NASA/CR—2000-210350

HOTCFGM-2D: A Coupled Higher-Order Theory for Cylindrical Structural Components With Bi-Directionally Graded Microstructures

Marek-Jerzy Pindera and Jacob Aboudi
University of Virgina, Charlottesville, Virginia

August 2000

The NASA STI Program Office . . . in Profile

Since its founding, NASA has been dedicated to the advancement of aeronautics and space science. The NASA Scientific and Technical Information (STI) Program Office plays a key part in helping NASA maintain this important role.

The NASA STI Program Office is operated by Langley Research Center, the Lead Center for NASA's scientific and technical information. The NASA STI Program Office provides access to the NASA STI Database, the largest collection of aeronautical and space science STI in the world. The Program Office is also NASA's institutional mechanism for disseminating the results of its research and development activities. These results are published by NASA in the NASA STI Report Series, which includes the following report types:

- TECHNICAL PUBLICATION. Reports of completed research or a major significant phase of research that present the results of NASA programs and include extensive data or theoretical analysis. Includes compilations of significant scientific and technical data and information deemed to be of continuing reference value. NASA's counterpart of peer-reviewed formal professional papers but has less stringent limitations on manuscript length and extent of graphic presentations.

- TECHNICAL MEMORANDUM. Scientific and technical findings that are preliminary or of specialized interest, e.g., quick release reports, working papers, and bibliographies that contain minimal annotation. Does not contain extensive analysis.

- CONTRACTOR REPORT. Scientific and technical findings by NASA-sponsored contractors and grantees.

- CONFERENCE PUBLICATION. Collected papers from scientific and technical conferences, symposia, seminars, or other meetings sponsored or cosponsored by NASA.

- SPECIAL PUBLICATION. Scientific, technical, or historical information from NASA programs, projects, and missions, often concerned with subjects having substantial public interest.

- TECHNICAL TRANSLATION. English-language translations of foreign scientific and technical material pertinent to NASA's mission.

Specialized services that complement the STI Program Office's diverse offerings include creating custom thesauri, building customized data bases, organizing and publishing research results . . . even providing videos.

For more information about the NASA STI Program Office, see the following:

- Access the NASA STI Program Home Page at ***http://www.sti.nasa.gov***

- E-mail your question via the Internet to help@sti.nasa.gov

- Fax your question to the NASA Access Help Desk at (301) 621-0134

- Telephone the NASA Access Help Desk at (301) 621-0390

- Write to:
  NASA Access Help Desk
  NASA Center for AeroSpace Information
  7121 Standard Drive
  Hanover, MD 21076

NASA/CR—2000-210350

HOTCFGM-2D: A Coupled Higher-Order Theory for Cylindrical Structural Components With Bi-Directionally Graded Microstructures

Marek-Jerzy Pindera and Jacob Aboudi
University of Virgina, Charlottesville, Virginia

Prepared under Contract NAS3–97190 and Grant NAG3–2252

National Aeronautics and
Space Administration

Glenn Research Center

August 2000

Acknowledgments

The support for this work was provided by the NASA Glenn Research Center through the Contract NAS3–97190. The authors thank Dr. Steven M. Arnold of the NASA Glenn Research Center, the technical monitor of this contract, for his valuable suggestions and comments in the course of this investigation.

Available from

NASA Center for Aerospace Information
7121 Standard Drive
Hanover, MD 21076
Price Code: A05

National Technical Information Service
5285 Port Royal Road
Springfield, VA 22100
Price Code: A05

PREFACE

This report summarizes the work performed under the contract **NAS3-97190** during the FY98-99 funding period. The objective of this two-year project was to develop and deliver to the NASA-Glenn Research Center a two-dimensional higher-order theory, and related computer codes, for the analysis and design of cylindrical functionally graded materials/structural components for use in advanced aircraft engines (e.g., combustor linings, rotor disks, heat shields, blisk blades). To satisfy this objective, two-dimensional version of the higher-order theory, HOTCFGM-2D, and four computer codes based on this theory, for the analysis and design of structural components functionally graded in the radial and circumferential directions were developed in the cylindrical coordinate system r–θ–z. This version of the higher-order theory is a significant generalization of the one-dimensional theory, HOTCFGM-1D, developed during the FY97 funding period under the contract **NAS3-96052** for the analysis and design of cylindrical structural components with radially graded microstructures. The generalized theory is applicable to thin multi-phased composite shells/cylinders subjected to steady-state thermomechanical, transient thermal and inertial loading applied uniformly along the axial direction such that the overall deformation is characterized by a constant average axial strain. The reinforcement phases are uniformly distributed in the axial direction, and arbitrarily distributed in the radial and circumferential direction, thereby allowing functional grading of the internal reinforcement in the r–θ plane.

The four computer codes *fgmc3dq.cylindrical.f*, *fgmp3dq.cylindrical.f*, *fgmgvips3dq.cylindrical.f*, and *fgmc3dq.cylindrical.transient.f* are research-oriented codes for investigating the effect of functionally graded architectures, as well as the properties of the multi-phase reinforcement, in thin shells subjected to thermomechanical and inertial loading, on the internal temperature, stress and (inelastic) strain fields. The reinforcement distribution in the radial and circumferential directions is specified by the user. The thermal and inelastic properties of the individual phases can vary with temperature. The inelastic phases are presently modeled by the power-law creep model generalized to multi-directional loading (within *fgmc3dq.cylindrical.f* and *fgmc3dq.cylindrical.transient.f* for steady-state and transient thermal loading, respectively), and incremental plasticity and GVIPS unified viscoplasticity theories (within the steady-state loading versions *fgmp3dq.cylindrical.f* and *fgmgvips3dq.cylindrical.f*).

Notice: The four computer codes *fgmc3dq.cylindrical.f*, *fgmp3dq.cylindrical.f*, *fgmgvips3dq.cylindrical.f*, and *fgmc3dq.cylindrical.transient.f* are being delivered to the NASA-Glenn Research Center strictly as research tools. The authors of the codes do not assume liability for application of the codes beyond research needs. Any questions or related items concerning these computer codes can be directed to either Professor Marek-Jerzy Pindera at the Civil Engineering & Applied Mechanics Department, University of Virginia, Charlottesville, VA 22903 (Tel: 804-924-1040, e-mail: marek@virginia.edu), or Professor Jacob Aboudi at the Department of Solid Mechanics, Materials & Structures, Faculty of Engineering, Tel-Aviv University, Ramat Aviv, Tel-Aviv69978, Israel (Tel: 972-3-640-8131, e-mail: aboudi@eng.tau.ac.il).

TABLE OF CONTENTS

1.0 INTRODUCTION

This final report summarizes the work funded under the contract **NAS3-97190** during the FY98-99 funding period. The objective of this two-year project was to develop and deliver to the NASA-Glenn Research Center a two-dimensional higher-order theory, and related computer codes, for the analysis and design of cylindrical functionally graded materials/structural components for use in advanced aircraft engines. This significant generalization of the one-dimensional theory developed during the F97 funding period allows the analysis and design of a wider class of aircraft engine structural components under more complex thermomechanical loading conditions than the axisymmetric loading capability of the one-dimensional theory [1] (e.g., combustor linings, rotor disks and shafts, heat shields, blisk blades subjected to combined steady-state thermomechanical and transient thermal and inertial loading). The theory and the related computer codes enable the designer to enhance the performance of aircraft engine structural components through the use of functionally graded architectures/microstructures. The analytical approach employed in the theory's construction explicitly couples microstructural and macrostructural effects in cylindrical bodies of revolution wherein the reinforcement phase or phases are spatially varied to improve thermo-mechanical performance (deformation, thermal fatigue resistance and life). It was shown previously that functionally graded structural components cannot be analyzed accurately using the standard micromechanics approach based on the representative volume concept coupled with macrostructural analysis in a noninteractive manner [2,3,4]. Such coupling is explicitly taken into account in the analytical framework of the higher-order theory, thereby providing the capability and means (through the related computer codes) to accurately analyze the response of cylindrical functionally graded structural components.

The work performed during the FY98-99 funding period resulted in the development of a two-dimensional version of the higher-order theory, HOTCFGM-2D, and four computer codes based on this theory, for the analysis and design of multi-phased composite thin shells/cylinders subjected to macroscopically uniform or nonuniform loading in the circumferential and radial directions applied uniformly along the axial direction. This version allows functional grading of the internal reinforcement in the r–θ plane, Figure 1. The reinforcement is in the form of continuous fibers, oriented in the axial or circumferential direction, or discontinuous inclusions with periodic spacing in the axial direction. The developed two-dimensional higher-order theory includes inertial body forces in the radial and circumferential directions due to angular acceleration, in addition to externally applied or transmitted loads, and temperature gradients in the r–θ plane. The temperature loading includes both steady-state and transient loading. As in the one-dimensional version, the development has been carried out in a manner that facilitates incorporation of inelastic and continuum-based damage constitutive theories for the response of the individual constituents, with robust integration algorithms [5,6]. At present, power-law creep model generalized to multiaxial loading, incremental plasticity and GVIPS unified viscoplasticity theories [7,8] are available within the three codes based on the steady-state version of the two-dimensional higher-order theory, *fgmc3dq.cylindrical.f*, *fgmp3dq.cylindrical.f*, and *fgmgvips3dq.cylindrical.f*. The code based on the version of the higher-order theory for transient thermal loading, *fgmc3dq.cylindrical.transient.f*, contains

power-law creep model. In addition, damage in the form of local fiber/matrix and matrix/matrix cracks has been incorporated into this code as a special case of a more general capability that admits the presence of internal cooling channels. The development of this capability was funded under the grant **NAG3-2252**, and is described in Appendix 7 in order to avoid unncecessary repetition. The combined capability that admits either cracks or cooling channels within a unified code provides the designer with a powerful and efficient code which is certainly preferable to two distinct codes.

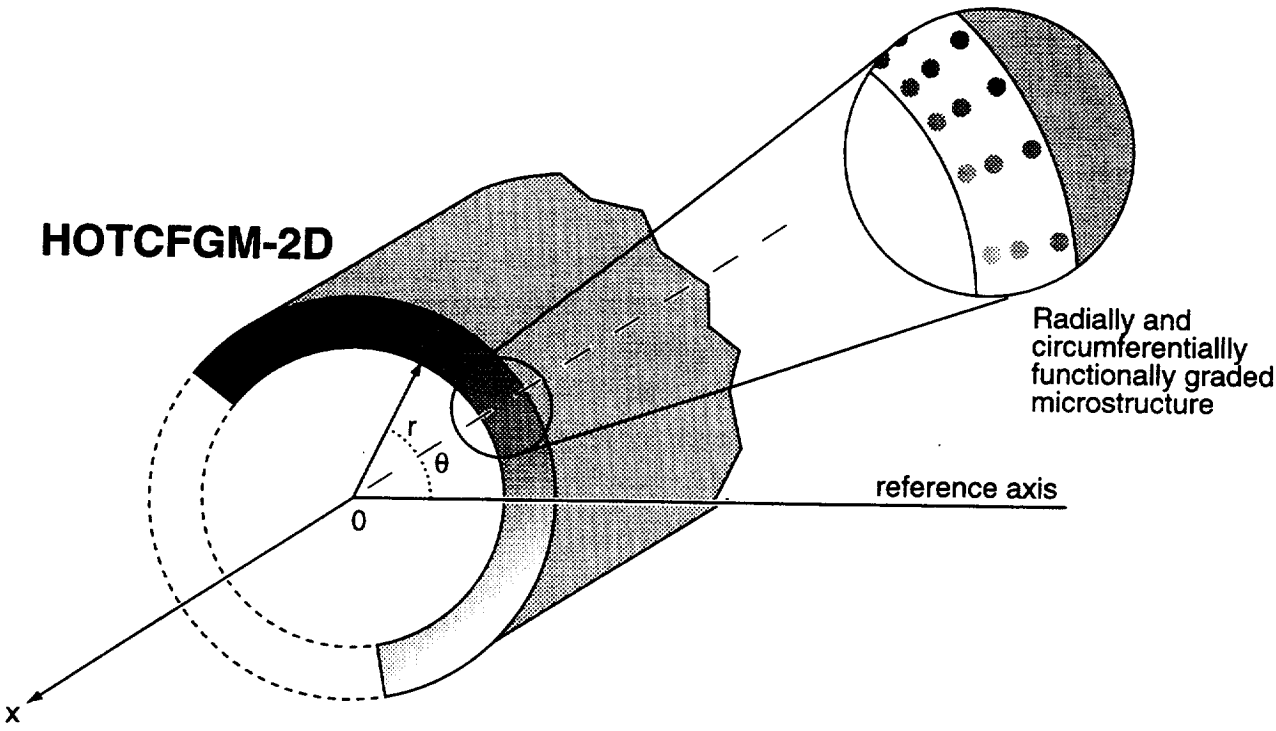

Figure 1. A geometric model for the cylindrical higher-order theory HOTCFGM-2D.

The four computer codes are research-oriented codes for investigating the effect of functionally graded architectures, as well as the properties of the multi-phase reinforcement, in thin shells/cylinders subjected to thermomechanical and inertial loading, on the internal temperature, stress and (inelastic) strain fields. The geometry of the investigated structural component, material properties of the phases, phase distributions in the radial and circumferential directions, and the applied loading in the r–θ plane are specified by the user in an easy-to-construct input data file described in more detail in section 3. The thermal and inelastic properties of the individual phases can vary with temperature and the elastic phases can be either isotropic or transversely isotropic. In the latter case, the axis of symmetry can be in the radial, circumferential or axial direction.

2.0 ANALYTICAL FOUNDATIONS OF HOTCFGM-2D

The developed theory is a significant generalization of an earlier version constructed by the authors for the analysis and design of cylindrical structural components with radially graded microstructures under axisymmetric thermomechanical loading [1]. The analytical framework is based on a second order representation of temperature and displacement fields within the subvolumes used to characterize the material's functionally graded microstructure, volumetric averaging of the various field quantities within these subvolumes, and subsequent satisfaction of the field equations within each subvolume in a volumetric sense, together with the imposition of boundary and continuity conditions in an average sense between adjacent subvolumes. This results in two systems of algebraic equations for the unknown coefficients that govern the temperature and displacement field in the individual subvolumes of a functionally graded cylinder. When thermal loading is of the steady-state type, the equations that govern the temperature field in each subvolume are solved first, and the results are subsequently used in the solution of the mechanical problem. When transient effects are included in thermal loading, the two sets of equations are solved simultaneously at each time increment of the applied thermal loading history. A brief outline of the construction of the two-dimensional higher-order theory for cylindrical functionally graded structural components under steady-state or transient thermal, and steady-state mechanical, loading is provided below. This construction is based on the previously developed theoretical framework for HOTCFGM-1D and includes the necessary modifications to account for two-dimensional steady-state thermomechanical and transient thermal loading and microstructural effects in the r–θ plane.

2.1 Analytical Model

The microstructure of the heterogeneous cylindrical structural element shown in Figure 1 is discretized into N_p and N_q cells in the r–θ plane. The generic cell (p,q) used to construct the composite consists of eight subcells designated by the triplet ($\alpha\beta\gamma$), where each index α, β, γ takes on the values 1 or 2 which indicate the relative position of the given subcell along the r, θ and z axis, respectively. The indices p and q, whose ranges are $p = 1, 2, ..., N_p$ and $q = 1, 2, ..., N_q$, identify the generic cell in the $r - \theta$ plane. The dimensions of the generic cell along the periodic z direction, l_1, l_2, are fixed for the given configuration, whereas the dimensions along the r and θ axes or the functionally graded directions, $d_1^{(p)}$, $d_2^{(p)}$, and $h_1^{(q)}$, $h_2^{(q)}$, can vary in an arbitrary fashion.

2.1.1 Thermal analysis

For the specified thermomechanical loading applied in the r–θ plane, an approximate solution for the temperature and displacement fields is constructed by first approximating the temperature distribution in each subcell of a generic cell using a quadratic expansion in the local coordinates $\bar{r}^{(\alpha)}$, $\bar{\theta}^{(\beta)}$, $\bar{z}^{(\gamma)}$,

$$T^{(\alpha\beta\gamma)} = T^{(\alpha\beta\gamma)}_{(000)} + \bar{r}^{(\alpha)} T^{(\alpha\beta\gamma)}_{(100)} + \bar{y}^{(\beta)} T^{(\alpha\beta\gamma)}_{(010)} + \frac{1}{2}(3\bar{r}^{(\alpha)2} - \frac{d_\alpha^{(p)2}}{4}) T^{(\alpha\beta\gamma)}_{(200)} + \frac{1}{2}(3\bar{y}^{(\beta)2} - \frac{h_\beta^{(q)2}}{4}) T^{(\alpha\beta\gamma)}_{(020)} + \frac{1}{2}(3\bar{z}^{(\gamma)2} - \frac{l_\gamma^2}{4}) T^{(\alpha\beta\gamma)}_{(002)} \quad (1)$$

where $\bar{y}^{(\beta)} = R^{(\alpha\beta\gamma)}\bar{\theta}^{(\beta)}$ and $R^{(\alpha\beta\gamma)}$ is the distance from the origin of the r–θ–z coordinate system to the center of the $(\alpha\beta\gamma)$ subcell. Given the six unknown coefficients associated with each subcell (i.e., $T^{(\alpha\beta\gamma)}_{(000)}$, ... , $T^{(\alpha\beta\gamma)}_{(002)}$) and eight subcells within each generic cell, $48N_pN_q$ unknown quantities must be determined for a composite with N_p rows and N_q columns of cells containing arbitrarily specified materials. These quantities are determined by first satisfying the heat conduction equation,

$$\frac{\partial q_r^{(\alpha\beta\gamma)}}{\partial \bar{r}^{(\alpha)}} + \frac{q_r^{(\alpha\beta\gamma)}}{R^{(\alpha\beta\gamma)} + \bar{r}^{(\alpha)}} + \frac{\partial q_\theta^{(\alpha\beta\gamma)}}{\partial \bar{y}^{(\beta)}} + \frac{\partial q_z^{(\alpha\beta\gamma)}}{\partial \bar{z}^{(\gamma)}} = -\rho c_p \dot{T}^{(\alpha\beta\gamma)} \tag{2}$$

as well as the first and second moment of this equation in each subcell in a volumetric sense in view of the employed temperature field approximation. In the above, ρ and c_p are the density and the heat capacity at constant pressure of the material occupying the $(\alpha\beta\gamma)$ subcell, and the rate of change of temperature with respect to time within the $(\alpha\beta\gamma)$ subcell is denoted by $\dot{T}^{(\alpha\beta\gamma)}$. The components $q_i^{(\alpha\beta\gamma)}$ $(i = r, \theta, z)$ of the heat flux vector in the the subcell $(\alpha\beta\gamma)$ of the (p,q)th cell in eqn (2) are derived from the temperature field according to

$$q_r^{(\alpha\beta\gamma)} = -k_r^{(\alpha\beta\gamma)} \frac{\partial T^{(\alpha\beta\gamma)}}{\partial \bar{r}^{(\alpha)}}, \quad q_\theta^{(\alpha\beta\gamma)} = -k_\theta^{(\alpha\beta\gamma)} \frac{\partial T^{(\alpha\beta\gamma)}}{\partial \bar{y}^{(\beta)}}, \quad q_z^{(\alpha\beta\gamma)} = -k_z^{(\alpha\beta\gamma)} \frac{\partial T^{(\alpha\beta\gamma)}}{\partial \bar{z}^{(\gamma)}} \tag{3}$$

where $k_i^{(\alpha\beta\gamma)}$ are the coefficients of heat conductivity of the material in the subcell $(\alpha\beta\gamma)$.

Subsequently, continuity of heat flux and temperature is imposed in an average sense at the interfaces separating adjacent subcells, as well as neighboring cells. Fulfillment of these field equations and continuity conditions, together with the imposed thermal boundary conditions applied to the bounding surface of the functionally graded material, provides the necessary $48N_pN_q$ equations for the $48N_pN_q$ unknown coefficients in the temperature field expansion of the form:

$$\bar{\boldsymbol{\kappa}}\,\dot{\mathbf{T}} = \bar{\mathbf{t}}(\mathbf{T}, t) = \mathbf{A}\mathbf{T}(t) + \dot{\mathbf{e}}(t) \tag{4}$$

where the structural thermal conductivity matrix $\bar{\boldsymbol{\kappa}}$ contains information on the geometry, thermal conductivities, densities and heat capacities of the subcells $(\alpha\beta\gamma)$ in the N_pN_q cells spanning the r and θ functionally graded directions, the thermal coefficient vector $\dot{\mathbf{T}}$ contains the unknown rates of change of the coefficients that describe the thermal field in each subcell, i.e.,

$$\dot{\mathbf{T}} = [\, \dot{\mathbf{T}}_{11}^{(111)}, \ldots, \dot{\mathbf{T}}_{N_pN_q}^{(222)} \,]$$

where $\dot{\mathbf{T}}_{pq}^{(\alpha\beta\gamma)} = [\, \dot{T}_{(000)}, \dot{T}_{(100)}, \dot{T}_{(010)}, \dot{T}_{(200)}, \dot{T}_{(020)}, \dot{T}_{(002)} \,]_{pq}^{(\alpha\beta\gamma)}$, and the modified thermal force vector $\bar{\mathbf{t}}$ contains information on the current temperature field in the individual subcells (obtained from the previous integration step) and the applied thermal boundary conditions.

The above system of equations is integrated using an implicit integration algorithm to generate the temperature field in the individual subcells at each point in time during the specified thermal loading history. The employed implicit algorithm is based on the discretization of eqn (4) as follows,

$$\bar{\kappa}\frac{\mathbf{T}(t+\Delta t)-\mathbf{T}(t)}{\Delta t} = \mathbf{A}[\theta\mathbf{T}(t+\Delta t)+(1.0-\theta)\mathbf{T}(t)]+\dot{\mathbf{e}}(t) \tag{5}$$

where θ is a weight factor which lies in the interval $0.5 \le \theta \le 1.0$. The above equation can be rewritten in the form,

$$[\mathbf{A}-\theta\Delta t\mathbf{B}]\mathbf{T}(t+\Delta t) = [\mathbf{A}+(1.0-\theta)\Delta t\mathbf{B}]\mathbf{T}(t)+\Delta t\dot{\mathbf{e}}(t) \tag{6}$$

Setting $\theta = 0.0$ produces the explicit algorithm which requires a very small Δt increment for convergence. With $\theta = 0.5$ or 1.0, Δt can be as large as 1.0, producing dramatic execution time reduction.

In the absence of transient thermal loading (i.e., steady-state case when the diffusion effects can be neglected), the right-hand side of eqn (2) becomes zero, and the final system of equations becomes:

$$\boldsymbol{\kappa}\,\mathbf{T} = \mathbf{t} \tag{7}$$

where the structural thermal conductivity matrix $\boldsymbol{\kappa}$ contains information on the geometry and thermal conductivities of the subcells $(\alpha\beta\gamma)$ in the N_pN_q cells spanning the r and θ functionally graded directions, the thermal coefficient vector $\mathbf{T}$ contains the unknown coefficients that describe the thermal field in each subcell, i.e.,

$$\mathbf{T}=[\,\mathbf{T}_{11}^{(111)},\ldots,\mathbf{T}_{N_pN_q}^{(222)}\,]$$

where $\mathbf{T}_{pq}^{(\alpha\beta\gamma)} = [\,T_{(000)}, T_{(100)}, T_{(010)}, T_{(200)}, T_{(020)}, T_{(002)}\,]_{pq}^{(\alpha\beta\gamma)}$, and the thermal force vector $\mathbf{t}$ contains information on the thermal boundary conditions.

2.1.2 Mechanical analysis

Once the temperature field is known, the resulting displacement and stress fields are determined by approximating the displacement field in each subcell of a generic cell by a quadratic expansion in the local coordinates $\bar{r}^{(\alpha)}$, $\bar{y}^{(\beta)}$, and $\bar{z}^{(\gamma)}$ as follows:

$$\mathbf{u}_r^{(\alpha\beta\gamma)} = W_{1(000)}^{(\alpha\beta\gamma)} + \bar{r}^{(\alpha)}W_{1(100)}^{(\alpha\beta\gamma)} + \bar{y}^{(\beta)}W_{1(010)}^{(\alpha\beta\gamma)} + \frac{1}{2}(3\bar{r}^{(\alpha)2} - \frac{1}{4}d_\alpha^{(p)2})W_{1(200)}^{(\alpha\beta\gamma)} + \frac{1}{2}(3\bar{y}^{(\beta)2} - \frac{1}{4}h_\beta^{(q)2})W_{1(020)}^{(\alpha\beta\gamma)} + \frac{1}{2}(3\bar{z}^{(\gamma)2} - \frac{1}{4}l_\gamma^2)W_{1(002)}^{(\alpha\beta\gamma)} \tag{8}$$

$$\mathbf{u}_\theta^{(\alpha\beta\gamma)} = W_{2(000)}^{(\alpha\beta\gamma)} + \bar{r}^{(\alpha)}W_{2(100)}^{(\alpha\beta\gamma)} + \bar{y}^{(\beta)}W_{2(010)}^{(\alpha\beta\gamma)} + \frac{1}{2}(3\bar{r}^{(\alpha)2} - \frac{1}{4}d_\alpha^{(p)2})W_{2(200)}^{(\alpha\beta\gamma)} + \frac{1}{2}(3\bar{y}^{(\beta)2} - \frac{1}{4}h_\beta^{(q)2})W_{2(020)}^{(\alpha\beta\gamma)} + \frac{1}{2}(3\bar{z}^{(\gamma)2} - \frac{1}{4}l_\gamma^2)W_{2(002)}^{(\alpha\beta\gamma)} \tag{9}$$

$$u_z^{(\alpha\beta\gamma)} = W_{3(000)}^{(\alpha\beta\gamma)} + \bar{z}^{(\gamma)} W_{3(001)}^{(\alpha\beta\gamma)} \tag{10}$$

where the unknown coefficients $W_{i(lmn)}^{(\alpha\beta\gamma)}$ (i = 1, 2, 3) are determined from conditions similar to those employed in the thermal problem. In this case, there are 104 unknown quantities in a generic cell (p,q). The determination of these quantities parallels that of the thermal problem with the thermal equations and quantities replaced by their mechanical analogues as briefly described below.

First, the heat conduction equation is replaced by the three equilibrium equations,

$$\frac{\partial \sigma_{rr}^{(\alpha\beta\gamma)}}{\partial \bar{r}^{(\alpha)}} + \frac{\partial \sigma_{r\theta}^{(\alpha\beta\gamma)}}{\partial \bar{y}^{(\beta)}} + \frac{\partial \sigma_{rz}^{(\alpha\beta\gamma)}}{\partial \bar{z}^{(\gamma)}} + \frac{\sigma_{rr}^{(\alpha\beta\gamma)} - \sigma_{\theta\theta}^{(\alpha\beta\gamma)}}{R^{(\alpha\beta\gamma)} + \bar{r}^{(\alpha)}} + F_r^{(\alpha\beta\gamma)} = 0 \tag{11}$$

$$\frac{\partial \sigma_{r\theta}^{(\alpha\beta\gamma)}}{\partial \bar{r}^{(\alpha)}} + \frac{\partial \sigma_{\theta\theta}^{(\alpha\beta\gamma)}}{\partial \bar{y}^{(\beta)}} + \frac{\partial \sigma_{\theta z}^{(\alpha\beta\gamma)}}{\partial \bar{z}^{(\gamma)}} + \frac{2\sigma_{r\theta}^{(\alpha\beta\gamma)}}{R^{(\alpha\beta\gamma)} + \bar{r}^{(\alpha)}} + F_\theta^{(\alpha\beta\gamma)} = 0 \tag{12}$$

$$\frac{\partial \sigma_{rz}^{(\alpha\beta\gamma)}}{\partial \bar{r}^{(\alpha)}} + \frac{\partial \sigma_{\theta z}^{(\alpha\beta\gamma)}}{\partial \bar{y}^{(\beta)}} + \frac{\partial \sigma_{zz}^{(\alpha\beta\gamma)}}{\partial \bar{z}^{(\gamma)}} + \frac{\sigma_{rz}^{(\alpha\beta\gamma)}}{R^{(\alpha\beta\gamma)} + \bar{r}^{(\alpha)}} = 0 \tag{13}$$

where $F_r^{(\alpha\beta\gamma)}$ and $F_\theta^{(\alpha\beta\gamma)}$ are the components of the body force due to the radial and angular acceleration. The components of the stress tensor, assuming that the material occupying the subcell $(\alpha\beta\gamma)$ of the (p,q,r)th cell is orthotropic, are related to the strain components through the generalized Hooke's law:

$$\sigma_{ij}^{(\alpha\beta\gamma)} = c_{ijkl}^{(\alpha\beta\gamma)} \left(\varepsilon_{kl}^{(\alpha\beta\gamma)} - \varepsilon_{kl}^{in(\alpha\beta\gamma)} \right) - \Gamma_{ij}^{(\alpha\beta\gamma)} T^{(\alpha\beta\gamma)} \tag{14}$$

where $c_{ijkl}^{(\alpha\beta\gamma)}$ are the elements of the stiffness tensor, $\varepsilon_{ij}^{in(\alpha\beta\gamma)}$ are the inelastic strain components, and the elements $\Gamma_{ij}^{(\alpha\beta\gamma)}$ of the so-called thermal tensor are the products of the stiffness tensor and the thermal expansion coefficients. In this investigation, we consider transversely isotropic elastic or isotropic inelastic materials. Hence, in the latter case, eqn (14) reduces to:

$$\sigma_{ij}^{(\alpha\beta\gamma)} = \lambda_{(\alpha\beta\gamma)} \varepsilon_{kk}^{(\alpha\beta\gamma)} \delta_{ij} + 2\mu_{(\alpha\beta\gamma)} \varepsilon_{ij}^{(\alpha\beta\gamma)} \delta_{ij} - 2\mu_{(\alpha\beta\gamma)} \varepsilon_{ij}^{in(\alpha\beta\gamma)} - \Gamma_{ij}^{(\alpha\beta\gamma)} T^{(\alpha\beta\gamma)} \tag{15}$$

where $\lambda_{(\alpha\beta\gamma)}$ and $\mu_{(\alpha\beta\gamma)}$ are the Lame's constants of the material filling the given subcell $(\alpha\beta\gamma)$. The components of the strain tensor in the individual subcells are, in turn, obtained from the strain-displacement relations.

Second, the continuity of tractions and displacements at the various interfaces replaces the continuity of heat fluxes and temperature. Finally, the boundary conditions involve the appropriate mechanical quantities.

Application of the above equations and conditions in a volumetric and average sense, respectively, produces a system of $104N_pN_q$ algebraic equations in the field variables within the cells of the

functionally graded composite of the form:

$$\mathbf{K}\,\mathbf{U} = \mathbf{f} + \mathbf{g} \tag{16}$$

where the structural stiffness matrix **K** contains information on the geometry and thermomechanical properties of the individual subcells ($\alpha\beta\gamma$) within the cells comprising the functionally graded composite, the displacement coefficient vector **U** contains the unknown coefficients that describe the displacement field in each subcell, i.e.,

$$\mathbf{U} = [\ \mathbf{U}_{11}^{(111)}, \ldots, \mathbf{U}_{N_q N_r}^{(222)}\ ]$$

where $\mathbf{U}_{qr}^{(\alpha\beta\gamma)} = [\ W_{1(000)}, \ldots, W_{3(001)}\ ]_{qr}^{(\alpha\beta\gamma)}$, and the mechanical force vector **f** contains information on the boundary conditions, body forces and the thermal loading effects generated by the applied temperature or heat flux. In addition, the inelastic force vector **g** appearing on the right hand side of eqn (16) contains inelastic effects given in terms of the integrals of the inelastic strain distributions $\varepsilon_{ij}^{in(\alpha\beta\gamma)}(\bar{r}^{(\alpha)}, \bar{y}^{(\beta)}, \bar{z}^{(\gamma)})$ that are represented by the coefficients $R_{ij(l,m,n)}^{(\alpha\beta\gamma)}$,

$$R_{ij(l,m,n)}^{(\alpha\beta\gamma)} = \mu_{(\alpha\beta\gamma)} \frac{\sqrt{(1+2l)(1+2m)(1+2n)}}{4} \int_{-1}^{1}\int_{-1}^{1}\int_{-1}^{1} \varepsilon_{ij}^{in(\alpha\beta\gamma)} P_l(\zeta_1^{(\alpha)}) P_m(\zeta_2^{(\beta)}) P_n(\zeta_3^{(\gamma)}) d\zeta_1^{(\alpha)} d\zeta_2^{(\beta)} d\zeta_3^{(\gamma)} \tag{17}$$

where the non-dimensionalized variables $\zeta_i^{(\cdot)}$'s, defined in the interval $-1 \le \zeta_i^{(\cdot)} \le 1$, are given in terms of the local subcell coordinates as follows: $\zeta_1^{(\alpha)} = \bar{r}^{(\alpha)} / (d_\alpha^{(p)}/2)$, $\zeta_2^{(\beta)} = \bar{y}^{(\beta)} / (h_\beta^{(q)}/2)$, and $\zeta_3^{(\gamma)} = \bar{z}^{(\gamma)} / (l_\gamma/2)$, and where $P_l(\cdot)$, $P_m(\cdot)$, and $P_n(\cdot)$ are Legendre polynomials of orders l, m and n. These integrals depend implicitly on the elements of the displacement coefficient vector **U**, requiring an incremental solution of eqn (16) at each point along the loading path. As mentioned previously, the solution of this system of equations follows that of the thermal problem in the case of steady-state thermal loading, while for transient thermal loading the two problems (thermal and mechanical) must be solved simultaneously. The outlined formulation is sufficiently general to admit either rate-independent incremental plasticity, rate-dependent creep or unified viscoplasticity constitutive theories.

3.0 DELIVERABLES

Brief descriptions of the features and capabilities of the four computer codes based on the outlined two-dimensional higher-order theory in the cylindrical coordinate system, *fgmc3dq.cylindrical.f*, *fgmp3dq.cylindrical.f*, *fgmgvips3dq.cylindrical.f*, and *fgmc3dq.cylindrical.transient.f*, for the analysis and design of radially and circumferentially functionally graded cylinders, delivered to the NASA-Glenn Research Center in fulfillment of the terms of the contract **NAS3-96052** are provided in the following sections.

3.1 Analysis Codes

The four computer codes *fgmc3dq.cylindrical.f*, *fgmp3dq.cylindrical.f*, *fgmgvips3dq.cylindrical.f*, and *fgmc3dq.cylindrical.transient.f* enable the user to investigate the internal temperature, stress and (inelastic) strain fields in cylindrical structural components with radial and circumferential functionally graded reinforcement in the form of continuous fibers or discontinuous inclusions, subjected to steady-state thermomechanical and transient thermal and inertial loading in the r–θ plane. Each of these Fortran codes is first compiled in order to generate an executable file called *a.out* which, in turn, is executed by typing the command of the same name at the unix prompt. The code *fgmp3dq.cylindrical.f* is employed when the inelastic material response of the individual homogeneous phases is modeled using the classical incremental plasticity theory, whereas *fgmc3dq.cylindrical.f* and *fgmgvips3dq.cylindrical.f* are employed for homogeneous phases modeled with the power-law creep model or the GVIPS unified viscoplasticity theory. These three codes have been developed for steady-state thermomechanical and inertial loading. The code *fgmc3dq.cylindrical.transient.f* has been developed for transient thermal and inertial loading of functionally graded cylinders containing phases whose response is described by the power-law creep model. This code also accommodates the presence of internal cooling channels, which can be specialized to cracks between the individual sucells in order to model damage.

The structure of the input data files is similar for these four codes and the definitions of the input variables associated with each READ statement are well-documented directly within the codes. A brief overview of the structure of the input data file is provided below for *fgmc3dq.cylindrical.f* and further elaborated upon in Appendix 1. An example of this input file is given in Appendix 2 for the problem of a functionally graded thermal barrier coating subjected to steady-state cyclic thermal loading investigated in the following section. The structure of the input data files for *fgmp3dq.cylindrical.f* and *fgmgvips3dq.cylindrical.f* is similar, with appropriate modifications for the slightly different capabilities of these two codes, i.e., use of incremental plasticity and GVIPS viscoplasticity in place of the power-law creep model. The structure of the input file for the code *fgmc3dq.cylindrical.transient.f* differs slightly from the input data file for the three codes developed for steady-state loading due to the additional information that must be provided about the material properties associated with transient thermal loading and the location and size of an internal crack or cooling channel and the type of boundary conditions applied to their faces. These differences are discussed in Appendices 5, 6 and 7.

The data is read from the input file *fgmc3dq.cylindrical.data* and the results are written to the two output files *fgmc3dq.cylindrical.out* and *fgmc3dq.cylindrical.plot*. The input data consists of four blocks. Block 1 is designated for the specification of the number of the individual phases, and their temperature-dependent material parameters, that make up the cylinder's functionally graded microstructure. Each phase is homogeneous and can be either elastic or inelastic. Elastic phases can be either isotropic or transversely isotropic. In the latter case, the axis of symmetry can be in the radial, circumferential or axial direction. Inelastic phases must be isotropic and are modeled by the power-law creep model generalized to multiaxial loading (or classical plasticity with isotropic hardening in conjunction with a bilinear representation of the elastoplastic stress-strain curve and GVIPS unified viscoplasticity theory in the case of *fgmp3dq.cylindrical.f* and *fgmgvips.cylindrical.f*).

Block 2 is designated for the specification of the cylinder geometry and architecture given by the inner radius of the cylinder, the number of subcells in the radial and circumferential directions, and their radial and circumferential dimensions. The assignment of different phases to the individual subcells is also specified in this block, as is the geometry and location of a crack or a cooling channel when *fgmc3dq.cylindrical.transient.f* is employed.

Block 3 is designated for the specification of the parameters employed for the loading history, integration of the two systems of equations for the unknown thermal and mechanical microvariables in the individual subcells, eqns (4) or (7) and (16), and the manner in which the results generated by the program are written to the output files *fgmc3dq.cylindrical.out* and *fgmc3dq.cylindrical.plot* (loading path and geometric locations). Information on the out-of-plane constraint during the applied loading history in the r–θ plane (plane strain or generalized plane strain) is also provided in this block together with the order of Legendre polynomials employed in approximating the inelastic strain field in the individual subcells, eqn (17), and the number of collocation points employed to integrate the inelastic strains.

Block 4 is designated for the specification of the external and (in the case of a crack/cooling channel) internal boundary conditions applied to the boundaries of the cylindrical shell in the r–θ plane, which can involve the simultaneous application of temperature or heat flux, and different combinations of tractions, displacements and displacement gradients discussed in Appendix 1. The magnitudes of these quantities are also specified in this block, but the actual thermal and mechanical loading histories which define the loading rates during different, user-specified time intervals are constructed within the two functions FUNCTION APPLIEDTR(TIME) and FUNCTION APPLIEDM(TIME) that reside within each of the four codes. The subroutine ANGULAR_VELOCITY allows the user to define the desired rotational loading history.

The input data is echoed to the output file *fgmc3dq.cylindrical.out*. In addition, this file contains temperature, stress and (plastic) strain fields in the individual subcells at the specified points of the loading history. An example of this output file is given in Appendix 3 for the problem of the previously mentioned functionally graded thermal barrier coating subjected to steady-state cyclic thermal loading. The output file *fgmc3dq.cylindrical.plot* contains temperature, stress and (plastic) strain distributions along the radial and circumferential cross sections of the functionally graded cylinder specified by the user that can

be used directly for plotting purposes. The plotting file for the above problem is given in Appendix 4.

The capabilities and options available within the four analysis codes are summarized in Table 1.

Table 1. Capabilities available within the analysis codes.

Type	Description
Functionally graded cylinder geometry	**Geometry**: thin-walled partial or fully enclosed cylinder with or without a crack/cooling channel **Reinforcement**: continuous or discontinuous **Grading**: arbitrarily nonuniform (user-specified) in the radial and circumferential directions; axially periodic
Constitutive models	**Elastic**: isotropic and transversely isotropic materials **Plastic**: incremental plasticity (Prandtl-Reuss relations) with isotropic hardening and bilinear representation of the elastoplastic stress-strain response (*fgmp3dq.cylindrical.f*) **Viscoplastic**: GVIPS unified viscoplasticity theory for isotropic materials (*fgmgvips.cylindrical.f*) **Creep**: power-law creep model generalized to multiaxial loading for isotropic materials (*fgmc3dq.cylindrical.f, fgmc3dq.cylindrical.transient.f*)
Phases	**Homogeneous**: all codes **Heterogeneous**: not available at present
Integration schemes	**Thermal problem**: forward Euler (steady-state loading), implicit (transient loading) **Mechanical problem**: successive elastic solutions (incremental plasticity) forward Euler (power-law creep, GVIPS viscoplasticity)
Loading capabilities	**Thermal**: steady-state, transient; heat flux or temperature specified on the boundaries **Mechanical**: steady-state; combinations of tractions, displacements, or displacement gradients specified on the boundaries **Inertial**: steady-state, transient rotation
Predictive capabilities	Temperature distributions in the r–θ plane Stress and (plastic) strain distributions in the r–θ plane

4.0 SUMMARY OF RESEARCH ACTIVITIES AND RESULTS

The development of the aforementioned computer codes was accompanied by the following investigations:

- Code validation
- Investigation of the response of cylindrical functionally graded thermal barrier coatings subjected to steady-state and transient thermal gradient loading (without and with an internal cooling channel in the case of transient loading)
- Investigation of the response of cylindrical functionally graded thermal barrier coatings subjected to combined thermal and rotational loading

These investigations demonstrate the accuracy and the utility of the higher-order theory in the analysis of MMC cylindrical components with or without grading as well as the developed codes' capability as analysis and design tools.

4.1 Validation Studies

The validation studies have been performed for both the steady-state and transient versions of the developed codes. The results of the validation studies for the steady-state version of the higher-order theory presented in this section have been generated using the material properties given in Table 2. The inelastic response of the individual phases was modeled using the incremental plasticity theory with isotropic hardening in conjunction with a bilinear representation of the elastoplastic stress-strain response.

Table 2. Thermoelastic and plastic parameters of Ti-24Al-11Nb alloy and SiC fibers.

Material	E (GPa)	ν	α (10^{-6}/°C)	κ (W/m-C)	Yield stress (MPa)	Hardening slope (GPa)
Ti-24Al-11Nb	110.3	0.26	9.44	8.0	371.6	23.0
SiC	399.9	0.25	4.0	17.6	N/A	N/A

4.1.1 Validation of the steady-state version of HOTCFGM-2D

The validation was based on the response of a homogeneous (unreinforced) cylinder subjected to an internal pressure, temperature gradient, pure shear, and steady-state rotation, a homogeneous curved beam subjected to pure bending, and a heterogeneous cylinder subjected to internal pressure. Both the elastic and elastoplastic responses of the homogeneous matrix material were considered. For the elastic cases, the results were subsequently compared with the exact analytical results as well as the corresponding results generated using the HOTCFGM-1D code based on one-directional version of the higher-order

theory developed during the first year of the investigation [1], when the loading was axisymmetric. For the inelastic cases involving axisymmetric loading for which analytical solutions were not available, comparison with the corresponding HOTCFGM-1D results provided the validation basis. In particular, the following cases were validated with very good agreement between the HOTCFGM-2D results and/or the analytical and the HOTCFGM-1D results.

- Homogeneous elastic cylinder subjected to internal pressure, temperature gradient, shear loading in the r-θ plane, and steady-state rotation (analytical solutions available).
- Homogeneous elastic curved beam subjected to pure bending (analytical solution available).
- Homogeneous elastoplastic cylinder subjected to internal pressure, temperature gradient, and steady-state rotation (comparison with HOTCFGM-1D).
- Four-layer elastoplastic cylinder subjected to temperature gradient and internal pressure (comparison with HOTCFGM-1D).
- Heterogeneous elastoplastic cylinder subjected to internal pressure (comparison with HOTCFGM-1D).

To illustrate the comparison with the exact analytical and HOTCFGM-1D solutions, four cases are chosen from the above. In Case I, we consider a homogeneous Ti-24Al-11Nb alloy cylinder with an inner radius of 0.020 m and an outer radius of 0.021 m (which produces a wall thickness to the innner radius ratio of 20). The cylinder was subjected to an inner pressure of 25 MPa (without an external pressure) and the results were generated using elastic and elastoplastic properties given in Table 2. In Case II, the same cylinder was subjected to a temperature gradient of 700°C produced by an applied inner radius temperature of 700°C and an outer radius temperature of 0°C. In Case III, we consider a curved beam, made of the same material and having the same radius of curvature and wall thickness as in the first two cases but with the elastoplastic response suppressed, subjected to a pure bending moment generated by the application of circumferential tractions at both ends obtained from an exact analytical elasticity solution [9]. Finally, for Case IV, we consider the response of a Ti-24Al-Nb cylinder reinforced by 10 through-thickness rows of SiC fibers, which is subjected to an internal pressure. The fiber volume fraction was 0.40. The cylinder had an inner radius of 0.020m and an outer radius of 0.022m (which produces a wall thickness to the inner radius ratio of 10). The 10-fiber configuration was discretized into 20 subcells across the cylinder's thickness. The applied internal pressure was 50 MPa with the external surface maintained traction-free.

For the first three cases, we compare the predictions of the elasticity solutions in the absence of plasticity and the predictions obtained from the HOTCFGM-2D code. We also include the predictions obtained from the HOTCFGM-1D code for the axisymmetric loadings (internal pressure and temperature gradient loading of the first two cases) as an additional check. In the presence of plasticity, the predictions obtained from the HOTCFGM-2D code are compared with those obtained from the HOTCFGM-1D code.

Case I: Thin-walled cylinder subjected to internal pressure

Figure 2 presents the predictions obtained from the exact elasticity solution and the HOTCFGM-1D and HOTCFGM-2D codes generated using both elastic of elastoplastic material parameters of the Ti-24Al-11Nb alloy for the axial (top), circumferential (middle) and radial (bottom) stress distributions through the cylinder's thickness. In the case of the axial stress, the predictions obtained from the two codes are identical in the elastic and elastoplastic cases, illustrating that the results generated by the more complicated HOTCFGM-2D code reduce to those generated by the HOTCFGM-1D code under axisymmetric loading. Virtually no difference is observed between the elasticity solution and the HOTCFGM-1D/2D predictions when the plasticity effects are suppressed.

Essentially the same results are obtained for the circumferential and radial stress distributions. The observed differences between the elasticity solution and the HOTCFGM-1D/2D predictions when the plasticity effects are suppressed are quite small, i.e, on the order of 2%.

Case II: Thin-walled cylinder subjected to temperature gradient

The temperature distributions obtained from the exact thermoelasticity solution of the considered temperature gradient problem and the HOTCFGM-1D and HOTCFGM-2D codes generated using both elastic and elastoplastic material parameters of the Ti-24Al-11Nb alloy varied linearly from 700° C at the inner radius to 0° C at the outer radius, as expected. It was verified that the temperature distributions were independent of whether elastic or elastoplastic material parameters were used since no thermomechanical coupling effects have been included in the development of the higher-order theory. Virtually no differences were observed between the analytical solution and the HOTCFGM-1D/2D results.

Figure 3 presents the resulting thermally-induced stress distributions through the cylinder's thickness for the axial (top), circumferential (middle) and radial (bottom) stresses obtained from the exact elasticity solution and the HOTCFGM-1D and HOTCFGM-2D codes. In the case of the axial stress, the predictions obtained from the two codes are identical in the elastic and elastoplastic cases. Some differences are observed at the inner radius between the elasticity solution and the HOTCFGM-1D/2D predictions when the plasticity effects are suppressed, which however decrease to zero halfway through the cylinder's thickness.

In the case of the circumferential stress distributions, the predictions of the two higher-order theory codes are again identical for both elastic and elastoplastic cases, and the correlation with the elasticity results is excellent when the plasticity effects are suppressed. Similar correlation between the elasticity results and the elastic HOTCFGM-1D/2D predictions is obtained for the radial stress, despite the substantially smaller magnitude of the radial stress distribution relative to the magnitudes of the axial and circumferential stress distributions.

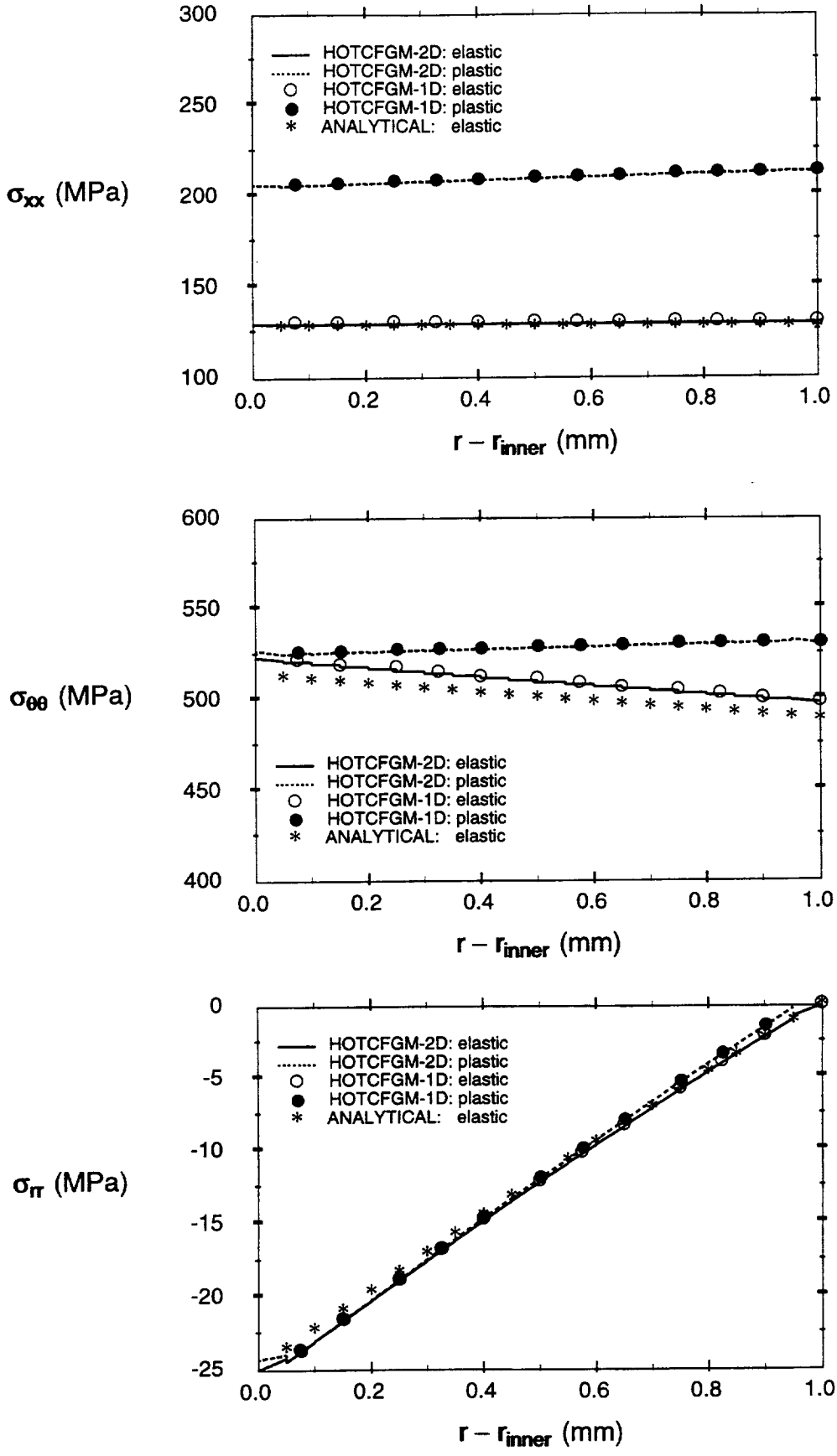

Figure 2. Comparison of HOTCFGM-2D, HOTCFGM-1D and exact solutions for an homogeneous elastic and elastoplastic cylinder subjected to an internal pressure: through-thickness axial stress (top); circumferential stress (middle); and radial stress (bottom) distributions.

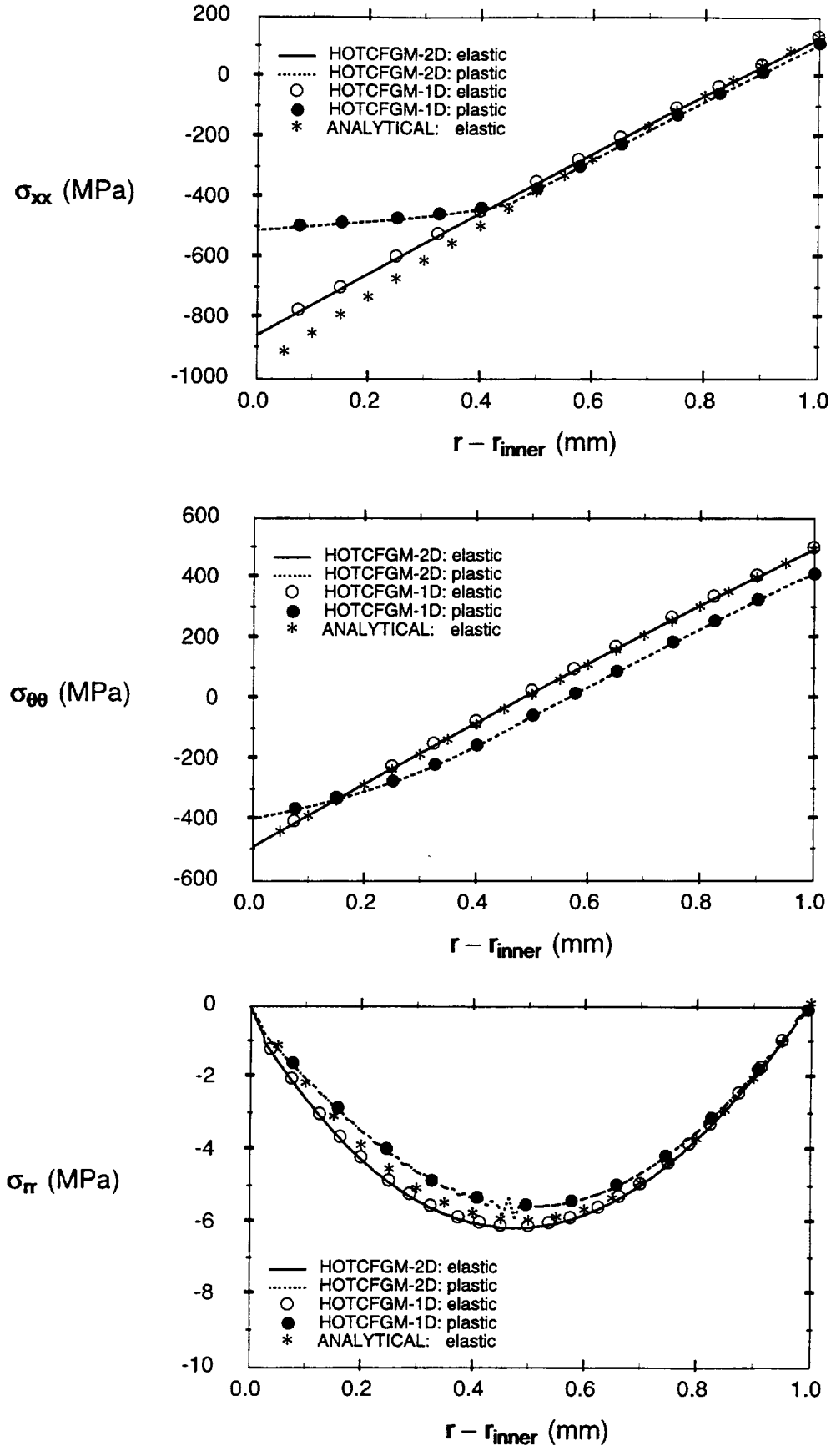

Figure 3. Comparison of HOTCFGM-2D, HOTCFGM-1D and exact solutions for an homogeneous elastic and elastoplastic cylinder subjected to a temperature gradient: through-thickness axial stress (top); circumferential stress (middle); and radial stress (bottom) distributions.

CASE III: Curved beam subjected to pure bending moment

Figure 4 presents the predictions obtained from the exact elasticity solution and the HOTCFGM-2D code generated using elastic parameters of the Ti-24Al-11Nb alloy for the circumferential (top) and radial (bottom) stress distributions through the curved beam's thickness. Excellent correlation between the analytical and higher-order predictions is observed for both stress components, despite the significantly lower magnitudes of the radial stress relative to the circumferential stress. We note the presence of the radial (through-thickness) stress which arises due to the beam's curvature (this stress component vanishes when the beam's curvature is zero).

CASE IV: SiC-fiber reinforced Ti-24Al-Nb cylinder subjected to internal pressure

Figures 5 and 6 present the comparison between the HOTCFGM-1D and HOTCFGM-2D predictions for the through-thickness axial (top), circumferential (middle) and radial (bottom) stress distributions in the SiC-fiber reinforced Ti-24Al-Nb cylinder subjected to an internal pressure of 50 MPa in the presence of plasticity. The distributions are given in the matrix-matrix and fiber-matrix representative cross sections (Figure 5 and 6, respectively). The differences between the HOTFGM-1D and HOTFGM-2D predictions are generally small, with smaller differences observed in the fiber-matrix than the matrix-matrix cross section.

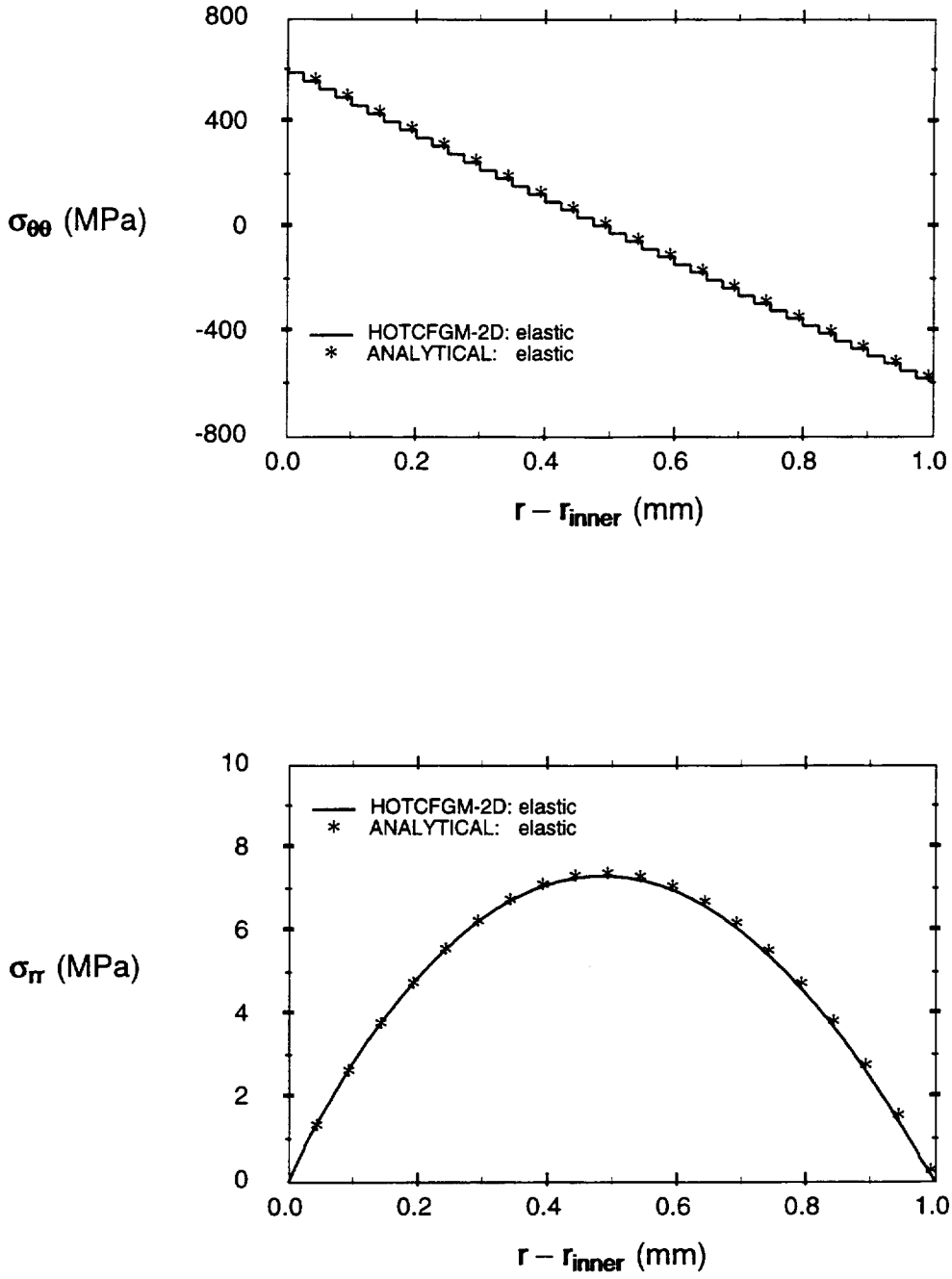

Figure 4. Comparison of HOTCFGM-2D and exact solutions for an homogeneous elastic curved beam subjected to a pure bending moment: through-thickness circumferential stress (top); and radial stress (bottom) distributions.

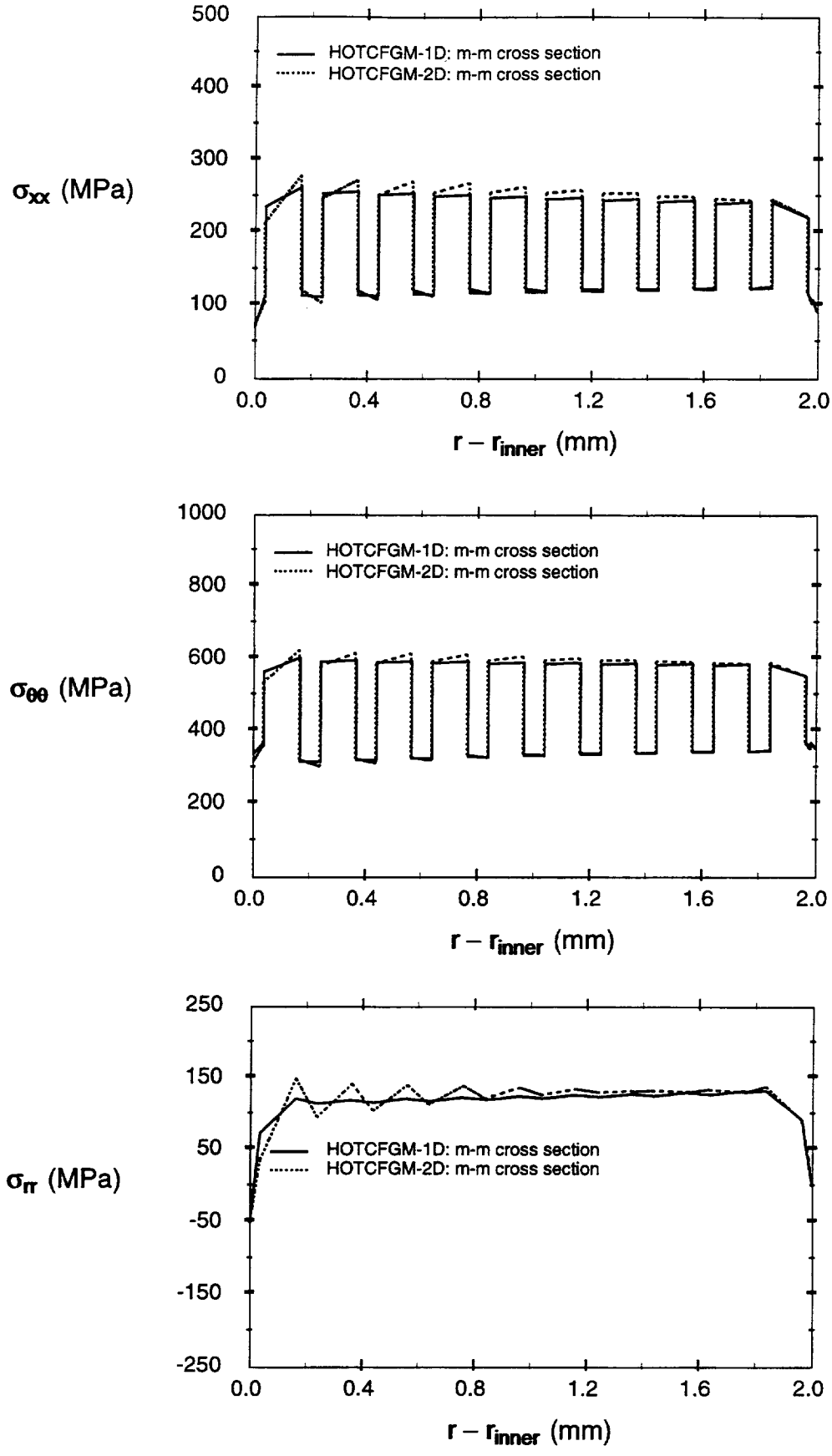

Figure 5. Comparison of HOTCFGM-1D and HOTCFGM-2D axial (top), circumferential (middle), and radial (bottom) stress distributions in a Ti-24Al-Nb cylinder with 10 through-thickness rows of SiC fibers subjected to an internal pressure: distributions in the matrix-matrix cross sections.

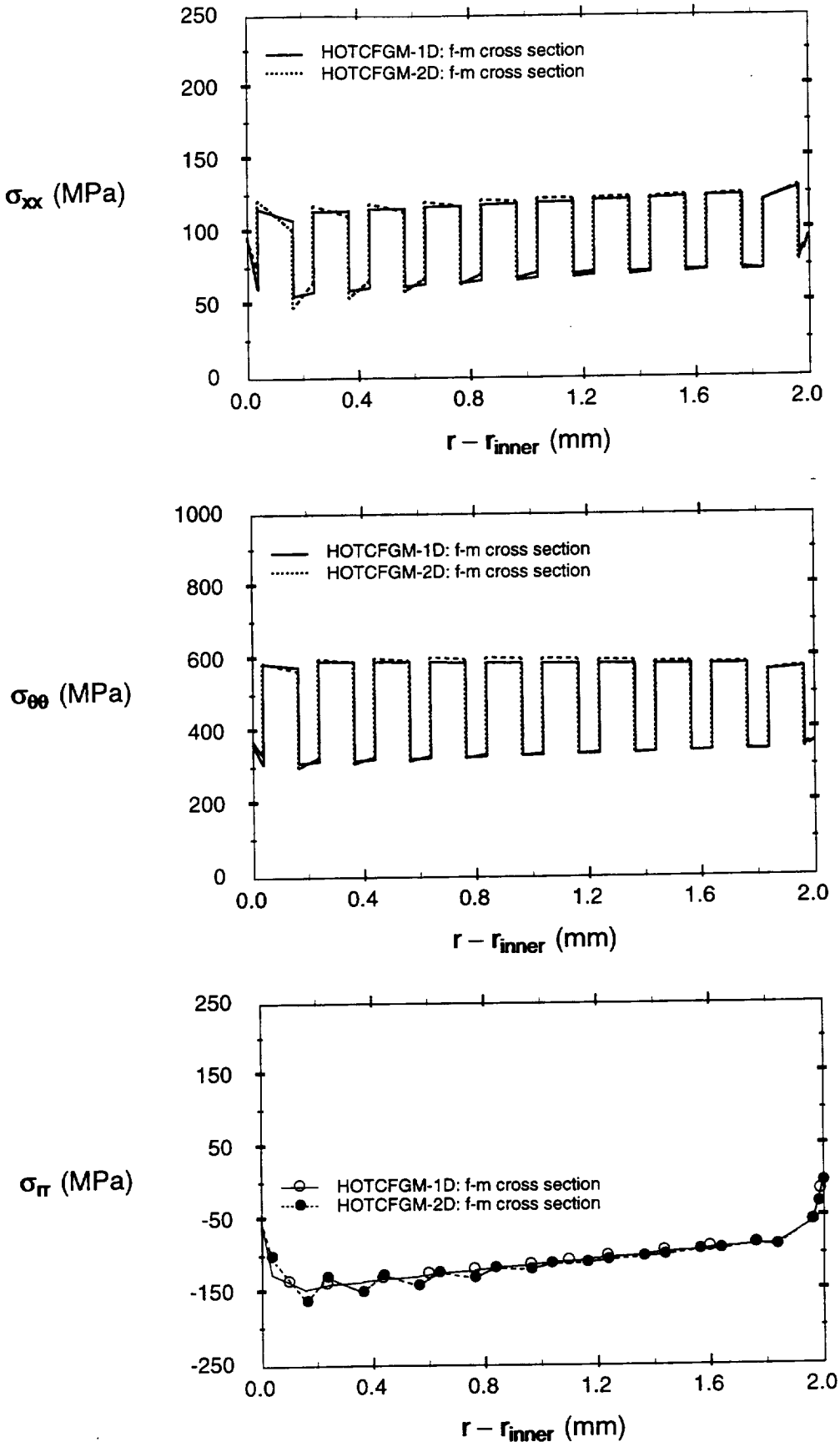

Figure 6. Comparison of HOTCFGM-1D and HOTCFGM-2D axial (top), circumferential (middle), and radial (bottom) stress distributions in a Ti-24Al-Nb cylinder with 10 through-thickness rows of SiC fibers subjected to an internal pressure: distributions in the fiber-matrix cross sections.

4.1.2 Validation of the transient version of HOTCFGM-2D

The validation of the transient thermal loading capability was carried out by comparing the predictions of the higher-order theory with a known analytical solution for the transient thermal problem of an infinite homogeneous slab instantaneously subjected to a temperature change on its upper and lower surfaces. The solution to this problem has been found in explicit form (a series solution) in Ref. [10] and subsequently programmed to generate numerical values for comparison with the higher-order theory predictions. The higher-order theory predictions were generated for the flat slab problem by setting the curvature to zero, which provided an additional and more demanding check on the theory's predictive capabilities.

Figure 7 presents a comparison between the higher-order predictions for the temperature distribution throughout the flat slab at different times with the programmed analytical results. The data is presented in nondimensional manner (nondimensional slab thickness x_1 / L where L is one half of the actual slab thickness, nondimensional temperature $T / T_{applied}$, and nondimensional time). As observed in the figure, virtually no difference is observed between the analytical solution and the higher-order theory results for all times. Further, the transient character of the solution is clearly evident in the generated data, demonstrating progressive homogenization of the temperature field throughout the slab thickness with increasing time.

4.2 Analysis of Functionally Graded TBCs

To investigate the response of cylindrical functionally graded thermal barrier coatings (TBCs) subjected to thermal loading involving a through-thickness temperature gradient, taking transient effects into account, a steel cylinder with the inner radius protected by a zirconia coating graded with CoCrAlY inclusions was considered. Both cyclic and Heaviside-type (or thermal shock) loading histories were employed. The ceramic coating was graded with the metallic bond coat material from the inner radius of 50 mm to the outer radius of 51 mm. The entire functionally graded coating was, in turn, bonded to the outer steel cylindrical substrate 1 mm thick. The representative cross section element of the investigated composite cylinder is shown in Figure 8, where the quasi-random distribution of the inclusion phases in the radial and circumferential directions is clearly evident. This is a much more realistic representation of functionally graded microstructures in thermal barrier coatings than previously employed in the context of the one-dimensional version of the theory, which is now possible with the generalization described in this report. The radial dimensions of the TBC-protected cylinder are the same as those employed in a previous investigation dealing with the effects of microstructural refinement on the response of functionally graded TBCs on flat substrates [11]. The transient thermo-mechanical analysis was performed on the representative cross section element (which is used to construct the entire composite cylinder in the circumferential direction), taking into account the symmetry conditions along the radial boundaries of the element. The results are compared with the corresponding results obtained when the transient effects are suppressed.

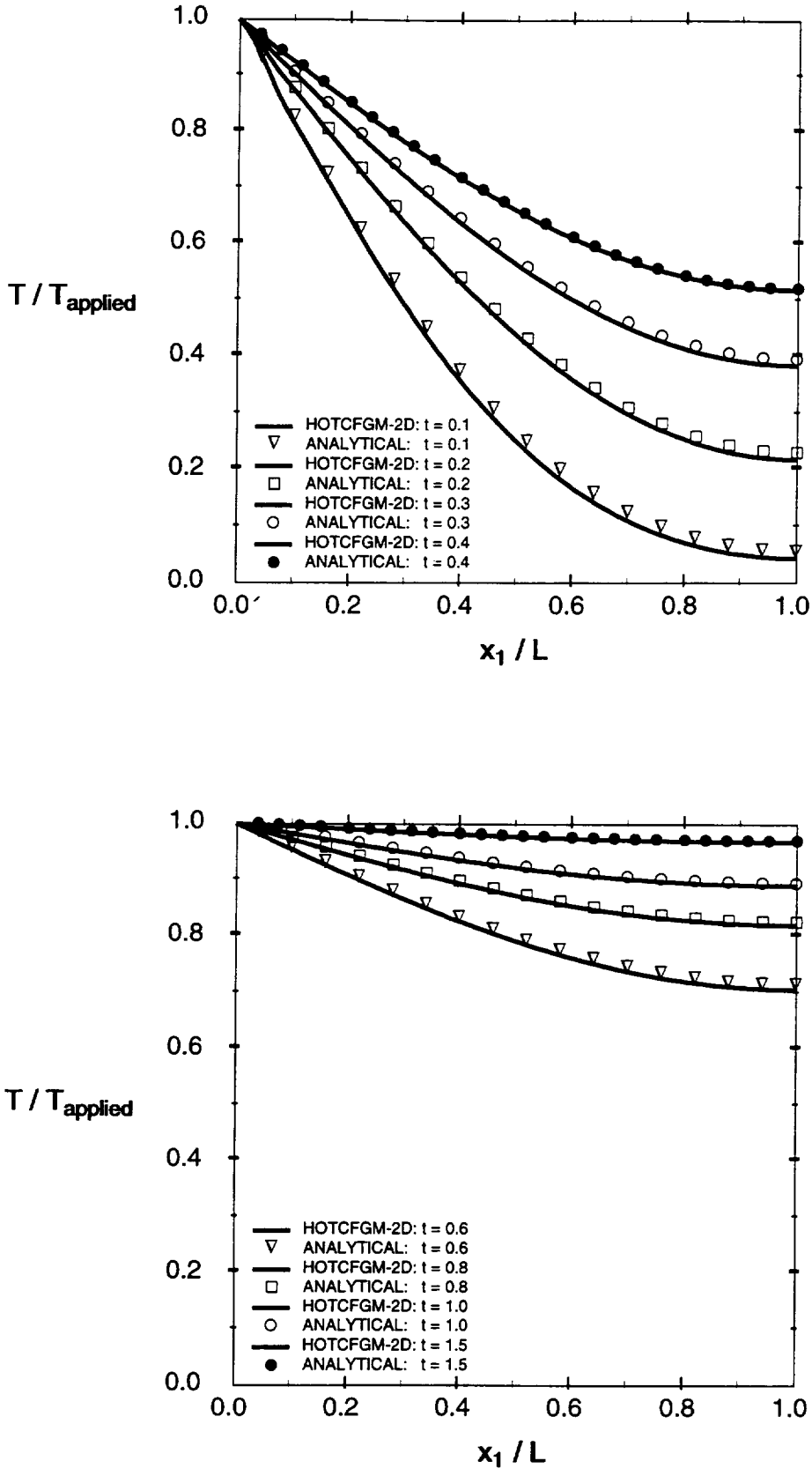

Figure 7. Temperature profiles in a slab subjected to an instantaneous temperature change on the upper and lower surfaces. Comparison of the higher-order theory predictions with an analytical solution.

The thermoelastic material parameters of the individual constituents of the functionally graded TBC configuration are given in Table 3.

Table 3. Thermoelastic material parameters of the TBC constituents.

Material	E (GPa)	ν	α (10^{-6}/K)	κ (W/m-K)	c_p ($m^2/(s^2K)$)	ρ (kg/m^3)
Zirconia top coat	36	0.20	8.0	0.50	272	6570
CoCrAlY bond coat	197	0.25	11.0	2.42	200	3000
Steel substrate	207	0.33	15.0	60.50	465	7830

Owing to the low conductivity of zirconia, and the significant temperature drop in the pure zirconia layers, the response of the CoCrAlY bond coat and the steel substrate was treated as elastic with temperature independent elastic parameters. The temperature-dependent inelastic response of the zirconia phase was modeled using the power-creep model generalized to multi-axial loading in the following manner:

$$\dot{\varepsilon}_{ij}^{in} = \frac{3F(\sigma_e)}{2\sigma_e}\sigma'_{ij} \tag{18}$$

where σ'_{ij} are the components of the stress deviator, $\sigma_e = \sqrt{3/2\sigma'_{ij}\sigma'_{ij}}$, and

$$F(\sigma_e) = A\sigma_e^n e^{-\Delta H/RT} \tag{19}$$

where the creep parameters A, n and ΔH are given in Table 4 and R = 8.317 J/(mole K). The thermoelastic and creep parameters also are the same as those in Ref. [11].

Table 4. Creep material parameters of the TBC constituents.

Material	A (Pa^{-n}/s)	n	ΔH (KJ/mole)
Zirconia top coat	1.89×10^{-6}	1.59	277
CoCrAlY bond coat	-	-	-
Steel substrate	-	-	-

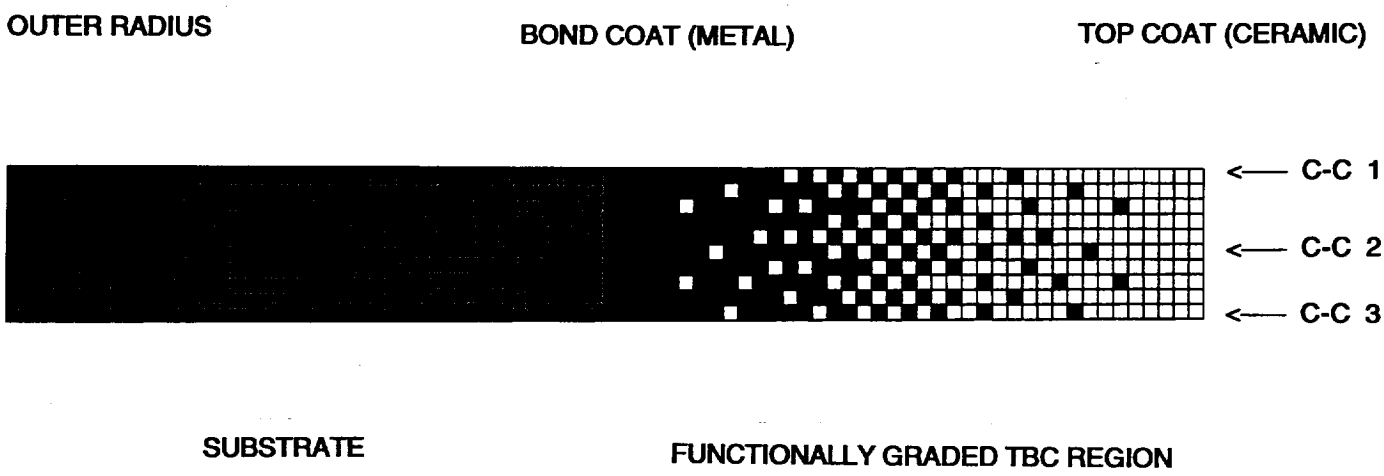

Figure 8. Repeating cross section element of a cylindrical structural component protected by a functionally graded thermal barrier coating.

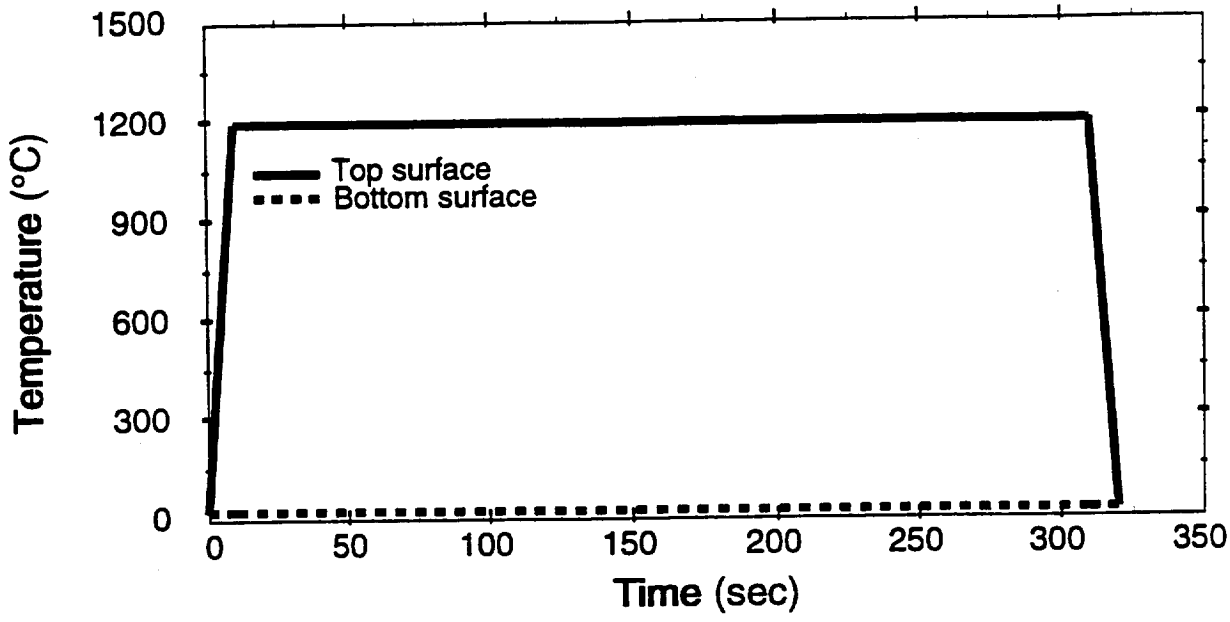

Figure 9. Thermal loading history.

4.2.1 Cyclic thermal loading

As the first step, we investigate the response of the considered thermal barrier coating subjected to cycling loading that involves heating of the inner radius from 25°C to 1200°C in 10 seconds, a hold period of 300 seconds, and a cooldown that lasts 10 seconds, Figure 9. The outer radius is kept at 25°C, producing a severe temperature gradient through the functionally graded coating's thickness.

Figure 10 presents the through-thickness temperature profiles in the three cross sections shown in Figure 8 at the end of the ramp, hold, and cooldown portions of the thermal cycle (t = 10, 310, and 320 seconds) generated taking into account transient effects. The profile at the end of the ramp portion of the thermal cycle is the same as the corresponding profile at the end of the hold period, indicating that the transient effects have died out by this point of the thermal loading history. This is further supported by the corresponding thermal profiles generated for the same thermal cycle under the assumption of steady-state conditions (not shown) which are virtually identical.

Figure 11 presents the corresponding through-thickness profiles of the circumferential stress $\sigma_{\theta\theta}$. Initially (at the end of the ramp period), the stress in the ceramic coating is compressive. However, considerable stress relaxation is observed in the ceramic-rich region at the end of the hold period which results in relatively high tensile circumferential stress upon cooldown in this region. These results are consistent with the results obtained for a flat functionally graded TBC in Ref. [11] under steady-state conditions using the same material properties, temperature history and through-thickness geometry, but different manner of grading.

Figure 12 presents the through-thickness circumferential stress profiles generated under the assumption of steady-state thermal cycling for comparison with those shown in Figure 11. At the end of the ramp portion, differences between transient and steady-state calculations are observed only in the ceramic region exposed to the elevated temperature where substantial creep and relaxation phenomena are occuring. This is most likely caused by the history dependence of the stress field in the presence of inelastic effects. For instance, the lower compressive circumferential stress at the ceramic (hot) surface of the TBC obtained from the transient analysis relative to the steady-state analysis after the end of the ramp period indicates initially higher stresses leading to greater relaxation. This is consistent with the heat diffusion mechanism which creates an initially higher constraint on material deformation in the regions of applied thermal loading relative to steady-state thermal loading (instantaneous heat diffusion). The differences between the steady-state and transient circumferential stress profiles in the ceramic region disappear at the end of the hold period.

The input, output and plot files for the case with the transient effects suppressed are given in Appendices 2, 3, and 4. The construction of the input file for the transient case is described in Appendix 5 where the differences between steady-state and transient input parameters are discussed. Appendix 6 provides the actual input file for the investigated transient case.

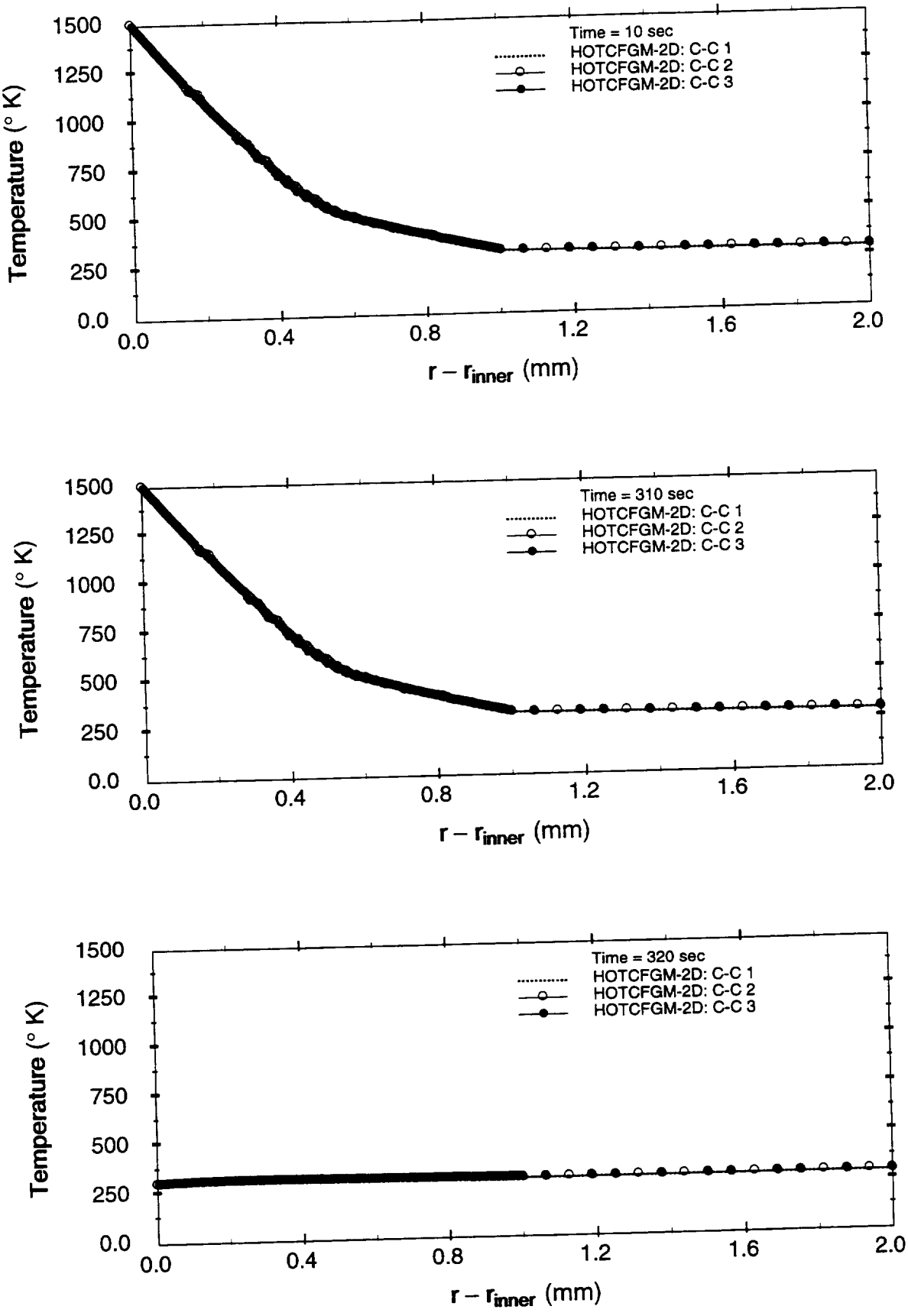

Figure 10. Transient through-thickness temperature profiles at t = 10 (top), 310 (middle), and 320 (bottom) seconds.

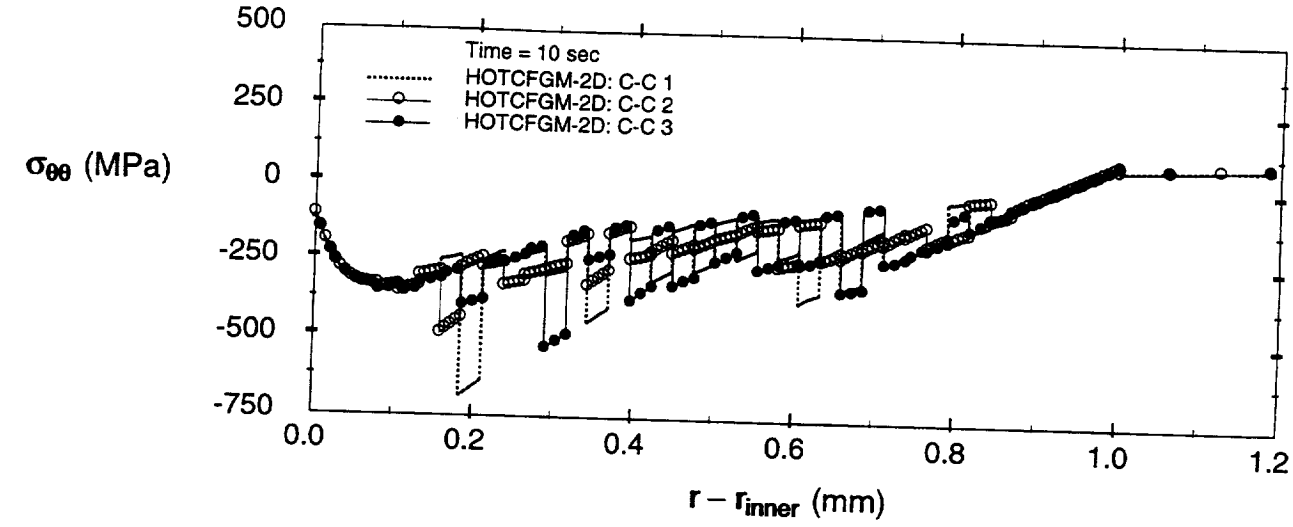

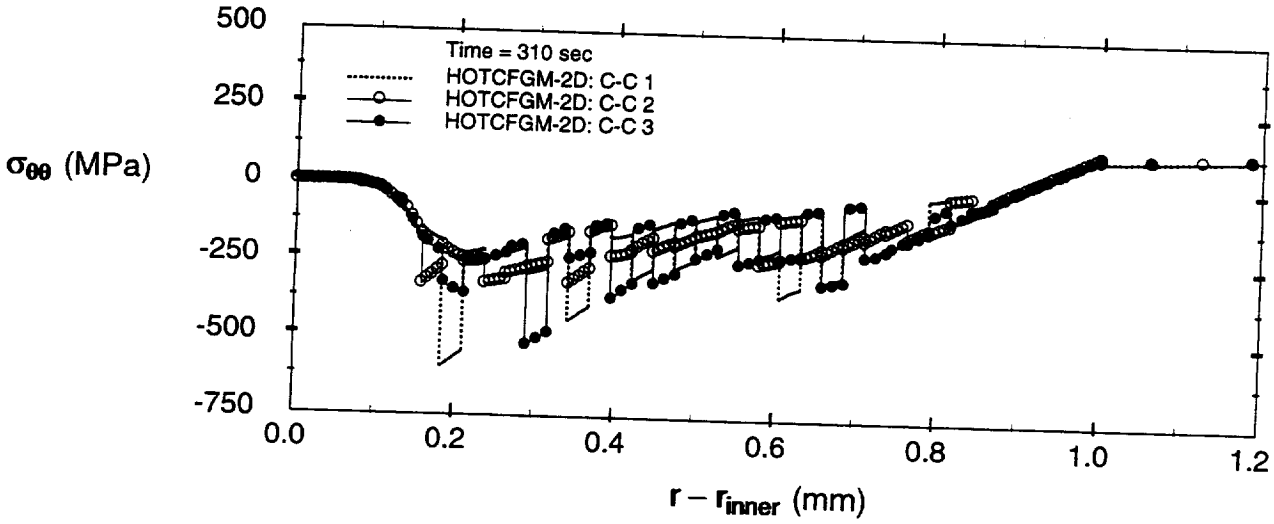

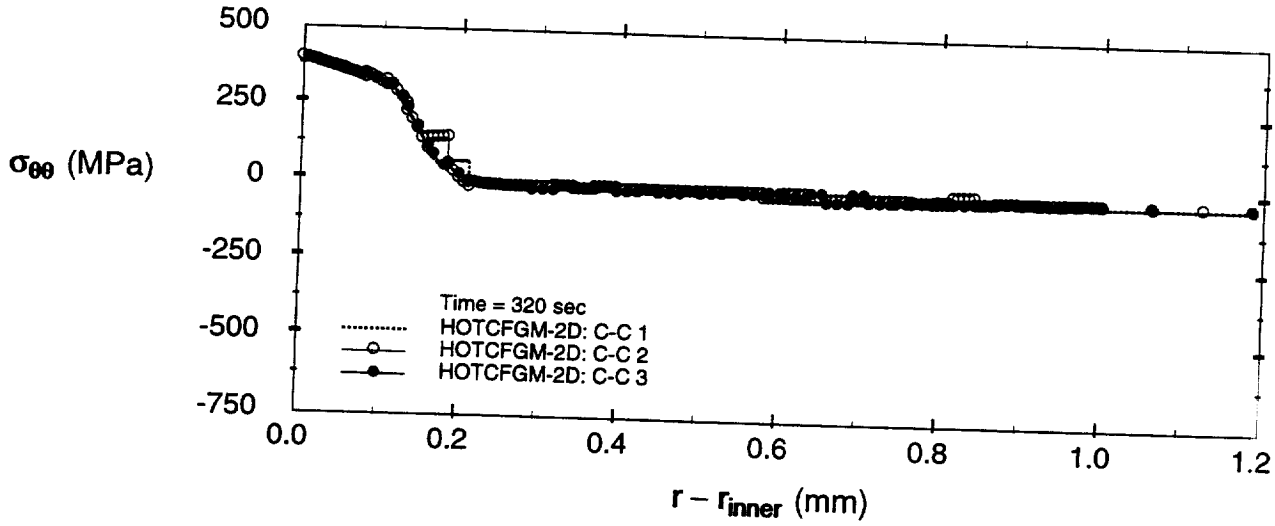

Figure 11. Transient through-thickness $\sigma_{\theta\theta}$ profiles at t = 10 (top), 310 (middle), and 320 (bottom) seconds.

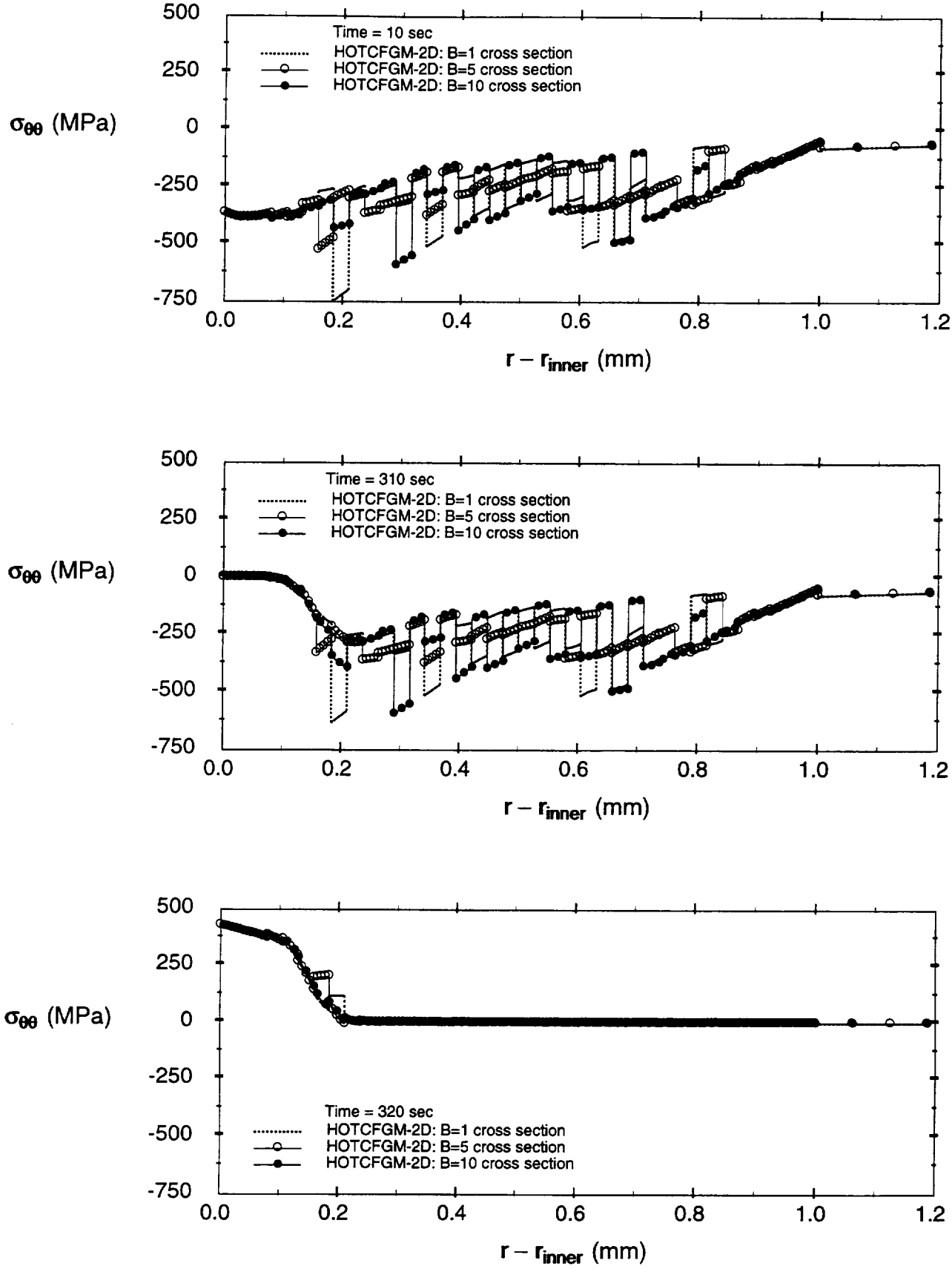

Figure 12. Steady-state through-thickness $\sigma_{\theta\theta}$ profiles at t = 10 (top), 310 (middle), and 320 (bottom) seconds.

4.2.2 Heaviside (thermal shock) loading

To better illustrate the transient thermal effects for the chosen TBC constituent material properties and geometry, instantaneous (Heaviside) thermal loading was applied to the inner radius of functionally graded TBC shown in Figure 8, while the outer radius was kept at room temperature. This was accomplished by decreasing the duration of the ramp portion of the thermal cycle shown in Figure 9 to a fraction of a second, and holding it at the upper temperature of 1200° C for 10 seconds.

Figure 13 presents the temperature distributions in the three cross sections (C-C 1, C-C 2, and C-C 3) of the functionally graded coating shown in Figure 8 at the times t= 0.01, 1.0 and 10 seconds. The transient thermal effects are quite apparent during the first second of heating. However, virtually no difference is observed in the thermal profiles at t = 1 and 10 seconds, indicating a very rapid decay of the transient effects (i.e., very rapid heat diffusion phenomenon). These results explain the absence of differences between transient and steady-state temperature distributions for the heating/hold/cooldown thermal cycle shown in Figure 9. In particular, the results presented at the end of the heatup and hold portions of the thermal cycle (t = 10 and 310 seconds) were essentially steady-state results due to the rapid decay of the transient effects for this particular material system as demonstrated in Figure 13.

Figures 14 and 15 present the corresponding circumferential stress and effective plastic strain distributions at the given times. The effect of thermal shock loading on the stress redistribution during the initial heat diffusion process (i.e., during the first second of heating) is quite apparent. The differences in the stress distributions at t = 1 and 10 seconds are due to the stress relaxation in the ceramic coating that occurs at the elevated temperature. Comparison with the results presented in the preceding section at t = 10 seconds, generated using a ramp function for initial heatup, indicates a greater amount of stress relaxation in the ceramic region. The evolution of plastic strain with time is also clearly visible and is clearly influenced by the heat diffusion process which provides the activation energy for creep strain.

4.2.3 Combined cyclic thermal and rotational loading

The mesh shown in Figure 8 also has been employed to demonstrate the transient rotational loading capability. In order to provide a basis for comparison, rotational loading involving a linear increase of the angular velocity from 0 to 10,000 radians/sec in 150 seconds, which was then kept constant, was superimposed on the temperature cycle employed in section 4.2.1.

Figures 16 and 17 present the circumferential stress and effective plastic strain distributions at t = 10, 310, and 320 seconds (which correspond to the end of the heatup, hold, and cooldown portions of the thermal cycle, respectively) for the combined thermal and rotational loading history. At t = 10 seconds, the stress and plastic strain distributions in the presence of the superposed rotational loading are indistinguishable from the corresponding distributions obtained from the pure thermal loading due to the small contribution from the rotational forces at this time. The effect becomes significant when the rotational velocity attains its maximum magnitude as observed at t = 310 and 320 seconds. In fact, the stress due to

the thermal loading is completely overshadowed by the rotationally-induced stress. The inelastic strains are affected to a substantially smaller degree since they are restricted to the inner ceramic region of the functionaly graded cylinder due to the assumption of linearly elastic behavior of the bond coat and substrate materials.

5.0 PLANS FOR FUTURE WORK

The capability developed during the FY98-98 funding period described in this report is currently being employed for the analysis and optimization of RLV thrust cell liner coatings under the grant **NAG3-2359**. The objective of this work is to identify an optimum blanching-resistant coating design for use on Cu-8Cr-4Nb thrust cell liners, leading to enhanced life/durability. This work in in direct support of the current collaborative effort among NASA-Glenn, MSFC and Rocketdyne to develop a new generation of blanching-resistant coatings for use on Cu-8Cr-4Nb thrust cell liners proposed for RLV applications. A preliminary investigation into the effects of interface roughness and oxide film thickness on the evolution of stress fields in duplex coatings on flat substrates, carried out with the higher-order theory, has confirmed the major failure mechanism by which plasma-sprayed coatings fail under spatially uniform thermal cycling [12]. This information will be employed in the ongoing RLV thrust cell liner coating study.

It has also been proposed to extend the completed higher-order theory for cylindrical functionally graded structural components by incorporating dynamic impact loading capability. This extension will make possible the assesssment of the effect of foreign object impact on the potential for damage evolution in advanced turbine blade coatings, for instance. The proposed work complements current nationwide efforts by a number of government agencies to develop a new generation of turbine blade coatings capable of operating longer in low-cost fuel environments containing different types of impurities. As the impact problem also plays an important role in a number of other technologically important applications that are important to the nation's security interests (graded body armour, for instance), the proposed work will significantly broaden the range of technologically important applications of the cylindrical higher-order theory.

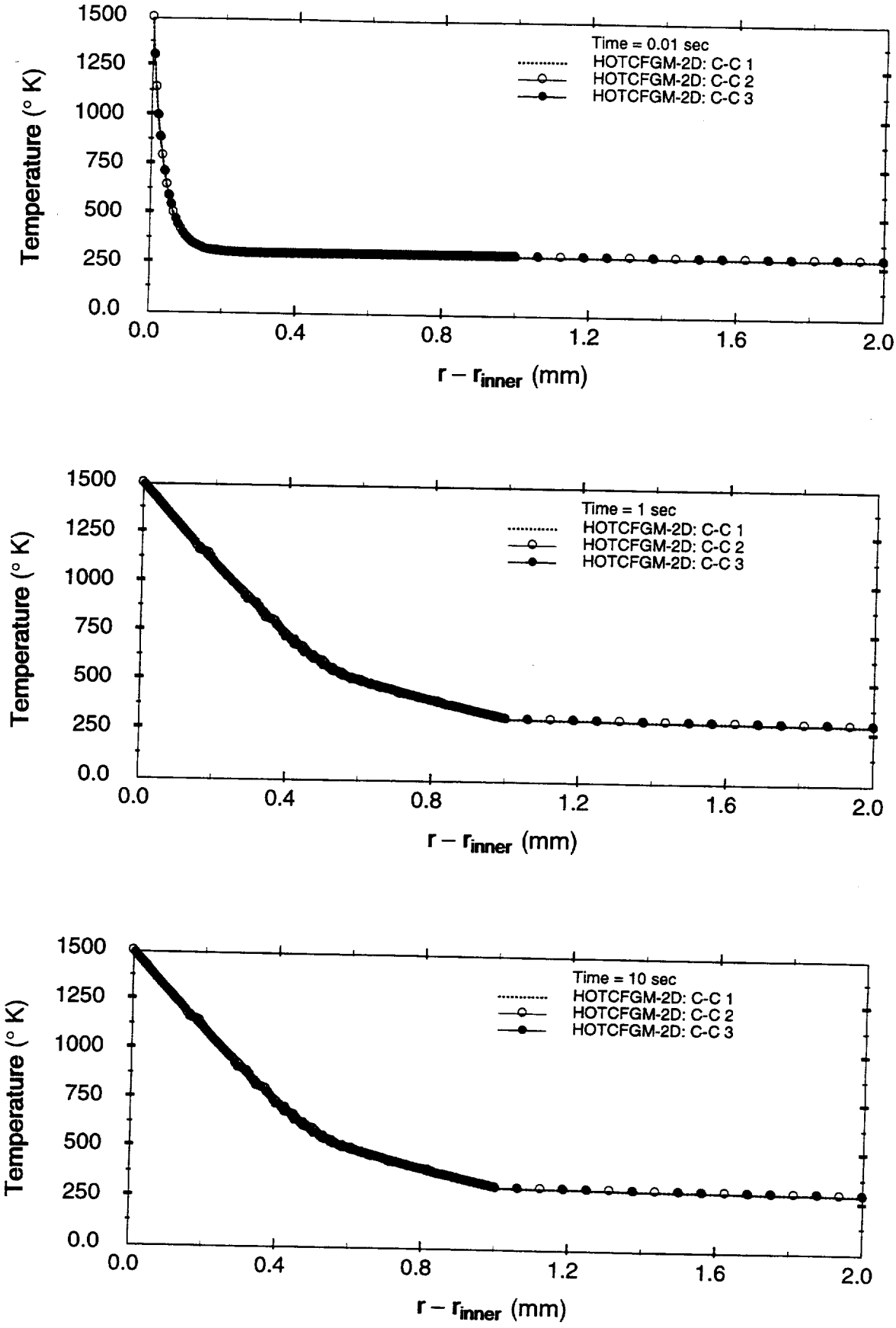

Figure 13. Transient through-thickness temperature profiles at t = 0.01 (top), 1.0 (middle), and 10 (bottom) seconds due to Heaviside thermal loading on the ceramic-rich surface.

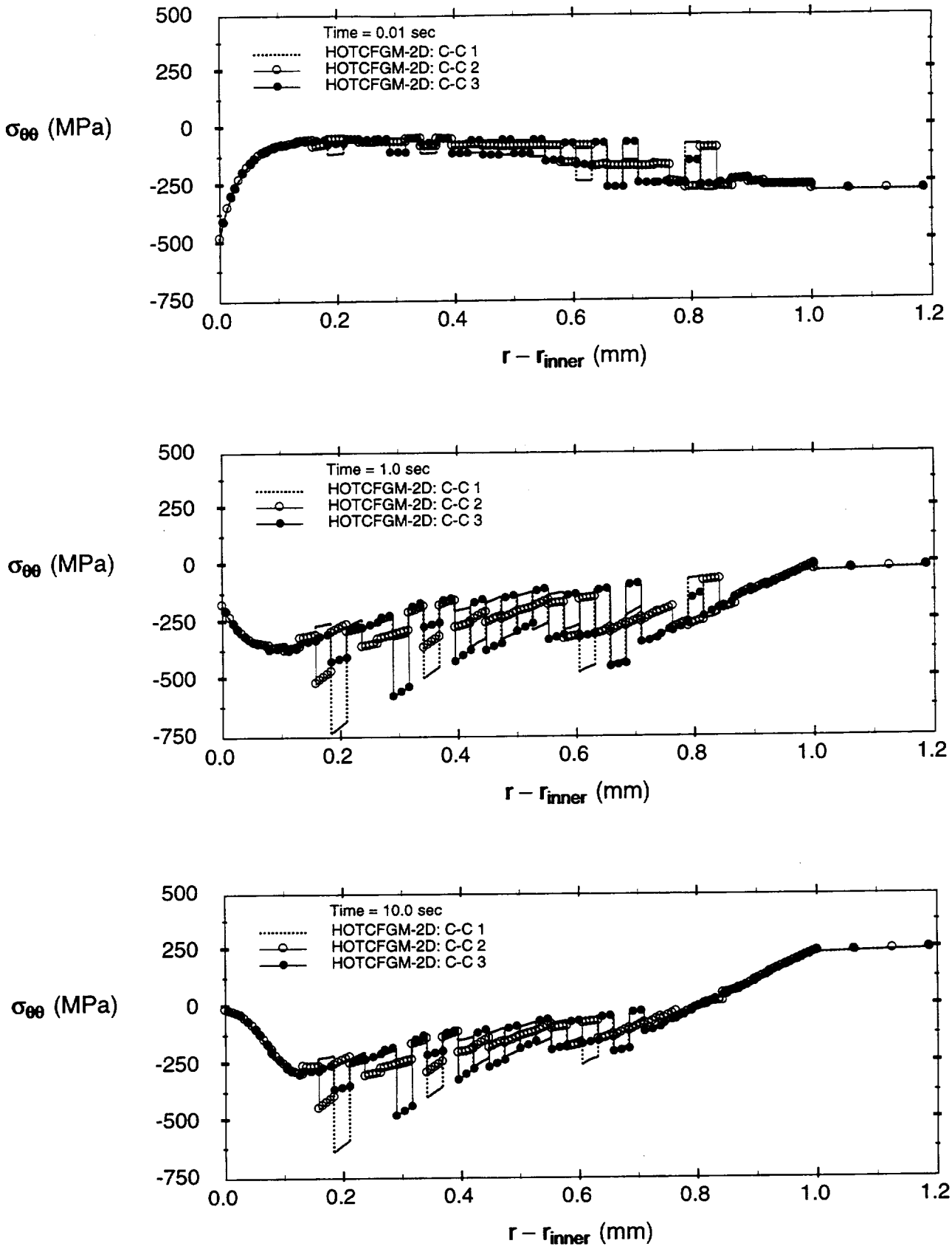

Figure 14. Transient through-thickness $\sigma_{\theta\theta}$ profiles at t = 0.01 (top), 0.1 (middle), and 1.0 (bottom) seconds due to Heaviside thermal loading on the ceramic-rich surface.

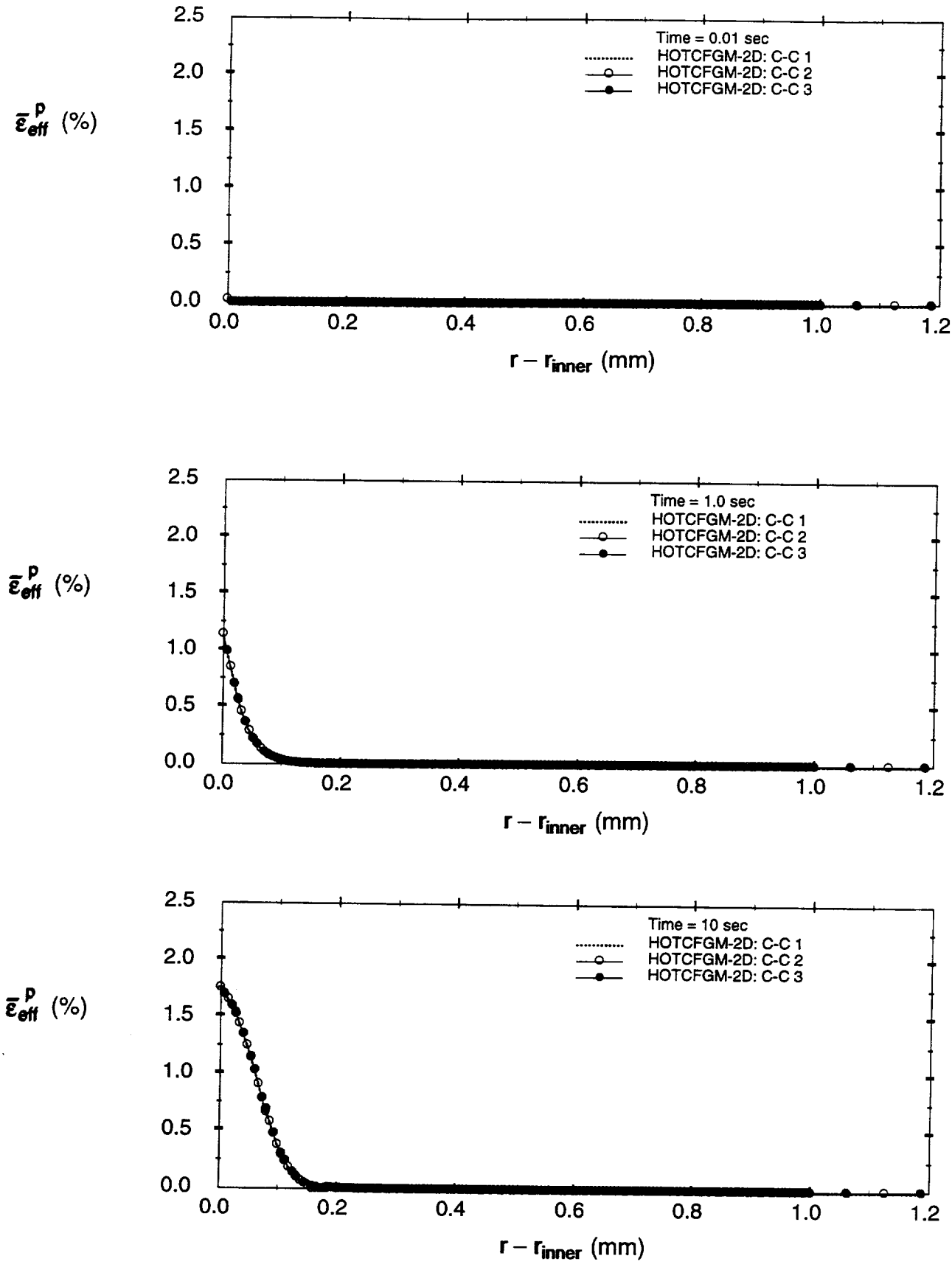

Figure 15. Transient through-thickness $\bar{\varepsilon}^{in}_{eff}$ profiles at t = 0.01 (top), 0.1 (middle), and 1.0 (bottom) seconds due to Heaviside thermal loading on the ceramic-rich surface.

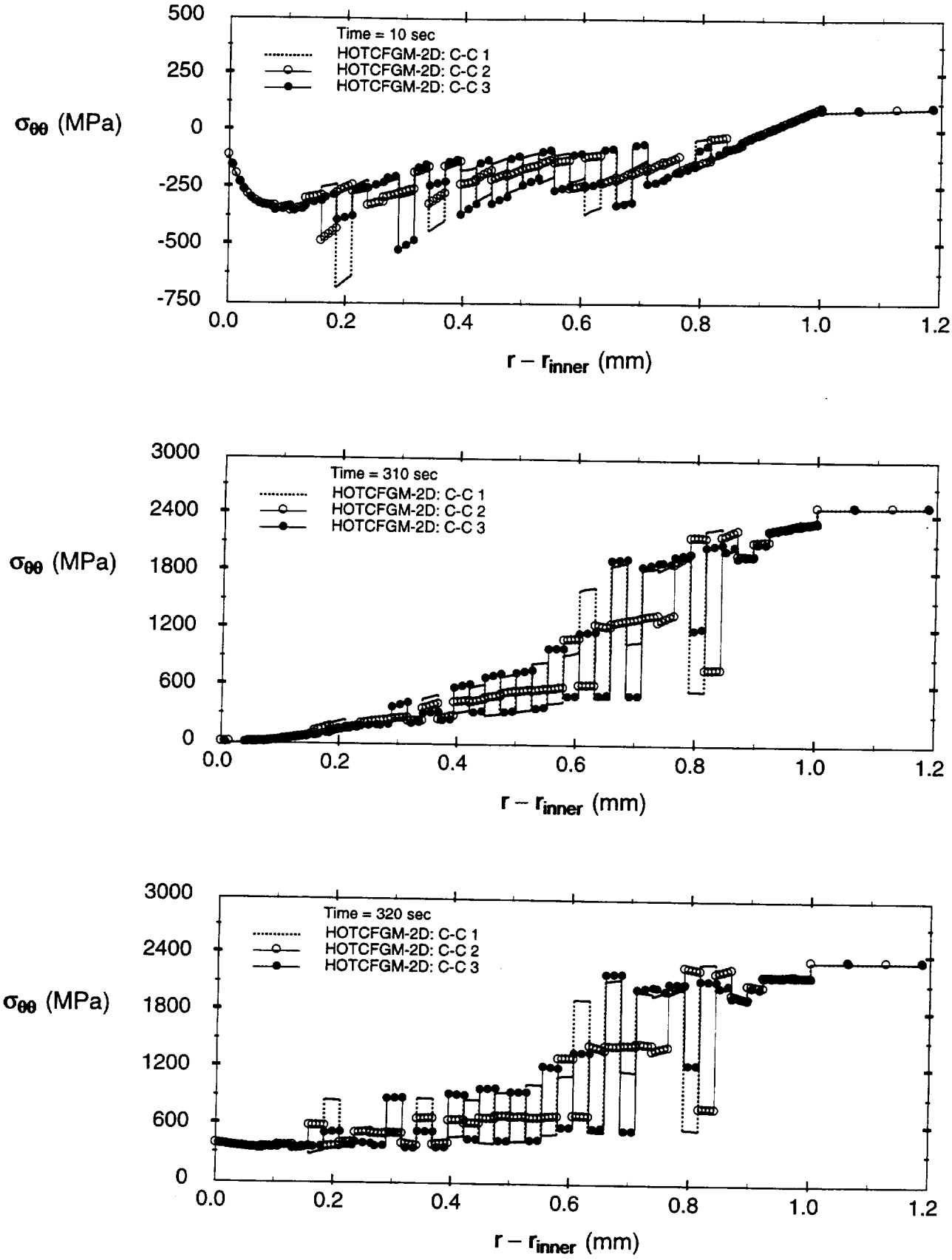

Figure 16. Transient through-thickness $\sigma_{\theta\theta}$ profiles at t = 10 (top), 310 (middle), and 320 (bottom) seconds due to combined thermal and rotational loading.

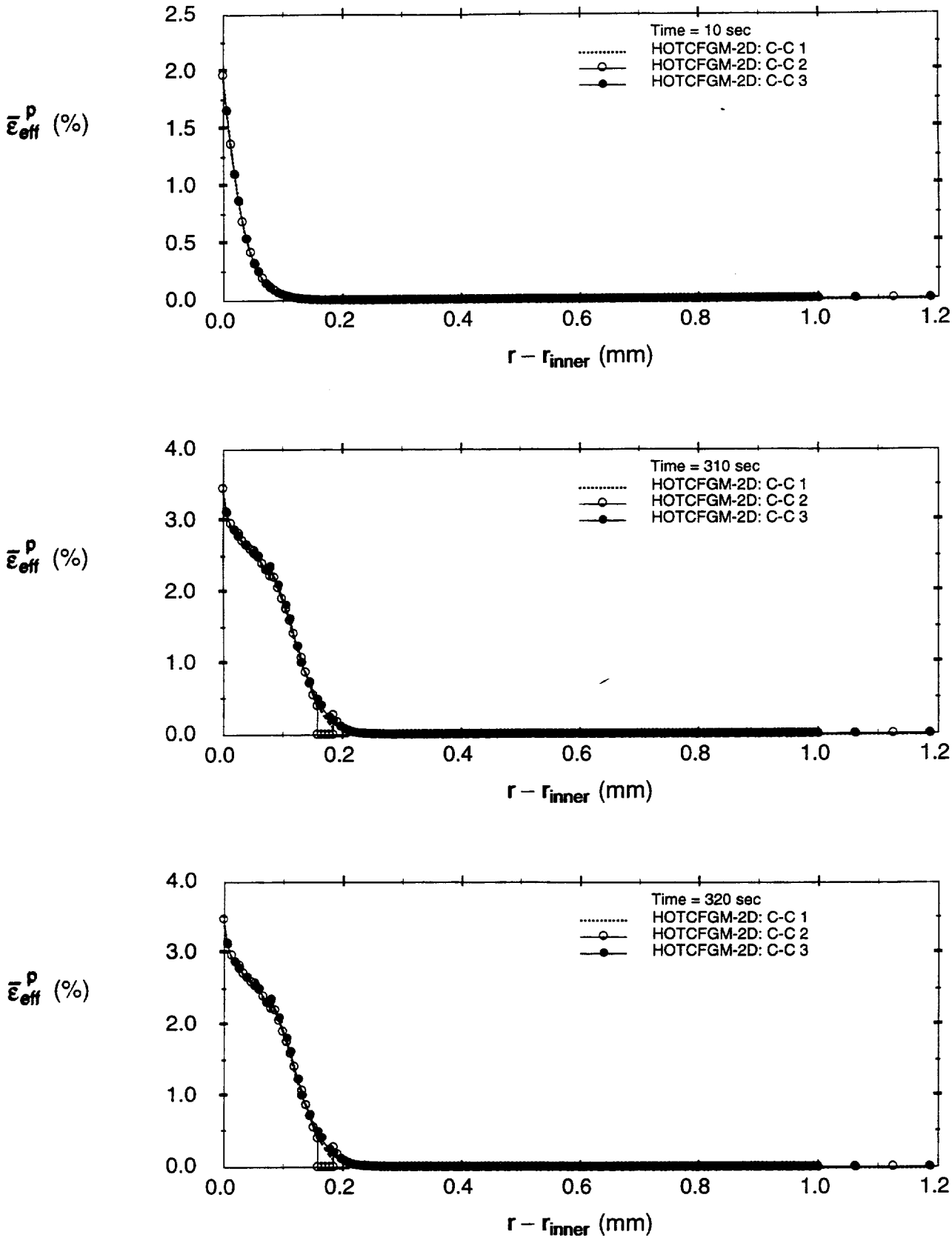

Figure 17. Transient through-thickness $\bar{\varepsilon}^{in}_{eff}$ profiles at t = 10 (top), 310 (middle), and 320 (bottom) seconds due to combined thermal and rotational loading.

6.0 REFERENCES

1. Pindera, M-J. and Aboudi, J. (1998), "HOTCFGM-1D: A Coupled Higher-Order Theory for Cylindrical Structural Components with Through-Thickness Functionally Graded Microstructures (Final Report)," *NASA Contractor Report 1998-207927*, NASA-Glenn Research Center, June 1998.

2. Pindera, M-J., Aboudi, J., and Arnold, S. M. (1994), "Thermo-Inelastic Analysis of Functionally Graded Materials: Inapplicability of the Classical Micromechanics Approach," in *Inelasticity and Micromechanics of Metal Matrix Composites*, G. Z. Voyiadjis and J. W. Ju (Eds.), pp. 273-305, Elsevier Science Publishers B.V., The Netherlands.

3. Pindera, M-J, Aboudi, J., and Arnold, S. M. (1995), "Limitations of the Uncoupled, RVE-Based Micromechanical Approach in the Analysis of Functionally Graded Composites," *Mechanics of Materials*, Vol. 20, No. 1, pp. 77-94.

4. Aboudi, J., Pindera, M-J., and Arnold, S. M. (1999), "Higher-Order Theory for Functionally Graded Materials," *Composites: Part B (Engineering)*, Vol. 30B, No. 8, pp. 777-832. .

5. Saleeb, A. F. and Li, W. (1995a), "Robust Integration Schemes for Generalized Viscoplasticity with Internal-State Variables. Part I: Theoretical Developments and Applications," *NASA CR 195452*, NASA-Lewis Research Center, Cleveland, OH.

6. Saleeb, A. F. and Li, W. (1995b), "Robust Integration Schemes for Generalized Viscoplasticity with Internal-State Variables. Part II: Algorithmic Developments and Implementation" *NASA CR 195453*, NASA-Lewis Research Center, Cleveland, OH.

7. Mendelson, A., *Plasticity: Theory and Applications*, Robert E. Krieger Publishing Company, Malabar, Florida, 1983 (reprint edition).

8. Arnold, S. M., Saleeb, A. F., and Castelli, M. G. (1994), "A Fully Associative, Nonlinear Kinematic, Unified Viscoplastic Model for Titanium Based Matrices," *NASA TM 106609*, NASA-Lewis Research Center, Cleveland, OH.

9. Timoshenko, S. P. and Goodier, J. N., *Theory of Elasticity*, McGraw-Hill Book Company, New York, pp. 71-75, 1970.

10. Carslaw, H. S. and Jager, J. C., "Conduction of Heat in Solids," Oxford University Press, 1992.

11. Pindera, M-J. and Aboudi, J., and Arnold, S. M. (1998), "Thermomechanical Analysis of Functionally Graded Thermal Barrier Coatings with Different Microstructural Scales," *J. American Ceramics Society*, Vol. 81(6), pp. 1525-1536.

12. Pindera, M-J., Aboudi, J., and Arnold, S. M. (2000), "Interface Roughness and Oxide Layer Thickness Effects on the Response of TBCs to Cyclic Thermal Loading," *Materials Science & Engineering A* (in press).

7.0 APPENDICES

7.1 Appendix 1

The input data file *fgmc3dq.cylindrical.data* is organized into four distinct blocks, as explained in section 3.1. The structure of the input data file, the variable names and their description read by the program are given below.

Block 1: Material properties for NMT materials at NTEMP identical temperatures

NMAT	number of materials
TREF	reference temperature
	begin sequential specification of different materials --> repeat NMAT times
MNAME	material name
RHO	density
ID	axis of symmetry indicator for transversely isotropic materials: ID=1 -> radial axis, ID=2 -> circumferential axis, ID=3 -> axial axis
NTEMP	number of temperatures at which CTE and creep properties are specified
CONDA,CONDT	axial and transverse thermal conductivities
EA,ET,GA	axial and transverse Young's moduli, and axial shear modulus
FNA,FNT	axial and transverse Poisson's ratios
	begin sequential CTE and creep material property input at a given temperature --> repeat NTEMP times
IT1, TEMP	temperature number (1, 2, . . . , NTEMP), temperature at which CTE and creep properties are specified
ALPHAATEMP,ALPHATTEMP	axial and transverse thermal expansion coefficients at TEMP
CREEPCOEFTEMP,POWERTEMP, HCREEPTEMP	creep parameters at TEMP
	end of CTE and creep property input at a given temperature
	end of material property input for NMAT materials at NTEMP temperatures

Note: the creep parameters are specified for the power-law model of the form given by eqns (18) and (19)

Block 2: Specification of the cylinder geometry and architecture

R0	inner radius (R0=0 -> flat plate option)
NALPHA,NBETA	number of subcells in the radial and circumferential directions (must be even)
	begin subcell dimensions specifications
IALPHA,XD	radial subcell number, radial subcell dimensions --> *repeat NALPHA times*
	if R0 is not zero
THETA	cirumferential subcell angle --> *repeat NBETA times*
	if R0=0
H1,H2	subcell dimensions in the θ direction -->*repeat NBETA/2 times*
	end of subcell dimensions specifications for NALPHA and NBETA subcells
L1,L2	subcell dimensions l_1 and l_2 in the out-of-plane direction
	begin subcell material assignment in each of the 2 r-θ *planes --> repeat 2 times*
	for each plane, start from the lower left corner with r *(ALPHA) directed up, and* θ *(BETA) directed to the right*
KGAMA	counter for the two planes (1 and then 2)
	material assignment for the IALPHAREAD subcell --> repeat NALPHA times
IALPHAREAD,MATNUM	counter, NALPHA × NBETA × 2 matrix containing material specification for each subcell --> *repeat NBETA times*
	end of subcell material assignment for NALPHA × NBETA × 2 subcells

Block 3: Specification of the loading and inelastic strain integration parameters, and write options

NINT	number of time steps for the integration of the global system of equations for the unknown thermal and mechanical microvariables
DTIME	time increment for the integration of the global system of equations
NSTEP	number of load increments between which output data is written to the *fgmc3dq.cylindrical.out* file
NPLOT1,....,NPLOT6	specification of the six times during the loading history at which output results are written to the *fgmc3dq.cylindrical.out* and *fgmc3dq.cylindrical.plot* files
KGAMPPLOT	r-θ plane indicator, indicates in which plane (1 or 2) output data for plotting purposes is to be generated
NBPLOT,JBETAPLOT	number of cross sections along the radial direction in which data is to be generated for plotting purposes, β subcell through which data is to be generated --> *repeat JBETAPLOT NBPLOT times*
ISIGNX2B	specifies the location within the particular β subcell through which data is to be generated when NBPLOT is not 0 (1 --> left face; 0 --> center: 2 --> right face) --> *repeat NBPLOT times*

NAPLOT,IALPHAPLOT	number of cross sections along the circumferential direction in which data is to be generated for plotting purposes, α subcell through which data is to be generated --> *repeat NAPLOT times*
ISIGNX1B	specifies the location within the particular α subcell through which data is to be generated when NAPLOT is not 0 (1 --> lower face; 0 --> center: 2 --> upper face) --> *repeat NAPLOT times*
IGPS	plane strain (0) or generalized plane strain (1) condition imposed in the out-of-plane direction
NLEG	order of Legendre polynomials for approximating the inelastic subcell strains in the three directions
J1	number of integration points for evaluating the inelastic subcell strains in the three directions

Block 4: Specification of thermal and meachanical boundary conditions in the r–θ *plane*

	specification of thermal boundary conditions at the inner and outer radii --> repeat NBETA times
LOADF1	thermal load indicator for the boundary β subcells at the inner radius (1 -> heat flux specified; 2 -> temperature specified)
AMPF1	heat flux/temperature amplitude for the boundary β subcells at the inner radius
LOADR1	thermal load indicator for the boundary β subcells at the outer radius (1 -> heat flux specified; 2 -> temperature specified)
AMPR1	heat flux/temperature amplitude for the boundary β subcells at the outer radius
	specification of thermal boundary conditions at the left and right faces --> repeat NALPHA times
LOADF2	thermal load indicator for the boundary α subcells at the left face (1 -> heat flux specified; 2 -> temperature specified)
AMPF2	heat flux/temperature amplitude for the boundary α subcells at the left face
LOADR2	thermal load indicator for the boundary α subcells at the right face (1 -> heat flux specified; 2 -> temperature specified)
AMPR2	heat flux/temperature amplitude for the boundary α subcells at the right face
	specification of mechanical boundary conditions at the inner and outer radii --> repeat NBETA times
LOADF1	mechanical load indicator for the boundary β subcells at the inner radius (1 -> σ_{rr} specified; 2 -> u_r specified; 3 -> $\partial u_r / \partial r$)
AMPF1	mechanical load amplitude for the boundary β subcells at the inner radius
LOADF1	mechanical load indicator for the boundary β subcells at the inner radius (1 -> $\sigma_{r\theta}$ specified; 2 -> u_θ specified; 3 -> $\partial u_\theta / \partial r$)

AMPF1	mechanical load amplitude for the boundary β subcells at the inner radius
LOADR1	mechanical load indicator for the boundary β subcells at the outer radius (1 -> σ_{rr} specified; 2 -> u_r specified; 3 -> $\partial u_r / \partial r$)
AMPR1	mechanical load amplitude for the boundary β subcells at the outer radius
LOADR1	mechanical load indicator for the boundary β subcells at the outer radius (1 -> $\sigma_{r\theta}$ specified; 2 -> u_θ specified; 3 -> $\partial u_\theta / \partial r$)
AMPR1	mechanical load amplitude for the boundary β subcells at the outer radius
	specification of mechanical boundary conditions at the left and right faces --> repeat NALPHA times
LOADF2	mechanical load indicator for the boundary β subcells at the left face (1 -> $\sigma_{\theta r}$ specified; 2 -> u_r specified; 3 -> $\partial u_r / \partial \theta$)
AMPF2	mechanical load amplitude for the boundary β subcells at the left face
LOADF2	mechanical load indicator for the boundary β subcells at the left face (1 -> $\sigma_{\theta\theta}$ specified; 2 -> u_θ specified; 3 -> $\partial u_\theta / \partial \theta$)
AMPF2	mechanical load amplitude for the boundary β subcells at the left face
LOADR2	mechanical load indicator for the boundary β subcells at the right face (1 -> $\sigma_{\theta r}$ specified; 2 -> u_r specified; 3 -> $\partial u_r / \partial \theta$)
AMPR2	mechanical load amplitude for the boundary β subcells at the right face
LOADR2	mechanical load indicator for the boundary β subcells at the right face (1 -> $\sigma_{\theta\theta}$ specified; 2 -> u_θ specified; 3 -> $\partial u_\theta / \partial \theta$)
AMPR2	mechanical load amplitude for the boundary β subcells at the right face

7.2 Appendix 2

The input file *fgmc3dq.cylindrical.data* for the steady-state cyclic thermal loading case described in section 4.2.1 is given below. The highlighted text, not to be included in the input deck, identifies the four blocks of the input data.

Block 1

```
3                                                    NMAT
300                                                  TREF
'MATERIAL 1'                                         MNAME
1                                                    RHO
1                                                    ID
1                                                    NTEMP
 0.50E+00     0.50E+00                               CONDA,CONDT
36.00E+09    36.00E+09    15.00E+09                  EA,ET,GA
 0.20E+00     0.20E+00                               FNA,FNT
 1            0                                      IT,TEMP
 8.00E-06     8.00E-06                               ALPHAATEMP,ALPHATTEMP
 1.89E-06     1.59       277.00E+03                  CREEPCOEFTEMP,POWERTEMP,HCREEPTEMP

'MATERIAL 2'
1
1
1
  2.42E+00     2.42E+00
197.00E+09   197.00E+09    78.80E+09
  0.25E+00     0.25E+00
1              0
11.00E-06    11.00E-06
 0.00E+00     1.00E+00     1.00E+00

'MATERIAL 3'
1
1
1
 60.50E+00    60.50E+00
207.00E+09   207.00E+09    79.60E+09
  0.30E+00     0.30E+00
1              0
 15.00E-06    15.00E-06
  0.00E+00     1.00E+00     1.00E+00
```

Block 2

```
50.00E+00                                            R0
42     10                                            NALPHA,NBETA

42    0.25E-0                                        NALPHA,XD(NALPHA)
41    0.25E-0                                        .
40    0.25E-0                                        .
39    0.25E-0                                        .
38    0.0263157E-0                                   .
37    0.0263157E-0                                   .
36    0.0263157E-0                                   .
35    0.0263157E-0                                   .
34    0.0263157E-0                                   .
33    0.0263157E-0                                   .
32    0.0263157E-0                                   .
31    0.0263157E-0                                   .
30    0.0263157E-0                                   .
```

```
29    0.0263157E-0                                .
28    0.0263157E-0                                .
27    0.0263157E-0                                .
26    0.0263157E-0                                .
25    0.0263157E-0                                .
24    0.0263157E-0                                .
23    0.0263157E-0                                .
22    0.0263157E-0                                .
21    0.0263157E-0                                .
20    0.0263157E-0                                .
19    0.0263157E-0                                .
18    0.0263157E-0                                .
17    0.0263157E-0                                .
16    0.0263157E-0                                .
15    0.0263157E-0                                .
14    0.0263157E-0                                .
13    0.0263157E-0                                .
12    0.0263157E-0                                .
11    0.0263157E-0                                .
10    0.0263157E-0                                .
 9    0.0263157E-0                                .
 8    0.0263157E-0                                .
 7    0.0263157E-0                                .
 6    0.0263157E-0                                .
 5    0.0263157E-0                                .
 4    0.0263157E-0                                .
 3    0.0263157E-0                                .
 2    0.0263157E-0                                .
 1    0.0263157E-0                                .

      0.02865 0.02865                             THETA(1),THETA(2)
      0.02865 0.02865                             .
      0.02865 0.02865                             .
      0.02865 0.02865                             .
      0.02865 0.02865                             THETA(NBETA-1),THETA(NBETA)

                                                  (or H1(1),H2(1) ... for flat plate)

      0.0263157E-0  0.0263157E-0                  L1,L2

 1                                                KGAMA
42    3  3  3  3  3  3  3  3  3  3                NALPHA,MATNUM(42,1,1) .... MATNUM(42,10,1
41    3  3  3  3  3  3  3  3  3  3
40    3  3  3  3  3  3  3  3  3  3
39    3  3  3  3  3  3  3  3  3  3
38    2  2  2  2  2  2  2  2  2  2
37    2  2  2  2  2  2  2  2  2  2
36    2  2  2  2  2  2  2  2  2  2
35    2  2  2  2  2  2  2  2  2  2
34    2  2  1  2  2  2  2  1  2  2
33    2  2  2  2  2  2  2  2  2  2
32    2  2  2  2  1  2  2  2  2  2
31    1  2  2  2  2  2  2  2  1  2
30    2  2  1  2  2  2  2  2  2  2
29    2  2  2  2  2  1  2  2  2  2
28    2  2  2  1  2  2  2  1  2  2
27    2  1  2  2  2  1  2  2  2  1
26    2  2  2  1  2  2  2  1  2  2
25    1  2  2  2  2  1  2  2  2  1
24    2  2  1  2  1  2  1  2  1  2
23    2  1  2  2  2  1  2  2  2  1
22    1  2  1  2  1  2  1  2  1  2
21    2  1  2  1  2  1  2  1  2  1
20    1  2  1  2  1  2  1  2  1  2
```

19	2	1	2	1	2	1	2	1	2	1
18	1	2	1	2	1	2	1	2	1	2
17	2	1	1	1	2	1	1	1	2	1
16	1	2	1	2	1	2	1	2	1	2
15	1	1	1	1	1	1	1	1	1	1
14	2	1	2	1	2	1	2	1	2	1
13	1	1	1	1	1	1	1	1	1	1
12	1	2	1	1	1	2	1	1	1	2
11	1	1	1	2	1	1	1	2	1	1
10	1	1	1	1	1	2	1	1	1	1
9	1	1	2	1	1	1	1	1	1	1
8	2	1	1	1	1	1	1	1	2	1
7	1	1	1	1	2	1	1	1	1	1
6	1	1	1	1	1	1	1	1	1	1
5	1	1	2	1	1	1	1	2	1	1
4	1	1	1	1	1	1	1	1	1	1
3	1	1	1	1	1	1	1	1	1	1
2	1	1	1	1	1	1	1	1	1	1
1	1	1	1	1	1	1	1	1	1	1

2

KGAMA

42	3	3	3	3	3	3	3	3	3	3
41	3	3	3	3	3	3	3	3	3	3
40	3	3	3	3	3	3	3	3	3	3
39	3	3	3	3	3	3	3	3	3	3
38	2	2	2	2	2	2	2	2	2	2
37	2	2	2	2	2	2	2	2	2	2
36	2	2	2	2	2	2	2	2	2	2
35	2	2	2	2	2	2	2	2	2	2
34	2	2	2	2	2	2	2	2	2	2
33	2	2	2	2	2	2	2	2	2	2
32	2	2	2	2	2	2	2	2	2	2
31	2	2	2	2	2	2	2	2	2	2
30	2	2	2	2	2	2	2	2	2	2
29	2	2	2	2	2	2	2	2	2	2
28	2	2	2	2	2	2	2	2	2	2
27	2	2	2	2	2	2	2	2	2	2
26	2	2	2	2	2	2	2	2	2	2
25	2	2	2	2	2	2	2	2	2	2
24	2	2	2	2	2	2	2	2	2	2
23	2	2	2	2	2	2	2	2	2	2
22	2	2	2	2	2	2	2	2	2	2
21	1	2	1	2	1	2	1	2	1	2
20	2	1	2	1	2	1	2	1	2	1
19	1	2	1	2	1	2	1	2	1	2
18	2	1	2	1	2	1	2	1	2	1
17	1	1	1	1	1	1	1	1	1	1
16	1	1	1	1	1	1	1	1	1	1
15	1	1	1	1	1	1	1	1	1	1
14	1	1	1	1	1	1	1	1	1	1
13	1	1	1	1	1	1	1	1	1	1
12	1	1	1	1	1	1	1	1	1	1
11	1	1	1	1	1	1	1	1	1	1
10	1	1	1	1	1	1	1	1	1	1
9	1	1	1	1	1	1	1	1	1	1
8	1	1	1	1	1	1	1	1	1	1
7	1	1	1	1	1	1	1	1	1	1
6	1	1	1	1	1	1	1	1	1	1
5	1	1	1	1	1	1	1	1	1	1
4	1	1	1	1	1	1	1	1	1	1
3	1	1	1	1	1	1	1	1	1	1
2	1	1	1	1	1	1	1	1	1	1
1	1	1	1	1	1	1	1	1	1	1

Block 3

```
 320                                                    NINT
   1.0                                                  DTIME
1000                                                    NSTEP
10  310  320  330  630  640                            NPLOT1 ... NPLOT6
1                                                       KGAMAPLOT
5   1  3  5  8 10                                       NBPLOT,JBETAPLOT(1) ... JBETAPLOT(5)
   -1  0  1  0  1                                       ISIGNX2B(1) ... ISIGNX2B(5)
0                                                       NAPLOT,IALPHAPLOT(1) ...
                                                        ISIGNX1B(1) ... ISIGNX1B(5)
10  310  320  330  630  640                            NPLOT1 ... NPLOT6

   0                                                    IGPS
   2                                                    NLEG
   5                                                    J1
```

Block 4

```
   2    2    2    2    2                               Thermal boundary conditions
   2    2    2    2    2                               LOADF1(1) ...
1200 1200 1200 1200 1200                               ... LOADF1(NBETA)
1200 1200 1200 1200 1200                               AMPF1(1) ...
                                                       ... AMPF1(NBETA)
   2    2    2    2    2
   2    2    2    2    2                               LOADR1(1) ...
   0    0    0    0    0                               ... LOADR1(NBETA)
   0    0    0    0    0                               AMPR1(1) ...
                                                       ... AMPR1(NBETA)
   1    1    1    1    1
   1    1    1    1    1                               LOADF2(1) ...
   1    1    1    1    1                               .
   1    1    1    1    1                               .
   1    1    1    1    1                               .
   1    1    1    1    1                               .
   1    1    1    1    1                               .
   1    1    1    1    1                               .
   1    1                                              ... LOADF2(NALPHA)
   0    0    0    0    0                               AMPF2(1) ...
   0    0    0    0    0                               .
   0    0    0    0    0                               .
   0    0    0    0    0                               .
   0    0    0    0    0                               .
   0    0    0    0    0                               .
   0    0    0    0    0                               .
   0    0                                              ... AMPF2(NALPHA)

   1    1    1    1    1                               LOADR2(1) ...
   1    1    1    1    1                               .
   1    1    1    1    1                               .
   1    1    1    1    1                               .
   1    1    1    1    1                               .
   1    1    1    1    1                               .
   1    1    1    1    1                               .
   1    1                                              ... LOADR2(NALPHA)
   0    0    0    0    0                               AMPR2(1)
   0    0    0    0    0                               .
   0    0    0    0    0                               .
   0    0    0    0    0                               .
   0    0    0    0    0                               .
```

```
0     0     0     0     0
0     0     0     0     0
0     0     0     0     0
0     0
```

```
.
.
.
... AMPR2(NALPHA)
```

```
Mechanical boundary conditions
```

```
1     1     1     1     1
1     1     1     1     1
0     0     0     0     0
0     0     0     0     0
```

```
LOADF1(1) ...
... LOADF1(NBETA)
AMPF1(1) ...
... AMPF1(NBETA)
```

```
1     1     1     1     1
1     1     1     1     1
0     0     0     0     0
0     0     0     0     0
```

```
LOADF1(1) ...
... LOADF1(NBETA)
AMPF1(1) ...
... AMPF1(NBETA)
```

```
1     1     1     1     1
1     1     1     1     1
0     0     0     0     0
0     0     0     0     0
```

```
LOADR1(1) ...
... LOADR1(NBETA)
AMPR1(1) ...
... AMPR1(NBETA)
```

```
1     1     1     1     1
1     1     1     1     1
0     0     0     0     0
0     0     0     0     0
```

```
LOADR1(1) ...
... LOADR1(NBETA)
AMPR1(1) ...
... AMPR1(NBETA)
```

```
1     1     1     1     1
1     1     1     1     1
1     1     1     1     1
1     1     1     1     1
1     1     1     1     1
1     1     1     1     1
1     1     1     1     1
1     1
0     0     0     0     0
0     0     0     0     0
0     0     0     0     0
0     0     0     0     0
0     0     0     0     0
0     0     0     0     0
0     0     0     0     0
0     0
```

```
LOADF2(1) ...
.
.
.
.
.
.
.
.
... LOADF2(NALPHA)
AMPF2(1) ...
.
.
.
.
.
.
.
.
... AMPF2(NALPHA)
```

```
2     2     2     2     2
2     2     2     2     2
2     2     2     2     2
2     2     2     2     2
2     2     2     2     2
2     2     2     2     2
2     2     2     2     2
2     2     2     2     2
2     2
0     0     0     0     0
0     0     0     0     0
0     0     0     0     0
0     0     0     0     0
0     0     0     0     0
0     0     0     0     0
0     0     0     0     0
0     0
```

```
LOADF2(1) ...
.
.
.
.
.
.
.
.
... LOADF2(NALPHA)
AMPF2(1) ...
.
.
.
.
.
.
.
.
... AMPF2(NALPHA)
```

```
1     1     1     1     1          LOADR2(1) ...
1     1     1     1     1          .
1     1     1     1     1          .
1     1     1     1     1          .
1     1     1     1     1          .
1     1     1     1     1          .
1     1     1     1     1          .
1     1     1     1     1          .
1     1                            ... LOADR2(NALPHA)
0     0     0     0     0          AMPR2(1) ...
0     0     0     0     0          .
0     0     0     0     0          .
0     0     0     0     0          .
0     0     0     0     0          .
0     0     0     0     0          .
0     0     0     0     0          .
0     0     0     0     0          .
0     0                            ... AMPR2(NALPHA)

2     2     2     2     2          LOADR2(1) ...
2     2     2     2     2          .
2     2     2     2     2          .
2     2     2     2     2          .
2     2     2     2     2          .
2     2     2     2     2          .
2     2     2     2     2          .
2     2                            ... LOADR(NALPHA)
0     0     0     0     0          AMPR2(1) ...
0     0     0     0     0          .
0     0     0     0     0          .
0     0     0     0     0          .
0     0     0     0     0          .
0     0     0     0     0          .
0     0     0     0     0          .
0     0                            ... AMPR2(NALPHA)
```

7.3 Appendix 3

The output file *fgmc3dq.cylindrical.out* generated by the input file *fgmc3dq.cylindrical.data* of Appendix 2 is given below.

```
**************************************************
**          FUNCTIONALLY GRADED COMPOSITES      **
**             (CYLINDRICAL COORDINATES)        **
**           IN RADIAL & ANGULAR DIRECTIONS     **
**                                              **
**        ( PERIODIC IN THE AXIAL DIRECTION )   **
**                                              **
**         DETERMINATION OF THE BEHAVIOR OF     **
**                                              **
**         FG COMPOSITES IN TWO DIRECTIONS      **
**              (WITH CREEPING PHASES)          **
**                                              **
**                  PROGRAMMED BY               **
**                  JACOB ABOUDI                **
**               MAY 1997, JULY 1999            **
**************************************************


************* INPUT DATA ECHO **************

                MATERIAL SPECIFICATION


NUMBER OF MATERIALS (NMAT) =  3

Tref =  0.300E+03


                   MATERIAL 1

DENSITY =    0.100E+01

AXIS OF SYMMETRY OF THE TRANSVERSELY ISOTROPIC MATERIAL IS : 1

 THERMAL CONDUCTIVITIES

KA    =  0.500E+00     KT    =  0.500E+00

 ELASTIC CONSTANTS

EA    =  0.360E+11     ET    =  0.360E+11     GA =  0.150E+11
NUA   =  0.200E+00     NUT   =  0.200E+00


NO. OF TEMPS AT WHICH THE CTE ARE & CREEP ARE GIVEN =  1

TEMP # =1        TEMP = 0.00E+00

CTE(AXIAL) =    0.80E-05    CTE(TRANSVERSE) =    0.80E-05

CREEP-COEFFICIENT = 0.189E-05     CREEP-POWER = 0.159E+01     ACTIVATION ENERGY = 0.277E+06
```

MATERIAL 2

DENSITY = 0.100E+01

AXIS OF SYMMETRY OF THE TRANSVERSELY ISOTROPIC MATERIAL IS : 1

THERMAL CONDUCTIVITIES

KA = 0.242E+01 KT = 0.242E+01

ELASTIC CONSTANTS

EA = 0.197E+12 ET = 0.197E+12 GA = 0.788E+11
NUA = 0.250E+00 NUT = 0.250E+00

NO. OF TEMPS AT WHICH THE CTE ARE & CREEP ARE GIVEN = 1

TEMP # =1 TEMP = 0.00E+00

CTE(AXIAL) = 0.11E-04 CTE(TRANSVERSE) = 0.11E-04

CREEP-COEFFICIENT = 0.000E+00 CREEP-POWER = 0.100E+01 ACTIVATION ENERGY = 0.100E+01

MATERIAL 3

DENSITY = 0.100E+01

AXIS OF SYMMETRY OF THE TRANSVERSELY ISOTROPIC MATERIAL IS : 1

THERMAL CONDUCTIVITIES

KA = 0.605E+02 KT = 0.605E+02

ELASTIC CONSTANTS

EA = 0.207E+12 ET = 0.207E+12 GA = 0.796E+11
NUA = 0.300E+00 NUT = 0.300E+00

NO. OF TEMPS AT WHICH THE CTE ARE & CREEP ARE GIVEN = 1

TEMP # =1 TEMP = 0.00E+00

CTE(AXIAL) = 0.15E-04 CTE(TRANSVERSE) = 0.15E-04

CREEP-COEFFICIENT = 0.000E+00 CREEP-POWER = 0.100E+01 ACTIVATION ENERGY = 0.100E+01

GEOMETRY SPECIFICATION

INNER RADIUS = R0 = 0.500E-01

NUMBER OF SUBCELLS IN THE X-1 DIRECTION = 42
NUMBER OF SUBCELLS IN THE X-2 DIRECTION = 10

NUMBER OF CELLS IN THE X-1 DIRECTION = 21
NUMBER OF CELLS IN THE X-2 DIRECTION = 5

XD(42) = 0.250E-03
XD(41) = 0.250E-03
XD(40) = 0.250E-03
XD(39) = 0.250E-03
XD(38) = 0.263E-04
XD(37) = 0.263E-04
XD(36) = 0.263E-04

```
XD( 35 ) =    0.263E-04
XD( 34 ) =    0.263E-04
XD( 33 ) =    0.263E-04
XD( 32 ) =    0.263E-04
XD( 31 ) =    0.263E-04
XD( 30 ) =    0.263E-04
XD( 29 ) =    0.263E-04
XD( 28 ) =    0.263E-04
XD( 27 ) =    0.263E-04
XD( 26 ) =    0.263E-04
XD( 25 ) =    0.263E-04
XD( 24 ) =    0.263E-04
XD( 23 ) =    0.263E-04
XD( 22 ) =    0.263E-04
XD( 21 ) =    0.263E-04
XD( 20 ) =    0.263E-04
XD( 19 ) =    0.263E-04
XD( 18 ) =    0.263E-04
XD( 17 ) =    0.263E-04
XD( 16 ) =    0.263E-04
XD( 15 ) =    0.263E-04
XD( 14 ) =    0.263E-04
XD( 13 ) =    0.263E-04
XD( 12 ) =    0.263E-04
XD( 11 ) =    0.263E-04
XD( 10 ) =    0.263E-04
XD(  9 ) =    0.263E-04
XD(  8 ) =    0.263E-04
XD(  7 ) =    0.263E-04
XD(  6 ) =    0.263E-04
XD(  5 ) =    0.263E-04
XD(  4 ) =    0.263E-04
XD(  3 ) =    0.263E-04
XD(  2 ) =    0.263E-04
XD(  1 ) =    0.263E-04

THETA(BETA)[deg] =   0.286E-01  0.286E-01  0.286E-01  0.286E-01  0.286E-01
                     0.286E-01  0.286E-01  0.286E-01  0.286E-01  0.286E-01

L1 =    0.263E-04     L2 =    0.263E-04


 TOTAL THICKNESS IN THE X-1 DIRECTION =  0.200E-02
 TOTAL ANGULAR SPAN [DEG]             =  0.287E+00
 TOTAL THICKNESS IN THE X-3 DIRECTION =  0.526E-04
 R0 / RADIAL THICKNESS =   0.250E+02
 TOTAL VOLUME =  0.268E-10


   SUBCELL MATERIAL ASSIGNMENT

            GAMMA = 1

   ALPHA =  42          3 3 3 3 3 3 3 3 3 3
   ALPHA =  41          3 3 3 3 3 3 3 3 3 3
   ALPHA =  40          3 3 3 3 3 3 3 3 3 3
   ALPHA =  39          3 3 3 3 3 3 3 3 3 3
   ALPHA =  38          2 2 2 2 2 2 2 2 2 2
   ALPHA =  37          2 2 2 2 2 2 2 2 2 2
   ALPHA =  36          2 2 2 2 2 2 2 2 2 2
   ALPHA =  35          2 2 2 2 2 2 2 2 2 2
   ALPHA =  34          2 2 1 2 2 2 2 1 2 2
   ALPHA =  33          2 2 2 2 2 2 2 2 2 2
   ALPHA =  32          2 2 2 2 1 2 2 2 2 2
   ALPHA =  31          1 2 2 2 2 2 2 2 1 2
   ALPHA =  30          2 2 1 2 2 2 2 2 2 2
   ALPHA =  29          2 2 2 2 2 1 2 2 2 2
   ALPHA =  28          2 2 2 1 2 2 2 1 2 2
   ALPHA =  27          2 1 2 2 2 1 2 2 2 1
   ALPHA =  26          2 2 2 1 2 2 2 1 2 2
   ALPHA =  25          1 2 2 2 2 1 2 2 2 1
```

ALPHA =	24	2 2 1 2 1 2 1 2 1 2
ALPHA =	23	2 1 2 2 2 1 2 2 2 1
ALPHA =	22	1 2 1 2 1 2 1 2 1 2
ALPHA =	21	2 1 2 1 2 1 2 1 2 1
ALPHA =	20	1 2 1 2 1 2 1 2 1 2
ALPHA =	19	2 1 2 1 2 1 2 1 2 1
ALPHA =	18	1 2 1 2 1 2 1 2 1 2
ALPHA =	17	2 1 1 1 2 1 1 1 2 1
ALPHA =	16	1 2 1 2 1 2 1 2 1 2
ALPHA =	15	1 1 1 1 1 1 1 1 1 1
ALPHA =	14	2 1 2 1 2 1 2 1 2 1
ALPHA =	13	1 1 1 1 1 1 1 1 1 1
ALPHA =	12	1 2 1 1 1 2 1 1 1 2
ALPHA =	11	1 1 1 2 1 1 1 2 1 1
ALPHA =	10	1 1 1 1 1 2 1 1 1 1
ALPHA =	9	1 1 2 1 1 1 1 1 1 1
ALPHA =	8	2 1 1 1 1 1 1 1 2 1
ALPHA =	7	1 1 1 1 2 1 1 1 1 1
ALPHA =	6	1 1 1 1 1 1 1 1 1 1
ALPHA =	5	1 1 2 1 1 1 1 2 1 1
ALPHA =	4	1 1 1 1 1 1 1 1 1 1
ALPHA =	3	1 1 1 1 1 1 1 1 1 1
ALPHA =	2	1 1 1 1 1 1 1 1 1 1
ALPHA =	1	1 1 1 1 1 1 1 1 1 1

GAMMA = 2

ALPHA =	42	3 3 3 3 3 3 3 3 3 3
ALPHA =	41	3 3 3 3 3 3 3 3 3 3
ALPHA =	40	3 3 3 3 3 3 3 3 3 3
ALPHA =	39	3 3 3 3 3 3 3 3 3 3
ALPHA =	38	2 2 2 2 2 2 2 2 2 2
ALPHA =	37	2 2 2 2 2 2 2 2 2 2
ALPHA =	36	2 2 2 2 2 2 2 2 2 2
ALPHA =	35	2 2 2 2 2 2 2 2 2 2
ALPHA =	34	2 2 2 2 2 2 2 2 2 2
ALPHA =	33	2 2 2 2 2 2 2 2 2 2
ALPHA =	32	2 2 2 2 2 2 2 2 2 2
ALPHA =	31	2 2 2 2 2 2 2 2 2 2
ALPHA =	30	2 2 2 2 2 2 2 2 2 2
ALPHA =	29	2 2 2 2 2 2 2 2 2 2
ALPHA =	28	2 2 2 2 2 2 2 2 2 2
ALPHA =	27	2 2 2 2 2 2 2 2 2 2
ALPHA =	26	2 2 2 2 2 2 2 2 2 2
ALPHA =	25	2 2 2 2 2 2 2 2 2 2
ALPHA =	24	2 2 2 2 2 2 2 2 2 2
ALPHA =	23	2 2 2 2 2 2 2 2 2 2
ALPHA =	22	2 2 2 2 2 2 2 2 2 2
ALPHA =	21	1 2 1 2 1 2 1 2 1 2
ALPHA =	20	2 1 2 1 2 1 2 1 2 1
ALPHA =	19	1 2 1 2 1 2 1 2 1 2
ALPHA =	18	2 1 2 1 2 1 2 1 2 1
ALPHA =	17	1 1 1 1 1 1 1 1 1 1
ALPHA =	16	1 1 1 1 1 1 1 1 1 1
ALPHA =	15	1 1 1 1 1 1 1 1 1 1
ALPHA =	14	1 1 1 1 1 1 1 1 1 1
ALPHA =	13	1 1 1 1 1 1 1 1 1 1
ALPHA =	12	1 1 1 1 1 1 1 1 1 1
ALPHA =	11	1 1 1 1 1 1 1 1 1 1
ALPHA =	10	1 1 1 1 1 1 1 1 1 1
ALPHA =	9	1 1 1 1 1 1 1 1 1 1
ALPHA =	8	1 1 1 1 1 1 1 1 1 1
ALPHA =	7	1 1 1 1 1 1 1 1 1 1
ALPHA =	6	1 1 1 1 1 1 1 1 1 1
ALPHA =	5	1 1 1 1 1 1 1 1 1 1
ALPHA =	4	1 1 1 1 1 1 1 1 1 1
ALPHA =	3	1 1 1 1 1 1 1 1 1 1
ALPHA =	2	1 1 1 1 1 1 1 1 1 1
ALPHA =	1	1 1 1 1 1 1 1 1 1 1

```
            PLOT IN SUBCELLS GAMMA =    1

 NO. OF PLOTTING FIELD DISTRIBUTIONS ALONG THE X1-DIRECTION IS :    5
     PLOTTING IN THE X1-DIRECTION STARTING FROM  X1=0   IN THE
     FOLLOWING SUBCELLS : BETA =     1     3     5     8    10
     IN THE FOLLOWING LOCATIONS:    -1     0     1     0     1

 NO. OF PLOTTING FIELD DISTRIBUTIONS ALONG THE X2-DIRECTION IS :    0
     PLOTTING IN THE X2-DIRECTION STARTING FROM  X2=0   IN THE
     FOLLOWING SUBCELLS :ALPHA =

   RESULTS ARE PLOTTED AT THE FOLLOWING 6 INCREMENTS :
         10      310      320      330      630      640

 NO. OF INTEGRATION INCREMENTS         =     320
 DTIME =    0.100E+01
 NO. OF PRINTING STEPS OF THE FIELD =      1000
 PLANE STRAIN CONDITIONS
 ORDER OF LEGENDRE POLYNOME =  2
 NUMBER OF INTEGRATION POINTS =  5


   ***************** OUTPUT ********************

        MATERIAL # = 1       VOLUME RATIO =  0.249E+00
        MATERIAL # = 2       VOLUME RATIO =  0.246E+00
        MATERIAL # = 3       VOLUME RATIO =  0.505E+00

        THE THERMAL LOADING CONDITIONS ( NSTAGE = 0 ) :


LOADF1= 2 2 2 2 2 2 2 2 2 2

AMPF1 =  0.120E+04  0.120E+04  0.120E+04  0.120E+04  0.120E+04
         0.120E+04  0.120E+04  0.120E+04  0.120E+04  0.120E+04

LOADR1= 2 2 2 2 2 2 2 2 2 2

AMPR1 =  0.000E+00  0.000E+00  0.000E+00  0.000E+00  0.000E+00
         0.000E+00  0.000E+00  0.000E+00  0.000E+00  0.000E+00


LOADF2= 1 1 1 1 1 1 1 1 1 1
        1 1 1 1 1 1 1 1 1 1
        1 1 1 1 1 1 1 1 1 1
        1 1 1 1 1 1 1 1 1 1
        1 1
AMPF2 =  0.000E+00  0.000E+00  0.000E+00  0.000E+00  0.000E+00
         0.000E+00  0.000E+00  0.000E+00  0.000E+00  0.000E+00
         0.000E+00  0.000E+00  0.000E+00  0.000E+00  0.000E+00
         0.000E+00  0.000E+00  0.000E+00  0.000E+00  0.000E+00
         0.000E+00  0.000E+00  0.000E+00  0.000E+00  0.000E+00
         0.000E+00  0.000E+00  0.000E+00  0.000E+00  0.000E+00
         0.000E+00  0.000E+00  0.000E+00  0.000E+00  0.000E+00
         0.000E+00  0.000E+00  0.000E+00  0.000E+00  0.000E+00
         0.000E+00  0.000E+00


LOADR2= 1 1 1 1 1 1 1 1 1 1
        1 1 1 1 1 1 1 1 1 1
        1 1 1 1 1 1 1 1 1 1
        1 1 1 1 1 1 1 1 1 1
        1 1
AMPR2 =  0.000E+00  0.000E+00  0.000E+00  0.000E+00  0.000E+00
         0.000E+00  0.000E+00  0.000E+00  0.000E+00  0.000E+00
         0.000E+00  0.000E+00  0.000E+00  0.000E+00  0.000E+00
         0.000E+00  0.000E+00  0.000E+00  0.000E+00  0.000E+00
         0.000E+00  0.000E+00  0.000E+00  0.000E+00  0.000E+00
         0.000E+00  0.000E+00  0.000E+00  0.000E+00  0.000E+00
         0.000E+00  0.000E+00  0.000E+00  0.000E+00  0.000E+00
```

```
          0.000E+00  0.000E+00  0.000E+00  0.000E+00  0.000E+00
          0.000E+00  0.000E+00

NUMBER OF NON-ZERO ELEMENTS OF [AT] =  29848

            THE THERMAL PROBLEM HAS BEEN SOLVED


         THE MECHANICAL LOADING CONDITIONS (NSTAGE = 1) :


LOADF1(1)= 1 1 1 1 1 1 1 1 1 1

AMPF1     =  0.000E+00  0.000E+00  0.000E+00  0.000E+00  0.000E+00
             0.000E+00  0.000E+00  0.000E+00  0.000E+00  0.000E+00

LOADF1(2)= 1 1 1 1 1 1 1 1 1 1

AMPF1     =  0.000E+00  0.000E+00  0.000E+00  0.000E+00  0.000E+00
             0.000E+00  0.000E+00  0.000E+00  0.000E+00  0.000E+00


LOADR1(1)= 1 1 1 1 1 1 1 1 1 1

AMPR1     =  0.000E+00  0.000E+00  0.000E+00  0.000E+00  0.000E+00
             0.000E+00  0.000E+00  0.000E+00  0.000E+00  0.000E+00

LOADR1(2)= 1 1 1 1 1 1 1 1 1 1

AMPR1     =  0.000E+00  0.000E+00  0.000E+00  0.000E+00  0.000E+00
             0.000E+00  0.000E+00  0.000E+00  0.000E+00  0.000E+00


LOADF2(1)= 1 1 1 1 1 1 1 1 1 1
           1 1 1 1 1 1 1 1 1 1
           1 1 1 1 1 1 1 1 1 1
           1 1 1 1 1 1 1 1 1 1
           1 1
AMPF2     =  0.000E+00  0.000E+00  0.000E+00  0.000E+00  0.000E+00
             0.000E+00  0.000E+00  0.000E+00  0.000E+00  0.000E+00
             0.000E+00  0.000E+00  0.000E+00  0.000E+00  0.000E+00
             0.000E+00  0.000E+00  0.000E+00  0.000E+00  0.000E+00
             0.000E+00  0.000E+00  0.000E+00  0.000E+00  0.000E+00
             0.000E+00  0.000E+00  0.000E+00  0.000E+00  0.000E+00
             0.000E+00  0.000E+00  0.000E+00  0.000E+00  0.000E+00
             0.000E+00  0.000E+00


LOADF2(2)= 2 2 2 2 2 2 2 2 2 2
           2 2 2 2 2 2 2 2 2 2
           2 2 2 2 2 2 2 2 2 2
           2 2 2 2 2 2 2 2 2 2
           2 2
AMPF2     =  0.000E+00  0.000E+00  0.000E+00  0.000E+00  0.000E+00
             0.000E+00  0.000E+00  0.000E+00  0.000E+00  0.000E+00
             0.000E+00  0.000E+00  0.000E+00  0.000E+00  0.000E+00
             0.000E+00  0.000E+00  0.000E+00  0.000E+00  0.000E+00
             0.000E+00  0.000E+00  0.000E+00  0.000E+00  0.000E+00
             0.000E+00  0.000E+00  0.000E+00  0.000E+00  0.000E+00
             0.000E+00  0.000E+00  0.000E+00  0.000E+00  0.000E+00
             0.000E+00  0.000E+00  0.000E+00  0.000E+00  0.000E+00
             0.000E+00  0.000E+00
```

```
LOADR2(1)= 1 1 1 1 1 1 1 1 1 1
           1 1 1 1 1 1 1 1 1 1
           1 1 1 1 1 1 1 1 1 1
           1 1 1 1 1 1 1 1 1 1
           1 1
AMPR2    =  0.000E+00  0.000E+00  0.000E+00  0.000E+00  0.000E+00
            0.000E+00  0.000E+00  0.000E+00  0.000E+00  0.000E+00
            0.000E+00  0.000E+00  0.000E+00  0.000E+00  0.000E+00
            0.000E+00  0.000E+00  0.000E+00  0.000E+00  0.000E+00
            0.000E+00  0.000E+00  0.000E+00  0.000E+00  0.000E+00
            0.000E+00  0.000E+00  0.000E+00  0.000E+00  0.000E+00
            0.000E+00  0.000E+00  0.000E+00  0.000E+00  0.000E+00
            0.000E+00  0.000E+00  0.000E+00  0.000E+00  0.000E+00
            0.000E+00  0.000E+00


LOADR2(2)= 2 2 2 2 2 2 2 2 2 2
           2 2 2 2 2 2 2 2 2 2
           2 2 2 2 2 2 2 2 2 2
           2 2 2 2 2 2 2 2 2 2
           2 2
AMPR2    =  0.000E+00  0.000E+00  0.000E+00  0.000E+00  0.000E+00
            0.000E+00  0.000E+00  0.000E+00  0.000E+00  0.000E+00
            0.000E+00  0.000E+00  0.000E+00  0.000E+00  0.000E+00
            0.000E+00  0.000E+00  0.000E+00  0.000E+00  0.000E+00
            0.000E+00  0.000E+00  0.000E+00  0.000E+00  0.000E+00
            0.000E+00  0.000E+00  0.000E+00  0.000E+00  0.000E+00
            0.000E+00  0.000E+00  0.000E+00  0.000E+00  0.000E+00
            0.000E+00  0.000E+00  0.000E+00  0.000E+00  0.000E+00
            0.000E+00  0.000E+00

NUMBER OF NON-ZERO ELEMENTS OF [A] =  87028


         INCREMENT =     1          TIME =  0.100E+01
              BETA =     1         ISIGN =  -1

X1=  0.132E-04   TEMPR=  0.417E+03   STRAINS=  0.138E-02  0.898E-04 -0.524E-07 -0.102E-09
                              CREEP STRAINS=  0.000E+00  0.000E+00  0.000E+00  0.000E+00
                                    STRESSES=  0.779E+04 -0.388E+08 -0.415E+08 -0.296E+05
X1=  0.395E-04   TEMPR=  0.412E+03   STRAINS=  0.131E-02  0.989E-04 -0.292E-07  0.342E-09
                              CREEP STRAINS=  0.000E+00  0.000E+00  0.000E+00  0.000E+00
                                    STRESSES= -0.132E+06 -0.367E+08 -0.396E+08  0.146E+06
X1=  0.658E-04   TEMPR=  0.406E+03   STRAINS=  0.124E-02  0.868E-04  0.171E-06 -0.590E-09
                              CREEP STRAINS=  0.000E+00  0.000E+00  0.000E+00  0.000E+00
                                    STRESSES= -0.320E+06 -0.348E+08 -0.376E+08 -0.674E+04
X1=  0.921E-04   TEMPR=  0.401E+03   STRAINS=  0.121E-02  0.459E-04  0.999E-06 -0.297E-09
                              CREEP STRAINS=  0.000E+00  0.000E+00  0.000E+00  0.000E+00
                                    STRESSES=  0.343E+06 -0.343E+08 -0.358E+08 -0.788E+06
X1=  0.118E-03   TEMPR=  0.396E+03   STRAINS=  0.117E-02  0.385E-04 -0.341E-06  0.153E-08
                              CREEP STRAINS=  0.000E+00  0.000E+00  0.000E+00  0.000E+00
                                    STRESSES=  0.104E+07 -0.337E+08 -0.341E+08 -0.641E+04
.
.
.

X1=  0.987E-03   TEMPR=  0.302E+03   STRAINS=  0.597E-05  0.997E-04 -0.117E-06  0.737E-10
                              CREEP STRAINS=  0.000E+00  0.000E+00  0.000E+00  0.000E+00
                                    STRESSES= -0.168E+06  0.145E+08 -0.113E+07  0.150E+05
X1=  0.112E-02   TEMPR=  0.301E+03   STRAINS= -0.380E-05  0.987E-04  0.373E-10 -0.447E-09
                              CREEP STRAINS=  0.000E+00  0.000E+00  0.000E+00  0.000E+00
                                    STRESSES= -0.260E+06  0.161E+08  0.344E+06  0.576E+04
X1=  0.137E-02   TEMPR=  0.301E+03   STRAINS= -0.148E-04  0.983E-04 -0.142E-09  0.424E-09
                              CREEP STRAINS=  0.000E+00  0.000E+00  0.000E+00  0.000E+00
                                    STRESSES= -0.213E+06  0.178E+08  0.214E+07 -0.177E+04
X1=  0.162E-02   TEMPR=  0.301E+03   STRAINS= -0.255E-04  0.977E-04 -0.177E-09 -0.418E-09
                              CREEP STRAINS=  0.000E+00  0.000E+00  0.000E+00  0.000E+00
                                    STRESSES= -0.984E+05  0.195E+08  0.396E+07 -0.557E+03
X1=  0.187E-02   TEMPR=  0.300E+03   STRAINS= -0.361E-04  0.972E-04  0.740E-09  0.418E-09
                              CREEP STRAINS=  0.000E+00  0.000E+00  0.000E+00  0.000E+00
                                    STRESSES= -0.497E+04  0.212E+08  0.574E+07  0.120E+04
```

```
      BETA =      3          ISIGN =    0
      .
      .
      .
      BETA =      5          ISIGN =    1
      .
      .
      .
      BETA =      8          ISIGN =    0
      .
      .
      .
      BETA =     10          ISIGN =    1
      .
      .
      .
INCREMENT =     10           TIME =  0.100E+02
      BETA =      1          ISIGN =   -1
      .
      .
      .
      BETA =     10          ISIGN =    1


INCREMENT =    310           TIME =  0.310E+03
      BETA =      1          ISIGN =   -1
      .
      .
      .
      BETA =     10          ISIGN =    1


INCREMENT =    320           TIME =  0.320E+03
      BETA =      1          ISIGN =   -1
      .
      .
      .
      BETA =     10          ISIGN =    1


END OF JOB
```

7.4 Appendix 4

The plotting file *fgmc3dq.cylindrical.plot* generated by the input file *fgmc3dq.cylindrical.data* of Appendix 2 is given below.

```
          INC=    1          BETA =     1          ISIGN =  -1

    X1          TEMPR          U1          U2          SIGMA1          SIGMA2          SIGMA3          SIGMA12          EPQ
0.0000E+00  0.4200E+03  0.4429E-05  0.1075E-06 -0.4733E-01 -0.3981E+08 -0.4252E+08 -0.1690E-02  0.0000E+00
0.6579E-05  0.4186E+03  0.4438E-05  0.5376E-07  0.3994E+04 -0.3931E+08 -0.4203E+08 -0.1482E+05  0.0000E+00
0.1316E-04  0.4173E+03  0.4447E-05  0.1023E-10  0.7787E+04 -0.3881E+08 -0.4153E+08 -0.2964E+05  0.0000E+00
0.1974E-04  0.4159E+03  0.4456E-05 -0.5375E-07  0.1138E+05 -0.3831E+08 -0.4103E+08 -0.4446E+05  0.0000E+00
0.2632E-04  0.4145E+03  0.4465E-05 -0.1075E-06  0.1477E+05 -0.3781E+08 -0.4054E+08 -0.5928E+05  0.0000E+00
0.2632E-04  0.4145E+03  0.4670E-05 -0.1076E-06  0.1453E+05 -0.3770E+08 -0.4052E+08 -0.5929E+05  0.0000E+00
0.3289E-04  0.4131E+03  0.4679E-05 -0.5383E-07 -0.5867E+05 -0.3722E+08 -0.4004E+08  0.4312E+05  0.0000E+00
0.3947E-04  0.4118E+03  0.4687E-05 -0.3424E-10 -0.1323E+06 -0.3674E+08 -0.3956E+08  0.1455E+06  0.0000E+00
0.4605E-04  0.4104E+03  0.4696E-05  0.5381E-07 -0.2065E+06 -0.3626E+08 -0.3909E+08  0.2479E+06  0.0000E+00
0.5263E-04  0.4090E+03  0.4704E-05  0.1077E-06 -0.2810E+06 -0.3578E+08 -0.3861E+08  0.3502E+06  0.0000E+00
 .
 .
 .
 .
 .
0.1000E-02  0.3016E+03  0.5158E-05  0.1077E-06 -0.2538E+06  0.1609E+08  0.4202E+06  0.1180E+05  0.0000E+00
0.1000E-02  0.3016E+03  0.5043E-05  0.1077E-06 -0.2572E+06  0.1516E+08 -0.5681E+06  0.1180E+05  0.0000E+00
0.1062E-02  0.3015E+03  0.5043E-05  0.5390E-07 -0.2573E+06  0.1561E+08 -0.1105E+06  0.8725E+04  0.0000E+00
0.1125E-02  0.3014E+03  0.5043E-05  0.4572E-10 -0.2604E+06  0.1607E+08  0.3439E+06  0.5755E+04  0.0000E+00
0.1187E-02  0.3013E+03  0.5042E-05 -0.5388E-07 -0.2666E+06  0.1652E+08  0.7953E+06  0.2892E+04  0.0000E+00
0.1250E-02  0.3012E+03  0.5042E-05 -0.1079E-06 -0.2760E+06  0.1697E+08  0.1244E+07  0.1348E+03  0.0000E+00
0.1250E-02  0.3012E+03  0.5064E-05 -0.1079E-06 -0.2694E+06  0.1687E+08  0.1218E+07 -0.2484E+03  0.0000E+00
0.1312E-02  0.3011E+03  0.5063E-05 -0.5399E-07 -0.2416E+06  0.1733E+08  0.1679E+07 -0.9611E+03  0.0000E+00
0.1375E-02  0.3010E+03  0.5062E-05 -0.4360E-10 -0.2130E+06  0.1779E+08  0.2141E+07 -0.1774E+04  0.0000E+00
0.1437E-02  0.3009E+03  0.5061E-05  0.5397E-07 -0.1836E+06  0.1825E+08  0.2604E+07 -0.2689E+04  0.0000E+00
0.1500E-02  0.3008E+03  0.5060E-05  0.1080E-06 -0.1534E+06  0.1871E+08  0.3068E+07 -0.3703E+04  0.0000E+00
0.1500E-02  0.3008E+03  0.5038E-05  0.1080E-06 -0.1557E+06  0.1861E+08  0.3038E+07 -0.3411E+04  0.0000E+00
0.1562E-02  0.3007E+03  0.5037E-05  0.5408E-07 -0.1263E+06  0.1907E+08  0.3499E+07 -0.2034E+04  0.0000E+00
0.1625E-02  0.3006E+03  0.5035E-05  0.4311E-10 -0.9841E+05  0.1952E+08  0.3958E+07 -0.5574E+03  0.0000E+00
0.1687E-02  0.3005E+03  0.5034E-05 -0.5405E-07 -0.7206E+05  0.1997E+08  0.4416E+07  0.1018E+04  0.0000E+00
0.1750E-02  0.3004E+03  0.5032E-05 -0.1082E-06 -0.4725E+05  0.2042E+08  0.4872E+07  0.2693E+04  0.0000E+00
0.1750E-02  0.3004E+03  0.5054E-05 -0.1082E-06 -0.2053E+05  0.2039E+08  0.4870E+07  0.2811E+04  0.0000E+00
0.1812E-02  0.3003E+03  0.5052E-05 -0.5416E-07 -0.1143E+05  0.2080E+08  0.5308E+07  0.1956E+04  0.0000E+00
0.1875E-02  0.3002E+03  0.5050E-05 -0.4340E-10 -0.4974E+04  0.2121E+08  0.5744E+07  0.1203E+04  0.0000E+00
0.1937E-02  0.3001E+03  0.5048E-05  0.5414E-07 -0.1165E+04  0.2162E+08  0.6177E+07  0.5514E+03  0.0000E+00
0.2000E-02  0.3000E+03  0.5045E-05  0.1084E-06  0.5467E-01  0.2202E+08  0.6608E+07 -0.5931E-02  0.0000E+00

          INC=    1          BETA =     3          ISIGN =   0
          .
          .
          .
          INC=    1          BETA =     5          ISIGN =   1
          .
          .
          .
          INC=    1          BETA =     8          ISIGN =   0
          .
          .
          .
          INC=    1          BETA =    10          ISIGN =   1
          .
          .
          .


          INC=   10          BETA =     1          ISIGN =  -1
          .
          .
          .
          .
          .
          .
          INC=  320          BETA =     1          ISIGN =  -1
          .
          .
          .
          INC=  320          BETA =    10          ISIGN =   1
```

7.5 Appendix 5

The input data file *fgmc3dq.cylindrical.transient.data* is organized into four distinct blocks, as explained in section 3.1. The structure of the input data file, the variable names and their description read by the program are given below. The structure is similar to that of the input data file for steady-state loading described in Appendix 1, with appropriate modifications that account for an additional material parameter for transient thermal loading (Block 1), four additional parameters that describe location and orientation of damage in the form of a crack (Block 2), an additional parameter for simultaneous integration of the thermal and mechanical governing equations (Block 3), eqns (4) and (16), and twenty-four additional parameters (only twelve are specified) for the boundary conditions applied to the crack faces (Block 4). These additional parameters are highlighted for clarity.

Block 1: Material properties for NMT materials at NTEMP identical temperatures

NMAT	number of materials
TREF	reference temperature
	begin sequential specification of different materials --> repeat NMAT times
MNAME	material name
RHO	density
ID	axis of symmetry indicator for transversely isotropic materials: ID=1 -> radial axis, ID=2 -> circumferential axis, ID=3 -> axial axis
NTEMP	number of temperatures at which CTE and creep properties are specified
CONDA,CONDT,**CVP**	axial and transverse thermal conductivities, specific heat
EA,ET,GA	axial and transverse Young's moduli, and axial shear modulus
FNA,FNT	axial and transverse Poisson's ratios
	begin sequential CTE and creep material property input at a given temperature --> repeat NTEMP times
IT1, TEMP	temperature number (1, 2, . . . , NTEMP), temperature at which CTE and creep properties are specified
ALPHAATEMP,ALPHATTEMP	axial and transverse thermal expansion coefficients at TEMP
CREEPCOEFTEMP,POWERTEMP, HCREEPTEMP	creep parameters at TEMP
	end of CTE and creep property input at a given temperature
	end of material property input for NMAT materials at NTEMP temperatures

Note: the creep parameters are specified for the power-law model of the form given by eqns (18) and (19)

Block 2: Specification of the cylinder geometry and architecture

R0	inner radius (R0=0 -> flat plate option)
NALPHA,NBETA	number of subcells in the radial and circumferential directions
IALPHAW1,IALPHAW2	beginning and ending α subcells of a crack -> for a crack in the θ direction, IALPHAW1 is the subcell below the crack (must be even) and IALPHAW2 is the subcell above the crack (must be odd); **note that 0 is specified for both parameters in the absence of a crack**
JBETAW1,JBETAW2	beginning and ending β subcells of a crack -> for a crack in the θ direction, JBETAW1 is the left corner β subcell (must be odd) and JBETAW2 is the right corner β subcell (must be even); **note that 0 is specified for both parameters in the absence of a crack**
	begin subcell dimensions specifications
IALPHA,XD	radial subcell number, radial subcell dimensions --> *repeat NALPHA times*
	if R0 is not zero
THETA	cirumferential subcell angle --> *repeat NBETA times*
	if R0=0
H1,H2	subcell dimensions in the θ direction -->*repeat NBETA/2 times*
	end of subcell dimensions specifications for NALPHA and NBETA subcells
L1,L2	subcell dimensions l_1 and l_2 in the out-of-plane direction
	begin subcell material assignment in each of the 2 r-θ planes --> repeat 2 times
	for each plane, start from the lower left corner with r (ALPHA) directed up, and θ (BETA) directed to the right
KGAMA	counter for the two planes (1 and then 2)
	material assignment for the IALPHAREAD subcell --> repeat NALPHA times
IALPHAREAD,MATNUM	counter, NALPHA $\times$ NBETA $\times$ 2 matrix containing material specification for each subcell --> *repeat NBETA times*
	end of subcell material assignment for NALPHA $\times$ NBETA $\times$ 2 subcells

Block 3: Specification of the loading and inelastic strain integration parameters, and write options

NINT	number of time steps for the integration of the global system of equations for the unknown thermal and mechanical microvariables
DTIME,**DTIME_TEMP**	time increments for the integration of the mechanical and thermal global systems of equations
NSTEP	number of load increments between which output data is written to the *fgmc3dq.cylindrical.out* file

NPLOT1,....,NPLOT4	specification of the four times during the loading history at which output results are written to the *fgmc3dq.cylinder.plot* file
KGAMPPLOT	r-θ plane indicator, indicates in which plane (1 or 2) output data for plotting purposes is to be generated
NBPLOT,JBETAPLOT	number of cross sections along the radial direction in which data is to be generated for plotting purposes, β subcell through which data is to be generated --> *repeat JBETAPLOT NBPLOT times*
ISIGNX2B	specifies the location within the particular β subcell through which data is to be generated when NBPLOT is not 0 (1 --> left face; 0 --> center: 2 --> right face) --> *repeat NBPLOT times*
NAPLOT,IALPHAPLOT	number of cross sections along the circumferential direction in which data is to be generated for plotting purposes, α subcell through which data is to be generated --> *repeat NAPLOT times*
ISIGNX1B	specifies the location within the particular α subcell through which data is to be generated when NAPLOT is not 0 (1 --> lower face; 0 --> center: 2 --> upper face) --> *repeat NAPLOT times*
IGPS	plane (0) or generalized plane strain (1) condition in the out-of-plane direction
NLEG	order of Legendre polynomials for approximating the inelastic subcell strains in the three directions
J1	number of integration points for evaluating the inelastic subcell strains in the three directions

Block 4: Specification of thermal and mechanical boundary conditions

	specification of thermal boundary conditions at the inner and outer radii --> repeat NBETA times
LOADFT1	thermal load indicator for the boundary β subcells at the inner radius (1 -> heat flux specified; 2 -> temperature specified)
AMPFT1	heat flux/temperature amplitude for the boundary β subcells at the inner radius
LOADRT1	thermal load indicator for the boundary β subcells at the outer radius (1 -> heat flux specified; 2 -> temperature specified)
AMPRT1	heat flux/temperature amplitude for the boundary β subcells at the outer radius
	specification of thermal boundary conditions at the left and right faces --> repeat NALPHA times
LOADFT2	thermal load indicator for the boundary α subcells at the left face (1 -> heat flux specified; 2 -> temperature specified)
AMPFT2	heat flux or temperature amplitude for the boundary α subcells at the left face
LOADRT2	thermal load indicator for the boundary α subcells at the right face (1 -> heat flux specified; 2 -> temperature specified)
AMPRT2	heat flux/temperature amplitude for the boundary α subcells at the right face

	specification of thermal boundary conditions at the lower and upper faces of a crack --> repeat NBETA times; **for a circumferential crack only**
LOADWFT1	thermal load indicator for the boundary β subcells at the lower crack face (1 -> heat flux specified; 2 -> temperature specified)
AMPWFT1	heat flux/temperature amplitude for the boundary β subcells at the lower crack face
LOADWRF1	thermal load indicator for the boundary β subcells at the upper crack face (1 -> heat flux specified; 2 -> temperature specified)
AMPWRT1	heat flux/temperature amplitude for the boundary β subcells at the upper crack face
	specification of thermal boundary conditions at the left and right faces of a crack--> repeat NALPHA times; **for a radial crack only**
LOADWFT2	thermal load indicator for the boundary α subcells at the left crack face (1 -> heat flux specified; 2 -> temperature specified)
AMPWFT2	heat flux/temperature amplitude for the boundary α subcells at the left crack face
LOADWRT2	thermal load indicator for the boundary α subcells at the right crack face (1 -> heat flux specified; 2 -> temperature specified)
AMPWRT2	heat flux/temperature amplitude for the boundary α subcells at the right crack face
	specification of mechanical boundary conditions at the inner and outer radii --> repeat NBETA times
LOADFM1	mechanical load indicator for the boundary β subcells at the inner radius (1 -> σ_{rr} specified; 2 -> u_r specified; 3 -> $\partial u_r / \partial r$)
AMPFM1	mechanical load amplitude for the boundary β subcells at the inner radius
LOADFM1	mechanical load indicator for the boundary β subcells at the inner radius (1 -> $\sigma_{r\theta}$ specified; 2 -> u_θ specified; 3 -> $\partial u_\theta / \partial r$)
AMPFM1	mechanical load amplitude for the boundary β subcells at the inner radius
LOADRM1	mechanical load indicator for the boundary β subcells at the outer radius (1 -> σ_{rr} specified; 2 -> u_r specified; 3 -> $\partial u_r / \partial r$)
AMPRM1	mechanical load amplitude for the boundary β subcells at the outer radius
LOADRM1	mechanical load indicator for the boundary β subcells at the outer radius (1 -> $\sigma_{r\theta}$ specified; 2 -> u_θ specified; 3 -> $\partial u_\theta / \partial r$)
AMPRM1	mechanical load amplitude for the boundary β subcells at the outer radius
	specification of mechanical boundary conditions at the left and right faces --> repeat NALPHA times
LOADFM2	mechanical load indicator for the boundary β subcells at the left face (1 -> $\sigma_{\theta r}$ specified; 2 -> u_r specified; 3 -> $\partial u_r / \partial \theta$)

AMPFM2	mechanical load amplitude for the boundary β subcells at the left face
LOADFM2	mechanical load indicator for the boundary β subcells at the left face (1 -> $\sigma_{\theta\theta}$ specified; 2 -> u_θ specified; 3 -> $\partial u_\theta / \partial\theta$)
AMPFM2	mechanical load amplitude for the boundary β subcells at the left face
LOADRM2	mechanical load indicator for the boundary β subcells at the right face (1 -> $\sigma_{\theta r}$ specified; 2 -> u_r specified; 3 -> $\partial u_r / \partial\theta$)
AMPRM2	mechanical load amplitude for the boundary β subcells at the right face
LOADRM2	mechanical load indicator for the boundary β subcells at the right face (1 -> $\sigma_{\theta\theta}$ specified; 2 -> u_θ specified; 3 -> $\partial u_\theta / \partial\theta$)
AMPRM2	mechanical load amplitude for the boundary β subcells at the right face
	specification of mechanical boundary conditions at the lower and upper faces of a crack --> repeat NBETA times; **for a circumferential crack only**
LOADWFM1	mechanical load indicator for the boundary β subcells at the lower crack face (1 -> σ_{rr} specified; 2 -> u_r specified; 3 -> $\partial u_r / \partial r$)
AMPWFM1	mechanical load amplitude for the boundary β subcells at the lower crack face
LOADWFM1	mechanical load indicator for the boundary β subcells at the lower crack face (1 -> $\sigma_{r\theta}$ specified; 2 -> u_θ specified; 3 -> $\partial u_\theta / \partial r$)
AMPWFM1	mechanical load amplitude for the boundary β subcells at the lower crack face
LOADWRM1	mechanical load indicator for the boundary β subcells at the upper crack face (1 -> σ_{rr} specified; 2 -> u_r specified; 3 -> $\partial u_r / \partial r$)
AMPWRM1	mechanical load amplitude for the boundary β subcells at the upper crack face
LOADWRM1	mechanical load indicator for the boundary β subcells at the upper crack face (1 -> $\sigma_{r\theta}$ specified; 2 -> u_θ specified; 3 -> $\partial u_\theta / \partial r$)
AMPWRM1	mechanical load amplitude for the boundary β subcells at the upper crack face
	specification of mechanical boundary conditions at the left and right faces of a crack --> repeat NALPHA times; **for a radial crack only**
LOADWFM2	mechanical load indicator for the boundary β subcells at the left crack face (1 -> $\sigma_{\theta r}$ specified; 2 -> u_r specified; 3 -> $\partial u_r / \partial\theta$)
AMPWFM2	mechanical load amplitude for the boundary β subcells at the left crack face
LOADWFM2	mechanical load indicator for the boundary β subcells at the left crack face (1 -> $\sigma_{\theta\theta}$ specified; 2 -> u_θ specified; 3 -> $\partial u_\theta / \partial\theta$)
AMPWFM2	mechanical load amplitude for the boundary β subcells at the left crack face
LOADWRM2	mechanical load indicator for the boundary β subcells at the right crack face (1 -> $\sigma_{\theta r}$ specified; 2 -> u_r specified; 3 -> $\partial u_r / \partial\theta$)
AMPWRM2	mechanical load amplitude for the boundary β subcells at the right crack face

LOADWRM2 mechanical load indicator for the boundary β subcells at the right crack face (1 -> $\sigma_{\theta\theta}$ specified; 2 -> u_θ specified; 3 -> $\partial u_\theta / \partial\theta$)

AMPWRM2 mechanical load amplitude for the boundary β subcells at the right crack face

7.6 Appendix 6

The input file *fgmc3dq.cylindrical.transient.data* for the case described in section 4.2.2 is given below. The highlighted text, not to be included in the input deck, identifies the four blocks of the input data.

Block 1

```
3                                                          NMAT
300                                                        TREF
'MATERIAL 1'                                               MNAME
6570E-09                                                   RHO
1                                                          ID
1                                                          NTEMP
 0.50E+03      0.50E+03     272.0E+06                      CONDA,CONDT,CVP
36.00E+06     36.00E+06     15.00E+06                      EA,ET,GA
 0.20E+00      0.20E+00                                    FNA,FNT
 1             0                                          IT,TEMP
 8.00E-06      8.00E-06                                   ALPHAATEMP,ALPHATTEMP
 1.11E-01      1.59        277.00E+03                     CREEPCOEFTEMP,POWERTEMP,HCREEPTEMP

'MATERIAL 2'
3000E-09
1
1
  2.42E+03     2.42E+03    200.00E+06
197.00E+06   197.00E+06     78.80E+06
  0.25E+00     0.25E+00
1              0
11.00E-06     11.00E-06
 0.00E+00      1.00E+00      1.00E+00

'MATERIAL 3'
7830E-09
1
1
 60.50E+03    60.50E+03     465.0E+06
207.00E+06   207.00E+06     79.60E+06
  0.30E+00     0.30E+00
1              0
 15.00E-06    15.00E-06
  0.00E+00     1.00E+00      1.00E+00
```

Block 2

```
50.00E+00                                                  R0
42     10                                                  NALPHA,NBETA
 0      0                                                  IALPHAW1,IALPHAW2
 0      0                                                  JBETAW1,JBETAW2

42    0.25E-0                                             NALPHA,XD(NALPHA)
41    0.25E-0                                             .
40    0.25E-0                                             .
39    0.25E-0                                             .
38    0.0263157E-0                                        .
37    0.0263157E-0                                        .
36    0.0263157E-0                                        .
35    0.0263157E-0                                        .
34    0.0263157E-0                                        .
33    0.0263157E-0                                        .
32    0.0263157E-0                                        .
```

```
31    0.0263157E-0
30    0.0263157E-0
29    0.0263157E-0
28    0.0263157E-0
27    0.0263157E-0
26    0.0263157E-0
25    0.0263157E-0
24    0.0263157E-0
23    0.0263157E-0
22    0.0263157E-0
21    0.0263157E-0
20    0.0263157E-0
19    0.0263157E-0
18    0.0263157E-0
17    0.0263157E-0
16    0.0263157E-0
15    0.0263157E-0
14    0.0263157E-0
13    0.0263157E-0
12    0.0263157E-0
11    0.0263157E-0
10    0.0263157E-0
 9    0.0263157E-0
 8    0.0263157E-0
 7    0.0263157E-0
 6    0.0263157E-0
 5    0.0263157E-0
 4    0.0263157E-0
 3    0.0263157E-0
 2    0.0263157E-0
 1    0.0263157E-0

      0.02865 0.02865                    THETA(1),THETA(2)
      0.02865 0.02865                    .
      0.02865 0.02865                    .
      0.02865 0.02865                    .
      0.02865 0.02865                    THETA(NBETA-1),THETA(NBETA)

                                         (or H1(1),H2(1) ... for flat plate)

      0.0263157E-0  0.0263157E-0         L1,L2

 1                                       KGAMA
42    3  3  3  3  3  3  3  3  3  3       NALPHA,MATNUM(42,1,1) .... MATNUM(42,10,1)
41    3  3  3  3  3  3  3  3  3  3
40    3  3  3  3  3  3  3  3  3  3
39    3  3  3  3  3  3  3  3  3  3
38    2  2  2  2  2  2  2  2  2  2
37    2  2  2  2  2  2  2  2  2  2
36    2  2  2  2  2  2  2  2  2  2
35    2  2  2  2  2  2  2  2  2  2
34    2  2  1  2  2  2  2  1  2  2
33    2  2  2  2  2  2  2  2  2  2
32    2  2  2  2  1  2  2  2  2  2
31    1  2  2  2  2  2  2  2  1  2
30    2  2  1  2  2  2  2  2  2  2
29    2  2  2  2  2  1  2  2  2  2
28    2  2  2  1  2  2  2  1  2  2
27    2  1  2  2  2  1  2  2  2  1
26    2  2  2  1  2  2  2  1  2  2
25    1  2  2  2  2  1  2  2  2  1
24    2  2  1  2  1  2  1  2  1  2
23    2  1  2  2  2  1  2  2  2  1
22    1  2  1  2  1  2  1  2  1  2
```

21	2	1	2	1	2	1	2	1	2	1
20	1	2	1	2	1	2	1	2	1	2
19	2	1	2	1	2	1	2	1	2	1
18	1	2	1	2	1	2	1	2	1	2
17	2	1	1	1	2	1	1	1	2	1
16	1	2	1	2	1	2	1	2	1	2
15	1	1	1	1	1	1	1	1	1	1
14	2	1	2	1	2	1	2	1	2	1
13	1	1	1	1	1	1	1	1	1	1
12	1	2	1	1	1	2	1	1	1	2
11	1	1	1	2	1	1	1	2	1	1
10	1	1	1	1	1	2	1	1	1	1
9	1	1	2	1	1	1	1	1	1	1
8	2	1	1	1	1	1	1	1	2	1
7	1	1	1	1	2	1	1	1	1	1
6	1	1	1	1	1	1	1	1	1	1
5	1	1	2	1	1	1	1	2	1	1
4	1	1	1	1	1	1	1	1	1	1
3	1	1	1	1	1	1	1	1	1	1
2	1	1	1	1	1	1	1	1	1	1
1	1	1	1	1	1	1	1	1	1	1

KGAMA

2										
42	3	3	3	3	3	3	3	3	3	3
41	3	3	3	3	3	3	3	3	3	3
40	3	3	3	3	3	3	3	3	3	3
39	3	3	3	3	3	3	3	3	3	3
38	2	2	2	2	2	2	2	2	2	2
37	2	2	2	2	2	2	2	2	2	2
36	2	2	2	2	2	2	2	2	2	2
35	2	2	2	2	2	2	2	2	2	2
34	2	2	2	2	2	2	2	2	2	2
33	2	2	2	2	2	2	2	2	2	2
32	2	2	2	2	2	2	2	2	2	2
31	2	2	2	2	2	2	2	2	2	2
30	2	2	2	2	2	2	2	2	2	2
29	2	2	2	2	2	2	2	2	2	2
28	2	2	2	2	2	2	2	2	2	2
27	2	2	2	2	2	2	2	2	2	2
26	2	2	2	2	2	2	2	2	2	2
25	2	2	2	2	2	2	2	2	2	2
24	2	2	2	2	2	2	2	2	2	2
23	2	2	2	2	2	2	2	2	2	2
22	2	2	2	2	2	2	2	2	2	2
21	1	2	1	2	1	2	1	2	1	2
20	2	1	2	1	2	1	2	1	2	1
19	1	2	1	2	1	2	1	2	1	2
18	2	1	2	1	2	1	2	1	2	1
17	1	1	1	1	1	1	1	1	1	1
16	1	1	1	1	1	1	1	1	1	1
15	1	1	1	1	1	1	1	1	1	1
14	1	1	1	1	1	1	1	1	1	1
13	1	1	1	1	1	1	1	1	1	1
12	1	1	1	1	1	1	1	1	1	1
11	1	1	1	1	1	1	1	1	1	1
10	1	1	1	1	1	1	1	1	1	1
9	1	1	1	1	1	1	1	1	1	1
8	1	1	1	1	1	1	1	1	1	1
7	1	1	1	1	1	1	1	1	1	1
6	1	1	1	1	1	1	1	1	1	1
5	1	1	1	1	1	1	1	1	1	1
4	1	1	1	1	1	1	1	1	1	1
3	1	1	1	1	1	1	1	1	1	1
2	1	1	1	1	1	1	1	1	1	1

```
1    1  1  1  1  1  1  1  1  1  1
```

Block 3

```
1000
   0.01  0.001
 100
   1 10  100  1000
   1
   5   1  3  5  8 10
   -1  0  1  0  1
   0
   0
   2
   5
```

```
NINT
DTIME,DTIME_TEMP
NSTEP
NPLOT1 ... NPLOT4
KGAMAPLOT
NBPLOT,JBETAPLOT(1) ... JBETAPLOT(5)
ISIGNX2B(1) ... ISIGNX2B(5)
NAPLOT,IALPHAPLOT(1) ...
IGPS
NLEG
J1
```

Block 4

```
   2    2    2    2    2
   2    2    2    2    2
1200 1200 1200 1200 1200
1200 1200 1200 1200 1200

   2    2    2    2    2
   2    2    2    2    2
   0    0    0    0    0
   0    0    0    0    0

   1    1    1    1    1
   1    1    1    1    1
   1    1    1    1    1
   1    1    1    1    1
   1    1    1    1    1
   1    1    1    1    1
   1    1    1    1    1
   1    1
   0    0    0    0    0
   0    0    0    0    0
   0    0    0    0    0
   0    0    0    0    0
   0    0    0    0    0
   0    0    0    0    0
   0    0    0    0    0
   0    0
   1    1    1    1    1
   1    1    1    1    1
   1    1    1    1    1
   1    1    1    1    1
   1    1    1    1    1
   1    1    1    1    1
   1    1    1    1    1
   1    1
   0    0    0    0    0
   0    0    0    0    0
   0    0    0    0    0
   0    0    0    0    0
   0    0    0    0    0
   0    0    0    0    0
   0    0    0    0    0
   0    0
```

```
External thermal boundary conditions
LOADF1(1) ...
... LOADF1(NBETA)
AMPF1(1) ...
... AMPF1(NBETA)

LOADR1(1) ...
... LOADR1(NBETA)
AMPR1(1) ...
... AMPR1(NBETA)

LOADF2(1) ...
.
.
.
.
.
.
.
... LOADF2(NALPHA)
AMPF2(1) ...
.
.
.
.
.
.
.
... AMPF2(NALPHA)

LOADR2(1) ...
.
.
.
.
.
.
.
... LOADR2(NALPHA)
AMPR2(1)
.
.
.
.
.
.
.
... AMPR2(NALPHA)
```

```
 1     1     1     1     1
 1     1     1     1     1
 0     0     0     0     0
 0     0     0     0     0

 1     1     1     1     1
 1     1     1     1     1
 0     0     0     0     0
 0     0     0     0     0

 1     1     1     1     1
 1     1     1     1     1
 0     0     0     0     0
 0     0     0     0     0

 1     1     1     1     1
 1     1     1     1     1
 0     0     0     0     0
 0     0     0     0     0

 1     1     1     1     1
 1     1     1     1     1
 1     1     1     1     1
 1     1     1     1     1
 1     1     1     1     1
 1     1     1     1     1
 1     1     1     1     1
 1     1     1     1     1
 1     1
 0     0     0     0     0
 0     0     0     0     0
 0     0     0     0     0
 0     0     0     0     0
 0     0     0     0     0
 0     0     0     0     0
 0     0     0     0     0
 0     0     0     0     0
 0     0

 2     2     2     2     2
 2     2     2     2     2
 2     2     2     2     2
 2     2     2     2     2
 2     2     2     2     2
 2     2     2     2     2
 2     2     2     2     2
 2     2     2     2     2
 2     2
 0     0     0     0     0
 0     0     0     0     0
 0     0     0     0     0
 0     0     0     0     0
 0     0     0     0     0
 0     0     0     0     0
 0     0     0     0     0
 0     0     0     0     0
 0     0

 1     1     1     1     1
 1     1     1     1     1
 1     1     1     1     1
 1     1     1     1     1
 1     1     1     1     1
```

```
External mechanical boundary conditions
LOADF1(1) ...
... LOADF1(NBETA)
AMPF1(1) ...
... AMPF1(NBETA)

LOADF1(1) ...
... LOADF1(NBETA)
AMPF1(1) ...
... AMPF1(NBETA)

LOADR1(1) ...
... LOADR1(NBETA)
AMPR1(1) ...
... AMPR1(NBETA)

LOADR1(1) ...
... LOADR1(NBETA)
AMPR1(1) ...
... AMPR1(NBETA)

LOADF2(1) ...
.
.
.
.
.
.
.
... LOADF2(NALPHA)
AMPF2(1) ...
.
.
.
.
.
.
.
.
... AMPF2(NALPHA)

LOADF2(1) ...
.
.
.
.
.
.
.
.
... LOADF2(NALPHA)
AMPF2(1) ...
.
.
.
.
.
.
.
.
... AMPF2(NALPHA)

LOADR2(1) ...
.
.
.
.
```

```
1     1     1     1     1              .
1     1     1     1     1              .
1     1     1     1     1              .
1     1                                ... LOADR2(NALPHA)
0     0     0     0     0              AMPR2(1) ...
0     0     0     0     0              .
0     0     0     0     0              .
0     0     0     0     0              .
0     0     0     0     0              .
0     0     0     0     0              .
0     0     0     0     0              .
0     0     0     0     0              .
0     0                                ... AMPR2(NALPHA)

2     2     2     2     2              LOADR2(1) ...
2     2     2     2     2              .
2     2     2     2     2              .
2     2     2     2     2              .
2     2     2     2     2              .
2     2     2     2     2              .
2     2     2     2     2              .
2     2     2     2     2              .
2     2                                ... LOADR(NALPHA)
0     0     0     0     0              AMPR2(1) ...
0     0     0     0     0              .
0     0     0     0     0              .
0     0     0     0     0              .
0     0     0     0     0              .
0     0     0     0     0              .
0     0     0     0     0              .
0     0                                ... AMPR2(NALPHA)
```

7.7 Appendix 7

This appendix describes the work performed under the grant **NAG3-2252** during the FY99 funding period. It is included in the final report for the contract **NAS3-97190** in order to avoid unnecessary repetition as the work performed under this grant involved the extension of the work performed under the above contract.

INTERNALLY-COOLED FUNCTIONALLY GRADED CYLINDERS

FINAL REPORT: Grant NAG3-2252

Prepared by:

Marek-Jerzy Pindera
Jacob Aboudi[1]

Civil Engineering and
Applied Mechanics Department
University of Virginia
Charlottesville, Virginia 22903

May 15, 2000

[1]Visiting Professor, Faculty of Engineering, Tel-Aviv University, Ramat-Aviv, Tel-Aviv 69978, Israel.

7.7.1 SUMMARY

This report summarizes the work performed under the grant **NAG3-2252** during the FY99 funding period. The objective was to extend the theory, and the related computer codes, for the analysis, optimization and design of cylindrical functionally graded materials/structural components for use in advanced aircraft engines (e.g., combustor linings, rotor disks, heat shields, blisk blades), developed under the contract **NAS3-97190**, as described in the main body of the report. This extension involved modification of the theoretical formulation of the developed two-dimensional version of the higher-order theory in cylindrical coordinates, and one of the computer codes, in order to accommodate the presence of channels or holes. This extension considerably broadens the theory's range of practical applications by enabling the analysis and design of **internally-cooled**, functionally graded cylindrical structural components. Applications involving advanced turbine blades and structural components for the reusable-launch vehicle (RLV) currently under development will benefit from the completed work.

7.7.2 PROJECT DESCRIPTION

The incorporation of the cooling-channel capability into the cylindrical higher-order theory involved the modification of the traction, displacement, temperature and heat flux continuity conditions across the boundaries defining the channel geometry, which would otherwise separate the interior subvolumes of the functionally graded material microstructure in the absence of the channel. These interior boundaries have been treated in the same manner as the exterior boundaries, with the above continuity conditions replaced by the corresponding interior boundary conditions. This replacement, in turn, modifies the way that the two global systems of equations, eqns (4) and (16) described in section 2.1 of the main body of the report, for the unknown thermal and displacement microvariables in the individual subvolumes,

$$\overline{\kappa}\,\dot{\mathbf{T}} = \overline{\mathbf{t}}(\mathbf{T},t) = \mathbf{A}\mathbf{T}(t) + \dot{\mathbf{e}}(t)$$

$$\mathbf{K}\,\mathbf{U} = \mathbf{f} + \mathbf{g}$$

are constructed and assembled. Efficient ways of assembling these reformulated equations have been implemented in order to facilitate the construction of the input data file for the related computer code. In fact, it was possible to incorporate the internal cooling channel capability into the analytical formulation and the developed computer code in a way that only slightly modifies the construction of the data file employed for the code without the internal cooling channel capability. For this reason, the two codes have been combined into the single code *fgmc3dq.cylinder.transient.f* described in the main body of the report. Further, by setting certain parameters that define the cooling channel geometry appropriately, damage in the form of radial or circumferential cracks can be accommodated efficiently within the same code, as required by the contract **NAS3-97190**.

7.7.3 APPLICATIONS

In order to demonstrate the internal cooling channel capability incorporated into the cylindrical two-dimensional higher-order theory and the related computer code, the problem described in section 4.2 dealing with a functionally graded TBCs subjected to Heaviside type thermal loading was investigated in the presence of a cooling channel. The TBC geometry was modified to include a cooling channel whose dimensions and location are shown in Figure A7.1. The boundaries of the cooling channel were maintained at room temperature and kept traction free, while the external loading was identical to the problem of section 4.2. The construction of the input data file *fgmc3dq.cylinder.transient.data* in the presence of the cooling channel is similar to the corresponding problem in the absence of the cooling channel. The differences are explained in section 7.7.4 while the affected sections of the actual data file are given in section 7.7.5. The format of the *fgmc3dq.cylinder.transient.out* and *fgmc3dq.cylinder.transient.plot* files is essentially the same as the format of the corresponding files in the absence of the cooling channel, with appropriate modifications in the *fgmc3dq.cylinder.transient.out* file that reflect the presence of the cooling channel and the related internal boundary conditions.

For efficient analysis of the genarated results, output is also written to PATRAN files that can then be quickly plotted using the **MACPOST** code developed at the NASA-Glenn Research Center. Figures A7.2 and A7.3 show the temperature and $\sigma_{\theta\theta}$ distributions generated using **MACPOST** at three different times during the thermal loading history for the TBC with an internal cooling channel. The corresponding distributions in the absence of the cooling channel are shown in Figures A7.4 and A7.5. Comparison of Figures A7.2 and A7.4 demonstrates the significant shielding effect that the presence of the cooling channel has on the temperature distribution within the functionally graded coating. This shielding effect also has a substantial impact on the resulting $\sigma_{\theta\theta}$ distribution as observed by comparing Figures A7.3 and A7.5.

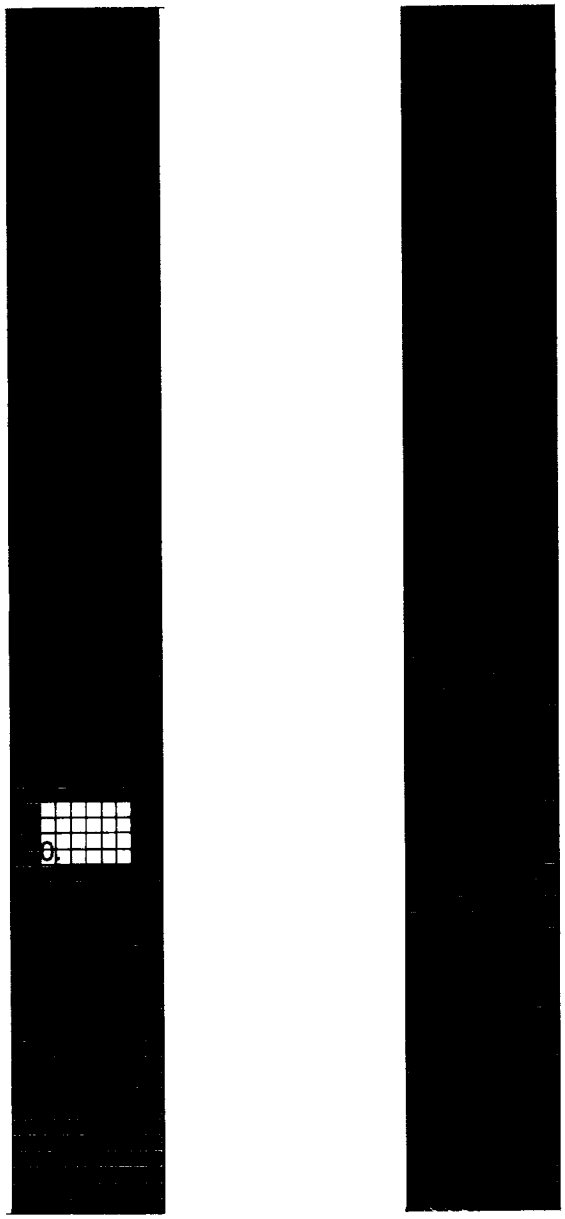

Figure A7.1. Repeating cross section element of a cylindrical structural component with (left) and without (right) a cooling channel in the functionally graded thermal barrier coating.

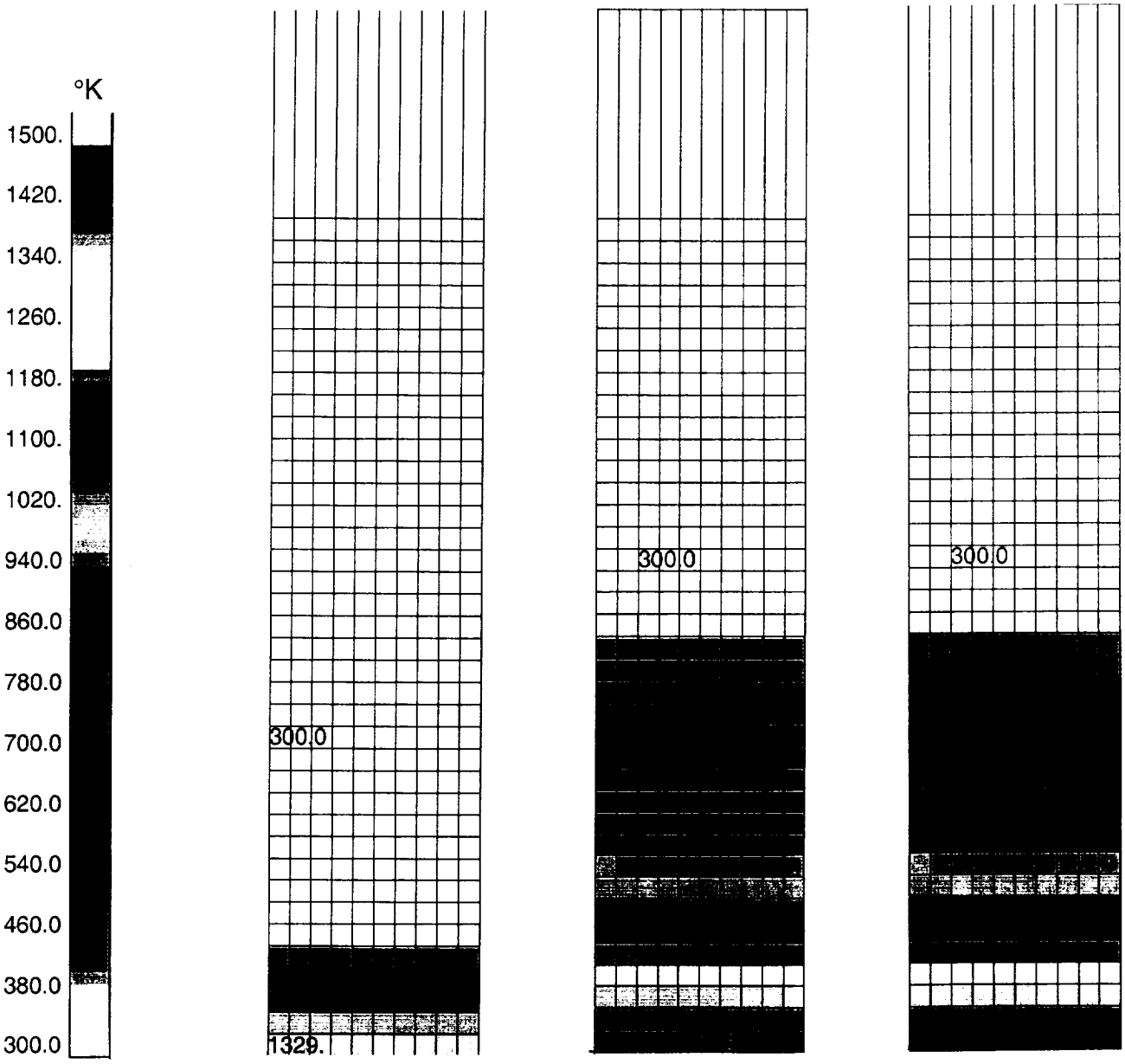

Figure A7.2. PATRAN-generated transient temperature distributions in the TBC with an internal cooling channel at t = 0.01 (left), 1.0 (middle), and 10 (right) seconds due to Heaviside thermal loading on the ceramic-rich surface.

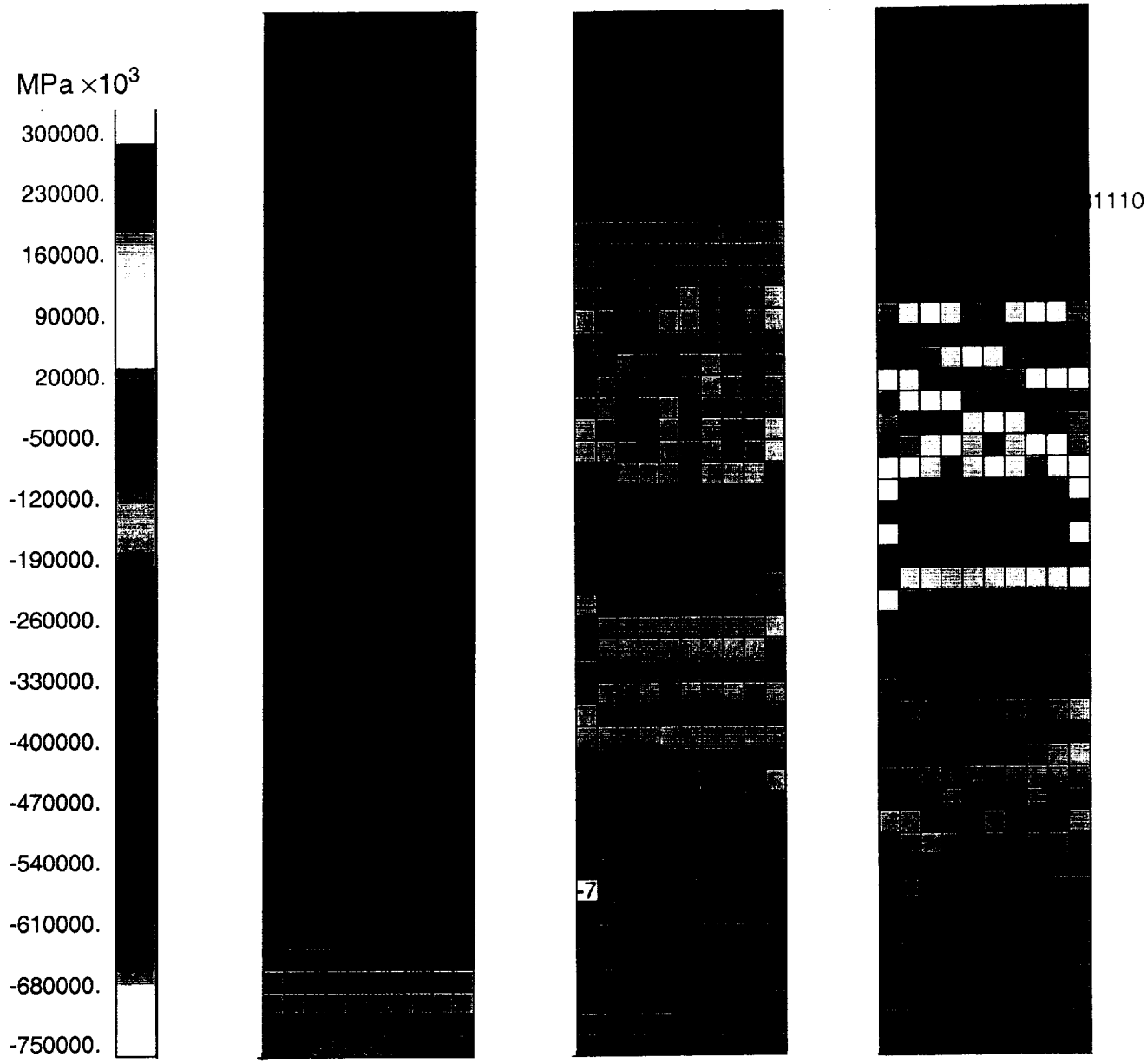

Figure A7.3. PATRAN-generated transient $\sigma_{\theta\theta}$ distributions in the TBC with an internal cooling channel at t = 0.01 (left), 1.0 (middle), and 10 (right) seconds due to Heaviside thermal loading on the ceramic-rich surface.

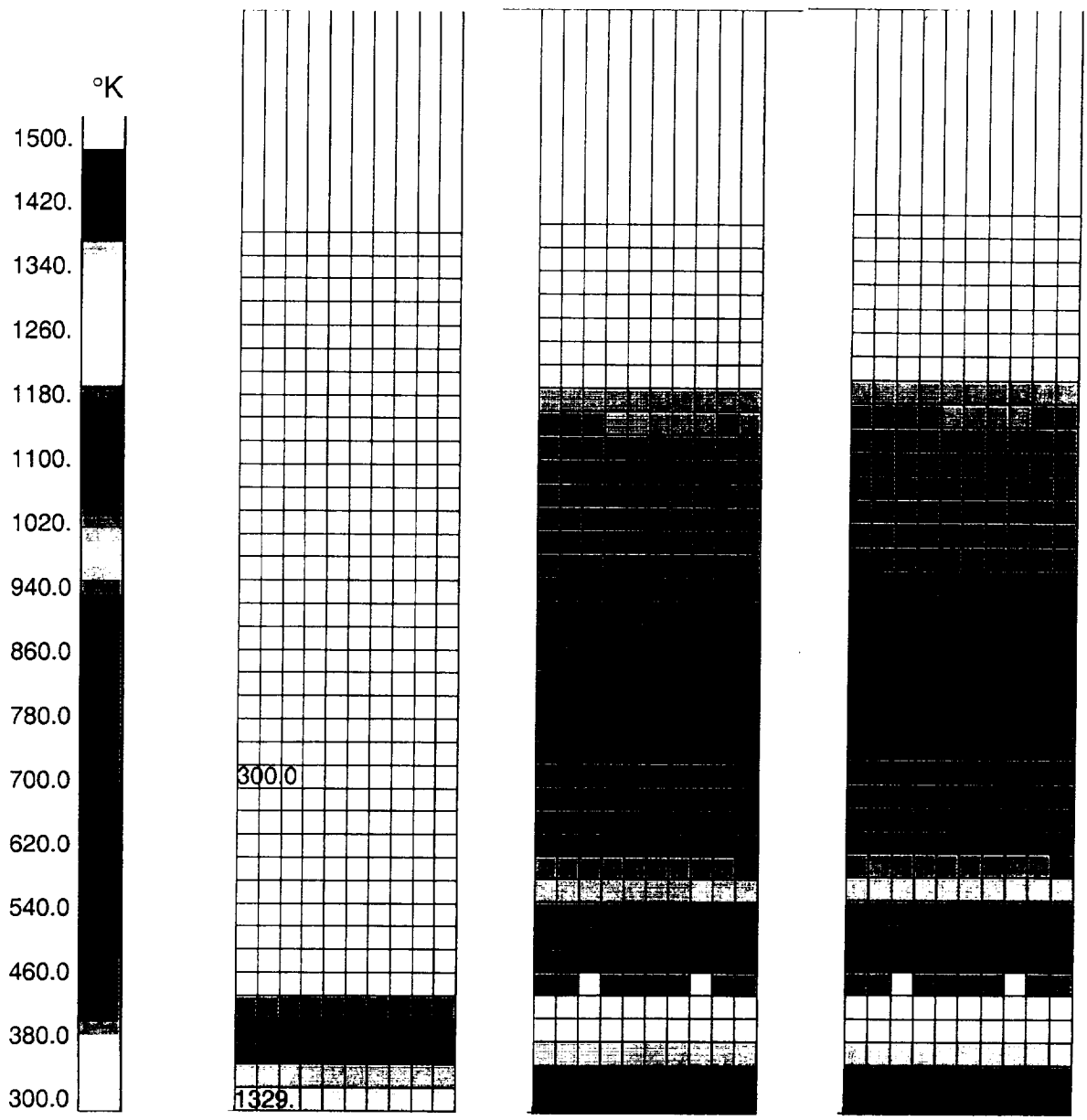

Figure A7.4. PATRAN-generated transient temperature distributions in the TBC without an internal cooling channel at t = 0.01 (left), 1.0 (middle), and 10 (right) seconds due to Heaviside thermal loading on the ceramic-rich surface.

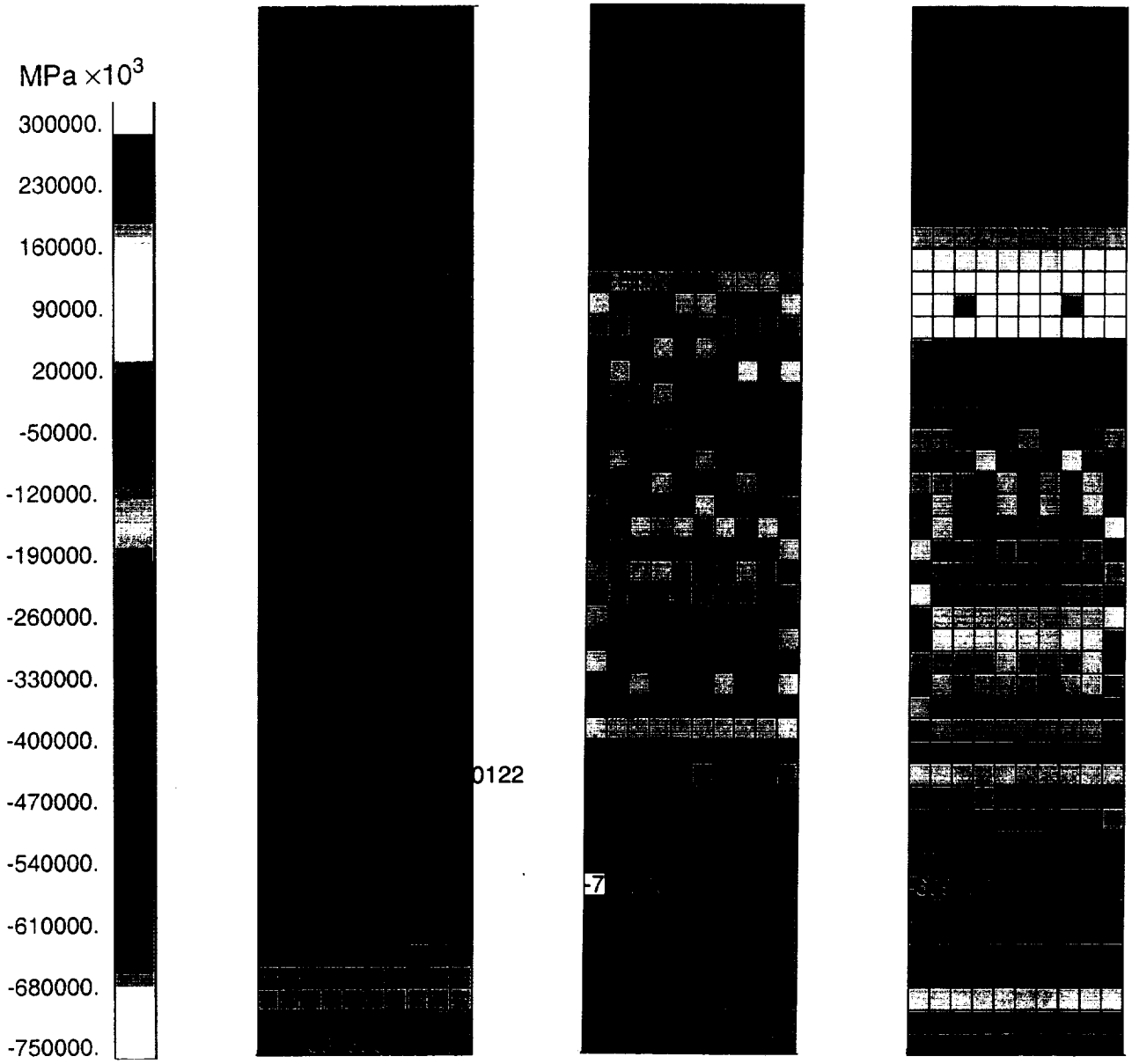

Figure A7.5. PATRAN-generated transient $\sigma_{\theta\theta}$ distributions in the TBC without an internal cooling channel at t = 0.01 (left), 1.0 (middle), and 10 (right) seconds due to Heaviside thermal loading on the ceramic-rich surface.

7.7.4 Construction of the input data file

The input data file *fgmc3dq.cylindrical.transient.data* that accounts for the presence of an internal cooling channel is organized in the same manner as the input data file described in Appendix 5 which accounts for the presence of an internal crack. There are some notable differences, however, with regard to how some of the parameters are specified. These parameters reside in Blocks 2 and 4, and the manner of specifying them is explained below. Blocks 1 and 3 remain unchanged.

Block 2: Specification of the cylinder geometry and architecture

R0	inner radius (R0=0 -> flat plate option)
NALPHA,NBETA	number of subcells in the radial and circumferential directions
IALPHAW1,IALPHAW2	beginning and ending α subcells of a cooling channel -> IALPHAW1 specifies the first empty α subcell (must be odd) and IALPHAW2 specifies the last empty α subcell (must be even)
JBETAW1,JBETAW2	beginning and ending β subcells of a cooling channel -> JBETAW1 specifies the first empty β subcell (must be odd) and JBETAW22 specifies the last empty β subcell (must be even)
	begin subcell dimensions specifications
IALPHA,XD	radial subcell number, radial subcell dimensions --> *repeat NALPHA times*
	if R0 is not zero
THETA	cirumferential subcell angle --> *repeat NBETA times*
	if R0=0
H1,H2	subcell dimensions in the θ direction -->*repeat NBETA/2 times*
	end of subcell dimensions specifications for NALPHA and NBETA subcells
L1,L2	subcell dimensions l_1 and l_2 in the out-of-plane direction
	begin subcell material assignment in each of the 2 r-θ *planes --> repeat 2 times*
	for each plane, start from the lower left corner with r *(ALPHA) directed up, and* θ *(BETA) directed to the right*
KGAMA	counter for the two planes (1 and then 2)
	material assignment for the IALPHAREAD subcell --> repeat NALPHA times
IALPHAREAD,MATNUM	counter, NALPHA $\times$ NBETA $\times$ 2 matrix containing material specification for each subcell --> *repeat NBETA times*; **note that subcells that compose a cooling channel are given the material assignment 0**
	end of subcell material assignment for NALPHA $\times$ NBETA $\times$ 2 subcells

Block 4: Specification of the thermal and mechanical boundary conditions

	specification of thermal boundary conditions at the inner and outer radii --> repeat NBETA times
LOADFT1	thermal load indicator for the boundary β subcells at the inner radius (1 -> heat flux specified; 2 -> temperature specified)
AMPFT1	heat flux/temperature amplitude for the boundary β subcells at the inner radius
LOADRT1	thermal load indicator for the boundary β subcells at the outer radius (1 -> heat flux specified; 2 -> temperature specified)
AMPRT1	heat flux/temperature amplitude for the boundary β subcells at the outer radius
	specification of thermal boundary conditions at the left and right faces --> repeat NALPHA times
LOADFT2	thermal load indicator for the boundary α subcells at the left face (1 -> heat flux specified; 2 -> temperature specified)
AMPFT2	heat flux/temperature amplitude for the boundary α subcells at the left face
LOADRT2	thermal load indicator for the boundary α subcells at the right face (1 -> heat flux specified; 2 -> temperature specified)
AMPRT2	heat flux/temperature amplitude for the boundary α subcells at the right face
	specification of thermal boundary conditions at the lower and upper faces of a cooling channel --> repeat NBETA times
LOADWFT1	thermal load indicator for the boundary β subcells at the lower face of a cooling channel (1 -> heat flux specified; 2 -> temperature specified)
AMPWFT1	heat flux/temperature amplitude for the boundary β subcells at the lower face of a cooling channel
LOADWRF1	thermal load indicator for the boundary β subcells at the upper face of a cooling channel (1 -> heat flux specified; 2 -> temperature specified)
AMPWRT1	heat flux/temperature amplitude for the boundary β subcells at the upper face of a cooling channel
	specification of thermal boundary conditions at the left and right faces of a cooling channel --> repeat NALPHA times
LOADWFT2	thermal load indicator for the boundary α subcells at the left face of a cooling channel (1 -> heat flux specified; 2 -> temperature specified)
AMPWFT2	heat flux/temperature amplitude for the boundary α subcells at the left face of a cooling channel
LOADWRT2	thermal load indicator for the boundary α subcells at the right face of a cooling channel (1 -> heat flux specified; 2 -> temperature specified)
AMPWRT2	heat flux/temperature amplitude for the boundary α subcells at the right face of a cooling channel

	specification of mechanical boundary conditions at the inner and outer radii --> repeat NBETA times
LOADFM1	mechanical load indicator for the boundary β subcells at the inner and outer radii (1 -> σ_{rr} specified; 2 -> u_r specified; 3 -> $\partial u_r / \partial r$)
AMPFM1	mechanical load amplitude for the boundary β subcells at the inner radius
LOADFM1	mechanical load indicator for the boundary β subcells at the inner radius (1 -> $\sigma_{r\theta}$ specified; 2 -> u_θ specified; 3 -> $\partial u_\theta / \partial r$)
AMPFM1	mechanical load amplitude for the boundary β subcells at the inner radius
LOADRM1	mechanical load indicator for the boundary β subcells at the outer radius (1 -> σ_{rr} specified; 2 -> u_r specified; 3 -> $\partial u_r / \partial r$)
AMPRM1	mechanical load amplitude for the boundary β subcells at the outer radius
LOADRM1	mechanical load indicator for the boundary β subcells at the outer radius (1 -> $\sigma_{r\theta}$ specified; 2 -> u_θ specified; 3 -> $\partial u_\theta / \partial r$)
AMPRM1	mechanical load amplitude for the boundary β subcells at the outer radius
	specification of mechanical boundary conditions at the left and right faces --> repeat NALPHA times
LOADFM2	mechanical load indicator for the boundary β subcells at the left face (1 -> $\sigma_{\theta r}$ specified; 2 -> u_r specified; 3 -> $\partial u_r / \partial \theta$)
AMPFM2	mechanical load amplitude for the boundary β subcells at the left face
LOADFM2	mechanical load indicator for the boundary β subcells at the left face (1 -> $\sigma_{\theta\theta}$ specified; 2 -> u_θ specified; 3 -> $\partial u_\theta / \partial \theta$)
AMPFM2	mechanical load amplitude for the boundary β subcells at the left face
LOADRM2	mechanical load indicator for the boundary β subcells at the right face (1 -> $\sigma_{\theta r}$ specified; 2 -> u_r specified; 3 -> $\partial u_r / \partial \theta$)
AMPRM2	mechanical load amplitude for the boundary β subcells at the right face
LOADRM2	mechanical load indicator for the boundary β subcells at the right face (1 -> $\sigma_{\theta\theta}$ specified; 2 -> u_θ specified; 3 -> $\partial u_\theta / \partial \theta$)
AMPRM2	mechanical load amplitude for the boundary β subcells at the right face
	specification of mechanical boundary conditions at the lower and upper faces of a cooling channel --> repeat NBETA times
LOADWFM1	mechanical load indicator for the boundary β subcells at the lower face of a cooling channel (1 -> σ_{rr} specified; 2 -> u_r specified; 3 -> $\partial u_r / \partial r$)
AMPWFM1	mechanical load amplitude for the boundary β subcells at the lower face of a cooling channel
LOADWFM1	mechanical load indicator for the boundary β subcells at the lower face of a cooling channel (1 -> $\sigma_{r\theta}$ specified; 2 -> u_θ specified; 3 -> $\partial u_\theta / \partial r$)

AMPWFM1	mechanical load amplitude for the boundary β subcells at the lower face of a cooling channel
LOADWRM1	mechanical load indicator for the boundary β subcells at the upper face of a cooling channel (1 -> σ_{rr} specified; 2 -> u_r specified; 3 -> $\partial u_r / \partial r$)
AMPWRM1	mechanical load amplitude for the boundary β subcells at the upper face of a cooling channel
LOADWRM1	mechanical load indicator for the boundary β subcells at the upper face of a cooling channel (1 -> $\sigma_{r\theta}$ specified; 2 -> u_θ specified; 3 -> $\partial u_\theta / \partial r$)
AMPWRM1	mechanical load amplitude for the boundary β subcells at the upper face of a cooling channel
	specification of mechanical boundary conditions at the left and right faces of a cooling channel --> repeat NALPHA times
LOADWFM2	mechanical load indicator for the boundary β subcells at the left face of a cooling channel (1 -> $\sigma_{\theta r}$ specified; 2 -> u_r specified; 3 -> $\partial u_r / \partial \theta$)
AMPWFM2	mechanical load amplitude for the boundary β subcells at the left face of a cooling channel
LOADWFM2	mechanical load indicator for the boundary β subcells at the left face of a cooling channel (1 -> $\sigma_{\theta\theta}$ specified; 2 -> u_θ specified; 3 -> $\partial u_\theta / \partial \theta$)
AMPWFM2	mechanical load amplitude for the boundary β subcells at the left face of a cooling channel
LOADWRM2	mechanical load indicator for the boundary β subcells at the right face of a cooling channel (1 -> $\sigma_{\theta r}$ specified; 2 -> u_r specified; 3 -> $\partial u_r / \partial \theta$)
AMPWRM2	mechanical load amplitude for the boundary β subcells at the right face of a cooling channel
LOADWRM2	mechanical load indicator for the boundary β subcells at the right face of a cooling channel (1 -> $\sigma_{\theta\theta}$ specified; 2 -> u_θ specified; 3 -> $\partial u_\theta / \partial \theta$)
AMPWRM2	mechanical load amplitude for the boundary β subcells at the right face of a cooling channel

7.7.5 Example of the input data file

The input file *fgmc3dq.cylindrical.transient.data* for the case described in section 7.7.3 is given below. The highlighted text, not to be included in the input deck, identifies the four blocks of the input data.

Block 1

```
3                                                    NMAT
300                                                  TREF
'MATERIAL 1'                                         MNAME
6570E-09                                             RHO
1                                                    ID
1                                                    NTEMP
 0.50E+03     0.50E+03    272.0E+06                  CONDA,CONDT,CVP
36.00E+06    36.00E+06    15.00E+06                  EA,ET,GA
 0.20E+00     0.20E+00                               FNA,FNT
 1            0                                      IT,TEMP
 8.00E-06     8.00E-06                               ALPHAATEMP,ALPHATTEMP
 1.11E-01     1.59       277.00E+03                  CREEPCOEFTEMP,POWERTEMP,HCREEPTEMP

'MATERIAL 2'
3000E-09
1
1
  2.42E+03    2.42E+03   200.00E+06
197.00E+06  197.00E+06    78.80E+06
  0.25E+00    0.25E+00
1             0
11.00E-06    11.00E-06
 0.00E+00     1.00E+00     1.00E+00

'MATERIAL 3'
7830E-09
1
1
 60.50E+03   60.50E+03    465.0E+06
207.00E+06  207.00E+06    79.60E+06
  0.30E+00    0.30E+00
1             0
 15.00E-06   15.00E-06
  0.00E+00    1.00E+00     1.00E+00
```

Block 2

```
50.00E+00                                            R0
42     10                                            NALPHA,NBETA
23     26                                            IALPHAW1,IALPHAW2
 3      8                                            JBETAW1,JBETAW2

42    0.25E-0                                        NALPHA,XD(NALPHA)
41    0.25E-0                                        .
40    0.25E-0                                        .
39    0.25E-0                                        .
38    0.0263157E-0                                   .
37    0.0263157E-0                                   .
36    0.0263157E-0                                   .
35    0.0263157E-0                                   .
34    0.0263157E-0                                   .
33    0.0263157E-0                                   .
32    0.0263157E-0                                   .
```

```
31    0.0263157E-0                          .
30    0.0263157E-0                          .
29    0.0263157E-0                          .
28    0.0263157E-0                          .
27    0.0263157E-0                          .
26    0.0263157E-0                          .
25    0.0263157E-0                          .
24    0.0263157E-0                          .
23    0.0263157E-0                          .
22    0.0263157E-0                          .
21    0.0263157E-0                          .
20    0.0263157E-0                          .
19    0.0263157E-0                          .
18    0.0263157E-0                          .
17    0.0263157E-0                          .
16    0.0263157E-0                          .
15    0.0263157E-0                          .
14    0.0263157E-0                          .
13    0.0263157E-0                          .
12    0.0263157E-0                          .
11    0.0263157E-0                          .
10    0.0263157E-0                          .
 9    0.0263157E-0                          .
 8    0.0263157E-0                          .
 7    0.0263157E-0                          .
 6    0.0263157E-0                          .
 5    0.0263157E-0                          .
 4    0.0263157E-0                          .
 3    0.0263157E-0                          .
 2    0.0263157E-0                          .
 1    0.0263157E-0                          .

      0.02865 0.02865                       THETA(1),THETA(2)
      0.02865 0.02865                       .
      0.02865 0.02865                       .
      0.02865 0.02865                       .
      0.02865 0.02865                       THETA(NBETA-1),THETA(NBETA)

                                            (or H1(1),H2(1) ... for flat plate)

      0.0263157E-0  0.0263157E-0            L1,L2

 1                                          KGAMA
42    3  3  3  3  3  3  3  3  3  3          NALPHA,MATNUM(42,1,1) .... MATNUM(42,10,1
41    3  3  3  3  3  3  3  3  3  3
40    3  3  3  3  3  3  3  3  3  3
39    3  3  3  3  3  3  3  3  3  3
38    2  2  2  2  2  2  2  2  2  2
37    2  2  2  2  2  2  2  2  2  2
36    2  2  2  2  2  2  2  2  2  2
35    2  2  2  2  2  2  2  2  2  2
34    2  2  1  2  2  2  2  1  2  2
33    2  2  2  2  2  2  2  2  2  2
32    2  2  2  2  1  2  2  2  2  2
31    1  2  2  2  2  2  2  2  1  2
30    2  2  1  2  2  2  2  2  2  2
29    2  2  2  2  2  1  2  2  2  2
28    2  2  2  1  2  2  2  1  2  2
27    2  1  2  2  2  1  2  2  2  1
26    2  2  0  0  0  0  0  0  2  2
25    1  2  0  0  0  0  0  0  2  1
24    2  2  0  0  0  0  0  0  1  2
23    2  1  0  0  0  0  0  0  2  1
22    1  2  1  2  1  2  1  2  1  2
```

21	2	1	2	1	2	1	2	1	2	1
20	1	2	1	2	1	2	1	2	1	2
19	2	1	2	1	2	1	2	1	2	1
18	1	2	1	2	1	2	1	2	1	2
17	2	1	1	1	2	1	1	1	2	1
16	1	2	1	2	1	2	1	2	1	2
15	1	1	1	1	1	1	1	1	1	1
14	2	1	2	1	2	1	2	1	2	1
13	1	1	1	1	1	1	1	1	1	1
12	1	2	1	1	1	2	1	1	1	2
11	1	1	1	2	1	1	1	2	1	1
10	1	1	1	1	1	2	1	1	1	1
9	1	1	2	1	1	1	1	1	1	1
8	2	1	1	1	1	1	1	1	2	1
7	1	1	1	1	2	1	1	1	1	1
6	1	1	1	1	1	1	1	1	1	1
5	1	1	2	1	1	1	1	2	1	1
4	1	1	1	1	1	1	1	1	1	1
3	1	1	1	1	1	1	1	1	1	1
2	1	1	1	1	1	1	1	1	1	1
1	1	1	1	1	1	1	1	1	1	1

2										KGAMA
42	3	3	3	3	3	3	3	3	3	3
41	3	3	3	3	3	3	3	3	3	3
40	3	3	3	3	3	3	3	3	3	3
39	3	3	3	3	3	3	3	3	3	3
38	2	2	2	2	2	2	2	2	2	2
37	2	2	2	2	2	2	2	2	2	2
36	2	2	2	2	2	2	2	2	2	2
35	2	2	2	2	2	2	2	2	2	2
34	2	2	2	2	2	2	2	2	2	2
33	2	2	2	2	2	2	2	2	2	2
32	2	2	2	2	2	2	2	2	2	2
31	2	2	2	2	2	2	2	2	2	2
30	2	2	2	2	2	2	2	2	2	2
29	2	2	2	2	2	2	2	2	2	2
28	2	2	2	2	2	2	2	2	2	2
27	2	2	2	2	2	2	2	2	2	2
26	2	2	0	0	0	0	0	0	2	2
25	2	2	0	0	0	0	0	0	2	2
24	2	2	0	0	0	0	0	0	2	2
23	2	2	0	0	0	0	0	0	2	2
22	2	2	2	2	2	2	2	2	2	2
21	1	2	1	2	1	2	1	2	1	2
20	2	1	2	1	2	1	2	1	2	1
19	1	2	1	2	1	2	1	2	1	2
18	2	1	2	1	2	1	2	1	2	1
17	1	1	1	1	1	1	1	1	1	1
16	1	1	1	1	1	1	1	1	1	1
15	1	1	1	1	1	1	1	1	1	1
14	1	1	1	1	1	1	1	1	1	1
13	1	1	1	1	1	1	1	1	1	1
12	1	1	1	1	1	1	1	1	1	1
11	1	1	1	1	1	1	1	1	1	1
10	1	1	1	1	1	1	1	1	1	1
9	1	1	1	1	1	1	1	1	1	1
8	1	1	1	1	1	1	1	1	1	1
7	1	1	1	1	1	1	1	1	1	1
6	1	1	1	1	1	1	1	1	1	1
5	1	1	1	1	1	1	1	1	1	1
4	1	1	1	1	1	1	1	1	1	1
3	1	1	1	1	1	1	1	1	1	1
2	1	1	1	1	1	1	1	1	1	1

```
1    1  1  1  1  1  1  1  1  1  1
```

Block 3

```
1000                                    NINT
   0.01  0.001                          DTIME,DTIME_TEMP
 100                                    NSTEP
   1 10  100  1000                      NPLOT1 ... NPLOT4
   1                                    KGAMAPLOT
   5   1  3  5  8 10                   NBPLOT,JBETAPLOT(1) ... JBETAPLOT(5)
   -1  0  1  0  1                       ISIGNX2B(1) ... ISIGNX2B(5)
   0                                    NAPLOT,IALPHAPLOT(1) ...
   0                                    IGPS
   2                                    NLEG
   5                                    J1
```

Block 4

```
                                        External thermal boundary conditions
   2    2    2    2    2                LOADF1(1) ...
   2    2    2    2    2                ... LOADF1(NBETA)
1200 1200 1200 1200 1200                AMPF1(1) ...
1200 1200 1200 1200 1200                ... AMPF1(NBETA)

   2    2    2    2    2                LOADR1(1) ...
   2    2    2    2    2                ... LOADR1(NBETA)
   0    0    0    0    0                AMPR1(1) ...
   0    0    0    0    0                ... AMPR1(NBETA)

   1    1    1    1    1                LOADF2(1) ...
   1    1    1    1    1                .
   1    1    1    1    1                .
   1    1    1    1    1                .
   1    1    1    1    1                .
   1    1    1    1    1                .
   1    1    1    1    1                .
   1    1    1    1    1                .
   1    1                               ... LOADF2(NALPHA)
   0    0    0    0    0                AMPF2(1) ...
   0    0    0    0    0                .
   0    0    0    0    0                .
   0    0    0    0    0                .
   0    0    0    0    0                .
   0    0    0    0    0                .
   0    0    0    0    0                .
   0    0    0    0    0                .
   0    0                               ... AMPF2(NALPHA)

   1    1    1    1    1                LOADR2(1) ...
   1    1    1    1    1                .
   1    1    1    1    1                .
   1    1    1    1    1                .
   1    1    1    1    1                .
   1    1    1    1    1                .
   1    1    1    1    1                .
   1    1    1    1    1                .
   1    1                               ... LOADR2(NALPHA)
   0    0    0    0    0                AMPR2(1)
   0    0    0    0    0                .
   0    0    0    0    0                .
   0    0    0    0    0                .
   0    0    0    0    0                .
   0    0    0    0    0                .
   0    0    0    0    0                .
   0    0    0    0    0                .
   0    0                               ... AMPR2(NALPHA)
```

```
                                        Window thermal boundary conditions
2     2     2     2     2     2         LOADWFT1(JBETAW1) ... LOADWFT1(JBETAW2)
0     0     0     0     0     0         AMPWFT1(JBETAW1) ... AMPWFT1(JBETAW2)
2     2     2     2     2     2         LOADWRT1(JBETAW1) ... LOADWRT1(JBETAW2)
0     0     0     0     0     0         AMPWRT1(JBETAW1) ... AMPWRT1(JBETAW2)

2     2     2     2                     LOADWFT2(IALPHAW1) ... LOADWFT2(IALPHAW2)
0     0     0     0                     AMPWFT2(IALPHAW1) ... AMPWFT2(IALPHAW2)

2     2     2     2                     LOADWRT2(IALPHAW1) ... LOADWRFT2(IALPHAW2)
0     0     0     0                     AMPWRT2(IALPHAW1) ... AMPWRT2(IALPHAW2)


                                        External mechanical boundary conditions
1     1     1     1     1               LOADF1(1) ...
1     1     1     1     1               ... LOADF1(NBETA)
0     0     0     0     0               AMPF1(1) ...
0     0     0     0     0               ... AMPF1(NBETA)

1     1     1     1     1               LOADF1(1) ...
1     1     1     1     1               ... LOADF1(NBETA)
0     0     0     0     0               AMPF1(1) ...
0     0     0     0     0               ... AMPF1(NBETA)

1     1     1     1     1               LOADR1(1) ...
1     1     1     1     1               ... LOADR1(NBETA)
0     0     0     0     0               AMPR1(1) ...
0     0     0     0     0               ... AMPR1(NBETA)

1     1     1     1     1               LOADR1(1) ...
1     1     1     1     1               ... LOADR1(NBETA)
0     0     0     0     0               AMPR1(1) ...
0     0     0     0     0               ... AMPR1(NBETA)

1     1     1     1     1               LOADF2(1) ...
1     1     1     1     1               .
1     1     1     1     1               .
1     1     1     1     1               .
1     1     1     1     1               .
1     1     1     1     1               .
1     1     1     1     1               .
1     1     1     1     1               .
1     1                                 ... LOADF2(NALPHA)
0     0     0     0     0               AMPF2(1) ...
0     0     0     0     0               .
0     0     0     0     0               .
0     0     0     0     0               .
0     0     0     0     0               .
0     0     0     0     0               .
0     0     0     0     0               .
0     0     0     0     0               .
0     0                                 ... AMPF2(NALPHA)

2     2     2     2     2               LOADF2(1) ...
2     2     2     2     2               .
2     2     2     2     2               .
2     2     2     2     2               .
2     2     2     2     2               .
2     2     2     2     2               .
2     2     2     2     2               .
2     2     2     2     2               .
2     2                                 ... LOADF2(NALPHA)
0     0     0     0     0               AMPF2(1) ...
0     0     0     0     0               .
```

```
0     0     0     0     0              .
0     0     0     0     0              .
0     0     0     0     0              .
0     0     0     0     0              .
0     0     0     0     0              .
0     0     0     0     0              .
0     0                                ... AMPF2(NALPHA)

1     1     1     1     1              LOADR2(1) ...
1     1     1     1     1              .
1     1     1     1     1              .
1     1     1     1     1              .
1     1     1     1     1              .
1     1     1     1     1              .
1     1     1     1     1              .
1     1     1     1     1              .
1     1                                ... LOADR2(NALPHA)
0     0     0     0     0              AMPR2(1) ...
0     0     0     0     0              .
0     0     0     0     0              .
0     0     0     0     0              .
0     0     0     0     0              .
0     0     0     0     0              .
0     0     0     0     0              .
0     0                                ... AMPR2(NALPHA)

2     2     2     2     2              LOADR2(1) ...
2     2     2     2     2              .
2     2     2     2     2              .
2     2     2     2     2              .
2     2     2     2     2              .
2     2     2     2     2              .
2     2     2     2     2              .
2     2     2     2     2              .
2     2                                ... LOADR(NALPHA)
0     0     0     0     0              AMPR2(1) ...
0     0     0     0     0              .
0     0     0     0     0              .
0     0     0     0     0              .
0     0     0     0     0              .
0     0     0     0     0              .
0     0     0     0     0              .
0     0                                ... AMPR2(NALPHA)


                                       Window mechanical boundary conditions
1     1     1     1     1     1        LOADWFM1(JBETAW1) ... LOADWFM1(JBETAW2)
0     0     0     0     0     0        AMPWFM1(JBETAW1) ... AMPWFM1(JBETAW2)
1     1     1     1     1     1        LOADWFM1(JBETAW1) ... LOADWFM1(JBETAW2)
0     0     0     0     0     0        AMPWFM1(JBETAW1) ... AMPWFM1(JBETAW2)

1     1     1     1     1     1        LOADWRM1(JBETAW1) ... LOADWRM1(JBETAW2)
0     0     0     0     0     0        AMPWRM1(JBETAW1) ... AMPWRM1(JBETAW2)

1     1     1     1     1     1        LOADWRM1(JBETAW1) ... LOADWRM1(JBETAW2)
0     0     0     0     0     0        AMPWRM1(JBETAW1) ... AMPWRM1(JBETAW2)

1     1     1     1                    LOADWFM2(JBETAW1) ... LOADWFM2(JBETAW2)
0     0     0     0                    AMPWFM2(JBETAW1) ... AMPWFM2(JBETAW2)

1     1     1     1                    LOADWFM2(JBETAW1) ... LOADWFM2(JBETAW2)
```

0	0	0	0	AMPWFM2(JBETAW1) ... AMPWFM2(JBETAW2)
1	1	1	1	LOADWRM2(JBETAW1) ... LOADWRM2(JBETAW2)
0	0	0	0	AMPWRM2(JBETAW1) ... AMPWRM2(JBETAW2)
1	1	1	1	LOADWRM2(JBETAW1) ... LOADWRM2(JBETAW2)
0	0	0	0	AMPWRM2(JBETAW1) ... AMPWRM2(JBETAW2)

REPORT DOCUMENTATION PAGE

Form Approved
OMB No. 0704-0188

1. AGENCY USE ONLY (*Leave blank*)	2. REPORT DATE	3. REPORT TYPE AND DATES COVERED
	August 2000	Final Contractor Report

4. TITLE AND SUBTITLE

HOTCFGM-2D: A Coupled Higher-Order Theory for Cylindrical Structural Components With Bi-Directionally Graded Microstructures

5. FUNDING NUMBERS

WU–523–31–13–00
NAS3–97190
NAG3–2252

6. AUTHOR(S)

Marek-Jerzy Pindera and Jacob Aboudi

7. PERFORMING ORGANIZATION NAME(S) AND ADDRESS(ES)

University of Virginia
Civil Engineering and Applied Mechanics Department
Charlottesville, Virginia 22903

8. PERFORMING ORGANIZATION REPORT NUMBER

E–12399

9. SPONSORING/MONITORING AGENCY NAME(S) AND ADDRESS(ES)

National Aeronautics and Space Administration
Washington, DC 20546–0001

10. SPONSORING/MONITORING AGENCY REPORT NUMBER

NASA CR—2000-210350

11. SUPPLEMENTARY NOTES

Marek-Jerzy Pindera and Jacob Aboudi, University of Virginia, Civil Engineering and Applied Mechanics Department Charlottesville, Virginia 22903; Jacob Aboudi, visiting Professor, Faculty of Engineering, Tel-Aviv University, Ramat-Aviv, Tel-Aviv 69978, Israel. Project Manager, S.M. Arnold, Structures and Acoustics Division, NASA Glenn Research Center, organization code 5920, (216) 433–3334.

12a. DISTRIBUTION/AVAILABILITY STATEMENT

Unclassified - Unlimited
Subject Categories: 24, 39, and 61 Distribution: Nonstandard

This publication is available from the NASA Center for AeroSpace Information, (301) 621–0390.

12b. DISTRIBUTION CODE

13. ABSTRACT ***(Maximum 200 words)***

This report summarizes the work performed under the contract NAS3-97190 during the FY98-99 funding period. The objective of this two-year project was to develop and deliver to the NASA-Glenn Research Center a two-dimensional higher-order theory, and related computer codes, for the analysis and design of cylindrical functionally graded materials/structural components for use in advanced aircraft engines (e.g., combustor linings, rotor disks, heat shields, brisk blades). To satisfy this objective, two-dimensional version of the higher-order theory, HOTCFGM-2D, and four computer codes based on this theory, for the analysis and design of structural components functionally graded in the radial and circumferential directions were developed in the cylindrical coordinate system r–θ–z. This version of the higher-order theory is a significant generalization of the one-dimensional theory, HOTCFGM-1D, developed during the FY97 funding period under the contract NAS3-96052 for the analysis and design of cylindrical structural components with radially graded microstructures. The generalized theory is applicable to thin multi-phased composite shells/cylinders subjected to steady-state thermomechanical, transient thermal and inertial loading applied uniformly along the axial direction such that the overall deformation is characterized by a constant average axial strain. The reinforcement phases are uniformly distributed in the axial direction, and arbitrarily distributed in the radial and circumferential direction, thereby allowing functional grading of the internal reinforcement in the r–θ plane. The four computer codes *fgmc3dq.cylindrical.f, fgmp3dq.cylindrical.f, fgmgvips3dq.cylindrical.f, and fgmc3dq.cylindrical.transient.f* are research-oriented codes for investigating the effect of functionally graded architectures, as well as the properties of the multi-phase reinforcement, in thin shells subjected to thermomechanical and inertial loading, on the internal temperature, stress and (inelastic) strain fields. The reinforcement distribution in the radial and circumferential directions is specified by the user. The thermal and inelastic properties of the individual phases can vary with temperature. The inelastic phases are presently modeled by the power-law creep model generalized to multi-directional loading (within *fgmc3dq.cylindrical.f* and *fgmc3dq.cylindrical.transient.f* for steady-state and transient thermal loading, respectively), and incremental plasticity and GVIPS unified viscoplasticity theories (within the steady-state loading versions *fgmp3dq.cylindrical.f* and *fgmgvips3dq.cylindrical.f*).

14. SUBJECT TERMS

Analysis; Elastic; Plastic; Thermal mechanical analysis; Functionally graded material

15. NUMBER OF PAGES

95

16. PRICE CODE

A05

17. SECURITY CLASSIFICATION OF REPORT	18. SECURITY CLASSIFICATION OF THIS PAGE	19. SECURITY CLASSIFICATION OF ABSTRACT	20. LIMITATION OF ABSTRACT
Unclassified	Unclassified	Unclassified	